Supervisory Model Predictive Control of Building Integrated Renewable and Low Carbon Energy Systems

by

Faramarz Sadr

BSc, MSc

Doctoral Thesis

Submitted in partial fulfilment of the requirements
for the award of Doctor of Philosophy of
Loughborough University

December 19, 2011

Abstract

To reduce fossil fuel consumption and carbon emission in the building sector, renewable and low carbon energy technologies are integrated in building energy systems to supply all or part of the building energy demand. In this research, an optimal supervisory controller is designed to optimize the operational cost and the CO_2 emission of the integrated energy systems. For this purpose, the building energy system is defined and its boundary, components (subsystems), inputs and outputs are identified. Then a mathematical model of the components is obtained. For mathematical modelling of the energy system, a unified modelling method is used. With this method, many different building energy systems can be modelled uniformly. Two approaches are used; multi-period optimization and hybrid model predictive control. In both approaches the optimization problem is deterministic, so that at each time step the energy consumption of the building, and the available renewable energy are perfectly predicted for the prediction horizon. The controller is simulated in three different applications. In the first application the controller is used for a system consisting of a micro-combined heat and power system with an auxiliary boiler and a hot water storage tank. In this application the controller reduces the operational cost and CO_2 emission by 7.31 percent and 5.19 percent respectively, with respect to the heat led operation. In the second application the controller is used to control a farm electrification system consisting of PV panels, a diesel generator and a battery bank. In this application the operational cost with respect to the common load following strategy is reduced by 3.8 percent. In the third application the controller is used to control a hybrid off-grid power system consisting of PV panels, a battery bank, an electrolyzer, a hydrogen storage tank and a fuel cell. In this application the controller maximizes the total stored energies in the battery bank and the hydrogen storage tank.

Key words: building energy system, integrated renewable energy, low carbon energy technology, CO_2 emission, supervisory control, optimal control, model predictive control, multi-period optimization, multi-parametric programming, explicit model predictive control

Acknowledgments

I would like to acknowledge Dr. Mahroo Eftekhari for the supervision of this thesis, and Loughborough University for providing the research grant.

Table of contents

List of figures

List of tables

Nomenclatures

ANN	Artificial Neural Network
A	total area of PV panels or solar collectors (gross area)(m^2)
AC	Alternating Current
Ah	Ampere-hour
B	energy bus
B_t	Benefits in year t
BMS	Building Management System
C	energy converter
C_{bw}	battery wear cost (£/kWh)
$C_{O\&M}$	hourly operation and maintenance cost (£/h)
C_{rep}	replacement cost of energy converter per hour (£/h)
C_t	costs in year t
CCHP	Combined Cooling, Heat and Power
CFTOC	Constrained Finite-Time Optimal Control
CHP	Combined Heat and Power
COP	Coefficient of Performance
$C_{\alpha d}$	unit price of energy carrier bought from the grid (£/kWh)
$C_{\alpha x}$	unit price of the energy sold to the grid (£/kWh)
DC	Direct Current
DDE	Dynamic Data Exchange
DHA	Discrete Hybrid Automata (Automaton)
E	stored energy (kWh)
E_α	stored energy of energy carrier type α (kWh)
$\dot{E}_\alpha$	storage rate (power) (kW)
EG	Event Generator
ESP	Energy Service Provider
F	diesel generator fuel consumption (litres/h)
F_i	proportionality factor of diesel generator fuel consumption with output power

F_o	proportionality factor of diesel generator fuel consumption with rated power of the diesel generator
FC	Fuel Cell
FLC	Fuzzy Logic Control
FSM	Finite State Machine
H	hub height of wind turbine (m)
H_{ref}	reference height for wind speed measurement (m)
HHV	Higher Heating Value (kWh/kg)
HMI	Human Machine Interface
HVAC	Heating, Ventilating and Air Conditioning
HYSDEL	Hybrid Systems Description Language
I_T	global solar radiation incident on the PV panel or solar collector ($\mathrm{kW/m^2}$)
I_S	standard amount of radiation used to rate the capacity of PV panel ($\mathrm{kW/m^2}$)
$K_{\alpha d}$	CO_2 emission factor of delivered power (kg/kWh)
$K_{\alpha x}$	CO_2 emission factor of exported power (kg/kWh)
LP	Linear Programming
LHV	Lower Heating Value (kWh/kg)
LT	lifetime (hours) of energy converter
LTI	Linear Time Invariant
M	stored mass (kg)
MILP	Mixed Integer Linear Programming
MLD	Mixed Logical Dynamic
MPC	Model Predictive Control
MPPT	Maximum Power Point Tracking (MPPT)
MS	Mode Selector
N_{bat}	number of batteries in the battery bank
N	number of time periods
N_c	control horizon
N_{con}	number of energy converters

N_p	prediction horizon
N_{ren}	number of renewable converters
NPV	Net Present Value
O&M	Operation and Maintenance
P	power (kW)
P_{hloss}	heat loss form hot water tank during a time step (kW)
PV	photovoltaic
$P_{\alpha c}$	input power α type to energy converter (kW)
$P_{\alpha d}$	delivered power from grid to building energy system (kW)
$P_{\alpha l}$	building load of energy type α (kW)
$P_{\alpha s}$	charging/discharging power to/from the storage devices (kW)
$P_{\alpha x}$	exported power from building energy system to grid (kW)
PWA	Piecewise Affine
Q_{bat}	currently stored amount of electricity in the battery (Ah)
$Q_{bat,\max}$	battery capacity (Ah)
$Q_{lifetime}$	lifetime throughput of a single battery (kWh)
Q_u	useful heat of solar collection (kW)
$Q_{\alpha c}$	output power type α from energy converter (kW)
R_α	power from renewable converters (kW)
SAS	Switched Affine System
SEC	specific energy consumption of the compressor between the electrolyzer and the hydrogen storage tank ($\mathrm{kW/m^3/min}$)
SOC	State of Charge
T_a	ambient (air) temperature (°C)
T_{av}	average solar collector fluid temperature (°C)
T_i	inlet temperature of fluid to solar collector (°C)
T_o	outlet temperature of fluid from solar collector (°C)
V_{nom}	nominal voltage of battery (V).
$\dot{V}$	volumetric flow rate of hydrogen ($\mathrm{m^3/min}$)

Y_{pv}	capacity of PV panel
a	coefficient of wind speed power law
a_0, a_1, a_2	thermal efficiency parameters of solar collector
d	discount rate
d_i	depth of discharge (%)
e	charging/discharging efficiency
f_i	number of cycles to failure
f_{pv}	derating factor of PV
$f_{\alpha d}$	primary energy factor of delivered power
$f_{\alpha x}$	primary energy factors of exported power
i	energy converter number
k	current sampling instant
$\dot{m}$	mass flow rate (kg/h)
r_α	interface efficiency of renewable energy
t	time step
u	manipulated input
v	wind speed (m/s)
v_{cin}	cut-in speed of wind turbine (m/s)
v_{cout}	cut-out speed of wind turbine (m/s)
v_{ref}	reference velocity of wind turbine (m/s)
y	actual output
$\hat{y}$	predicted output
wt	wind turbine
x	state
$\alpha, \beta, \gamma, ..., \omega$	energy carrier
δ	binary variable
σ	self discharge rate of the battery
ΔT	temperature difference between the inlet temperature of fluid to collector and ambient (°C)
Δt	time step length (h)

η	efficiency
η_{rt}	battery roundtrip efficiency

Vectors and Matrices

$\mathbf{P}$	input power vector to the converter
$\mathbf{Q}$	output power vector from the converter
$\mathbf{\Psi}$	conversion efficiency matrix
$\mathbf{P_d}$	delivered power to the energy system
$\mathbf{\Phi}$	storage efficiency matrix
$\mathbf{\dot{E}}$	power to or from the storage device
$\mathbf{E}$	stored energy
$\mathbf{P}_{c_i}$	input power to converter
$\mathbf{R}_i$	renewable energy
$\mathbf{P_l}$	load
$\mathbf{P_x}$	exported power

Subscripts and superscripts

b	boiler
bat	battery
c	cool, cooling
ch	charging
chi	chiller
chp	combined heat and power generator
comp	compressor
cs	stored cool
dch	discharging
do	diesel oil
fc	fuel cell
e	electricity
ely	electrolyzer
dsl	diesel generator

g	gas
h	heat, heating
h_2	hydrogen
h_{in}	input heat to absorption chiller
hp	heat pump
hwt	hot water tank
pv	photovoltaic panel
r	rated power
sc	solar collector
wt	wind turbine

Chapter 1
Introduction

1.1 Introduction to building integrated renewable and low carbon energy systems

The energy used in buildings contributes roughly half of the UK's total carbon dioxide (CO_2) emissions (27 per cent to homes and a further 17 per cent to non-domestic buildings) (DCLG, 2008). CO_2 is the main greenhouse gas, which is causing global warming and climate change. Utilisation of renewable and low carbon energy technologies for building energy supply systems are key methods for reducing CO_2 emission from the building sector and thus for tackling climate change. This approach helps to reduce the UK's dependence on fossil fuels, and also decreases the impacts of energy price rises.

For the above reasons, the UK Government's July 2007 Building A Greener Future – Policy Statement (DCLG, 2006a) announced that all new homes will be zero carbon from 2016. In addition, in the 2008 budget the Government's ambition was announced to be that all new non-domestic buildings should be zero carbon from 2019.

Low and Zero Carbon (LZC) is the term which is applied to renewable sources of energy and also to technologies, which are either significantly more efficient than traditional solutions, or which emit less carbon in providing heating, cooling or power. There are a number of LZC technologies that can be integrated into new and existing buildings. Table 1.1.1 summarises some of these technologies, from

simple, heat or electricity based renewables, to technologies that supply both electricity and heat.

Table 1.1.1 LZC technologies integrated in buildings (ECI, 2005)

Technology	Heat only	Heat and electricity	Electricity only
Low carbon	Heat pumps	Gas fired CHP in community heating Gas fired micro-CHP (Stirling engine) Gas fired micro-CHP (fuel cells)	_
Zero carbon	Solar hot water Biomass* Geothermal	Biomass* in micro-CHP (e.g. Stirling engines)	Photovoltaics Wind

* Biomass fuel has net zero carbon impact, since carbon emissions released by combustion of biomass are equivalent to the carbon absorbed during fuel crop growth

Of the LZC technologies that can be integrated in buildings, some are complementary (e.g. wind turbines and photovoltaic panels could both be installed at a site, each contributing to the electricity supply under different conditions), whereas others can be mutually exclusive (e.g. it is unlikely that ground source heat pumps will be installed at a site which already has a heat source such as biomass). Table 1.1.2 indicates those technologies which can be effectively installed as a combination (identified by '√'), together with those technologies which are unlikely to be complementary and therefore would not generally be installed together (identified by '×').

Renewable energies are mostly intermittent in nature and are not available on demand time. For example a photolytic panel (PV) generates electricity in the day time, but the peak electricity consumption of a home is usually in the early morning or night-time. In addition, on cloudy days the generated electricity may be less than the demand. Wind is also intermittent and the electricity produced by wind turbines is highly unpredictable.

In order to harvest as much energy as possible from renewable energy resources, it is essential to store the extra energy when surplus energy exists, and use the stored energy when there is an energy deficit.

Table 1.1.2 Combination of LCZ technologies (Shearer and Anderson, 2005)

	Solar thermal	Photovoltaics	District heating	Combined heat and power	Ground source heat pumps	Wind power	Biomass
Solar thermal		√			√	√	
Photovoltaics						√	
District heating				√	×		√
Combined heat and power					×		√
Ground source heat pumps							×
Wind power							
Biomass							

√ technologies which are generally complementary

× technologies which can be mutually exclusive

Energy storage is also important for load management in low carbon technologies. For example heat to power ratios of micro-CHP and building do not coincide. During the operation of micro-CHP systems, extra heat or electricity can be stored and used later when there is a heat or electricity deficit. In heat pump applications also, heat can be produced at night-time when electricity is cheaper, and stored for the peak time when the electricity is more expensive.

In building applications, electricity can be stored in a battery or hydrogen tank. In the latter case, electricity is used for the decomposition of water into hydrogen and oxygen, and the hydrogen is compressed and stored in the tank. The stored hydrogen is used for electricity generation by fuel cell.

For heat and cool storage, two main methods are used in buildings. These methods are sensible heat storage, normally in hot water tanks, and latent heat storage with phase change material.

1.2 Introduction to optimization of building energy system

In many areas of science and technology, there is more than one way to achieve a specific goal. Optimization techniques aim to find the optimum solution for pre-defined objectives. For a building energy system, in particular, given the building energy needs, optimization techniques can be used to determine the most efficient selection of the equipment types, system structure (topology), equipment sizes and system operation, in order to reduce the costs or CO_2 emission.

1.2.1 Selection of the energy equipment types

Different renewable, low carbon and conventional equipment can be used to supply electricity, heating and cooling demand of buildings. For example, the heating demand of a building can be supplied by solar collector, CHP, heat pump, hot water boiler (fuelled by biomass or natural gas), or a combination of these equipment. For energy storage also, different energy storage devices can be selected. For example, for heat storage, the existing alternatives would be the hot water tank and phase change material. The optimization technique is used to determine the best component type(s) that will have minimum initial cost, running cost and/or CO_2 emission.

1.2.2 Optimization of the energy system structure

The selected energy equipment of the building can be connected in different ways. The structure of the connection, determines the energy flow from one piece of equipment to the other. For example a heat pump and a solar collector can be connected in series or parallel. The optimization determines the best arrangement of equipment, which will result in minimum running cost and/or CO_2 emission.

1.2.3 Optimization of the energy equipment sizes

Having selected the energy equipment and system structure, the equipment sizes should be optimized in order to minimize the initial cost of the building energy system.

The above three optimizations determine the optimum equipment and structure of the building energy system. However, in order to reduce energy consumption, the building energy system needs to operate efficiently.

1.2.4 Optimization of the energy system operation

For a given building energy system (with specific component types, structure and sizes), under specified conditions, optimization of the system operation determines optimum power flows between grids, energy converters, storage devices and building loads, in order to reduce the operational cost and CO_2 emission.

1.3 Motivation and challenges

The motivation for this research is the minimization of the operational cost and the CO_2 emission of the building integrated renewable and low carbon energy systems by the efficient storage of energy and the management of the operation of equipment and energy flows. The effect of this minimization is important and considerable, because it is related to the whole lifetime of the system. In addition, considering the increasing trend of utilization of renewable and low carbon energy technologies in the building sector, this can further reduce the CO_2 emission level in the UK.

The minimization of energy consumption and CO_2 emission can be accomplished by using a supervisory controller. In the building energy system, each of the renewable, low carbon, conventional and energy storage subsystems

has its own local control system and can be operated independently. The supervisory controller can optimize the operation of the whole energy system by considering the predicted energy demand and the available renewable energy for the next day and the price/CO_2 emission of the non-renewable energies. The controller can calculate the optimum operation set point of the individual subsystems, as well as the optimum amounts of energy storage, energy import/export from/to the grid.

1.4 Aim

The main aim of the research is to develop a supervisory controller to integrate renewable and low carbon energy systems in buildings. The controller will optimize the energy generation and storage in the building so as to reduce CO_2 emissions.

1.5 Objectives

The objectives of this thesis are:

- To develop mathematical models of typical energy system components
- To select the appropriate structure of the optimal supervisory controller for integrating the different renewable and low carbon energy systems
- To validate the supervisory controller by using various modelling and simulation techniques
- To assess the effectiveness of the controller in reducing operational cost and CO_2 emission by comparing typical systems with and without the controller in place

1.6 Hypotheses

By validation and assessing the performance of the designed supervisory controller for different types of building integrated renewable and low carbon energy systems, the hypotheses can be tested in this research can be stated as:

Hypothesis 1: *In order to reduce operational cost and* CO_2 *emission of the building integrated renewable and low carbon energy system, could a supervisory controller to be designed to determine:*

- *How much energy should be charged or discharged from energy storage devices?*
- *Which one of the low carbon and conventional energy converters should be operated and how much should be their output power?*
- *How much energy should be imported from or exported to the grid?*

Hypothesis 2: *Would the supervisory model predictive controller be a unified (generic) controller that can be tailored and used in all types of integrated renewable and low carbon energy systems in buildings.*

It is assumed that the supervisory model predictive controller could follow the electrical and thermal load set points of the building, and handle input, state and output constraints.

1.7 Contribution

Considerable research has been done in the area of controlling building integrated renewable and low carbon energy systems, however in the existing research each of the designed controllers has been for a specific energy system and cannot be used in other systems. Another limitation of the designed controllers is the dependency of the controllers on sophisticated and expensive hardware and software which in practice makes their application difficult, especially for small and medium size buildings.

This research has contributed substantially to obtaining a unified (generic) method for the supervisory controller design, which optimally controls the operation of building integrated renewable and low carbon energy systems. By utilization of this method, sophisticated operational schedules can be considered in the design of the supervisory controller, including sequential operation of the equipment and delays in the start/stop of the subsystems. In addition the design of the supervisory hybrid model predictive controller for the building energy system and the explicit implementation of this controller are novel approaches in this research.

1.8 Outline of the thesis

The remainder of this thesis is organized as follows:

Chapter 2 critically reviews the background of the energy utilization, energy price, CO_2 emission and related policies and regulations. In this chapter some application samples of the building integrated renewable and low carbon energy systems are presented. This chapter critically reviews the existing control and management methods for the building integrated renewable and low carbon energy systems, and highlights the use of model predictive control as an innovative method for the supervisory control of these systems.

In Chapter 3 the building energy system and its connection to energy infrastructures is discussed. The required data for controlling the building energy system, which include prediction of the weather conditions, the available renewable energy and the building's electrical, heating and cooling loads, are fully described.

The mathematical modelling of subsystems is described in **Chapter 4** together with mathematical model of the building energy system's components. These components include energy converters and energy storage devices.

Chapter 5 covers the supervisory model predictive controller design. In this chapter the concept of supervisory controller is explained and two approaches for designing the model predictive controller are described. The first approach is based on multi-period optimization and the second approach is based on hybrid model predictive control. For the optimization purposes, economic, CO_2 emission and primary energy objective functions are formulated in this chapter.

Chapter 6 describes three applications of the designed supervisory controller. In application 1, the building energy system consists of a micro combined heat and power (micro-CHP) system, a boiler (or auxiliary heat) and a hot water storage tank. In application 2, the energy system consists of PV panels, a diesel generator and a battery bank. In application 3, the energy system consists of PV panels, a battery bank, an electrolyzer and a fuel cell. In each application, the results are presented and discussed.

The conclusion of the thesis is presented in **Chapter 7**. This chapter starts with a summary of the thesis. The conclusions are then explained, recommendations to industry are provided, and the limitations of the work are described.

Chapter 2

Literature review

This chapter consists of four sections. In section one, a background regarding energy utilization in the building sector and its contribution in CO_2 emission is explained. Then the role of renewable energies is highlighted and incentives, regulations and policies for the utilization of renewable energies and low carbon emission technologies in the UK are described. In section two, samples of research and applications concerning the integration of renewable energies in buildings are presented. In section three, a literature review about the control and management methods of the building integrated renewable and low carbon energy systems is given. Section four is a review of optimization problems related to the supervisory model predictive controller deign.

2.1 Background

2.1.1 World and the UK energy consumption

World energy consumption increases continuously. Most of the world's energy need is supplied by fossil fuels. According to the International Energy Outlook 2010 (EIA, 2010), in 2007 the total energy consumption of the world was 495 Quadrillion Btu and 86 percent of this energy was supplied by fossil fuels. In the IEO2010 Reference case, world energy consumption increases by 49 percent, or 1.4 percent per year, from 495 quadrillion Btu in 2007 to 739 quadrillion Btu in 2035 (Figure 2.1.1).

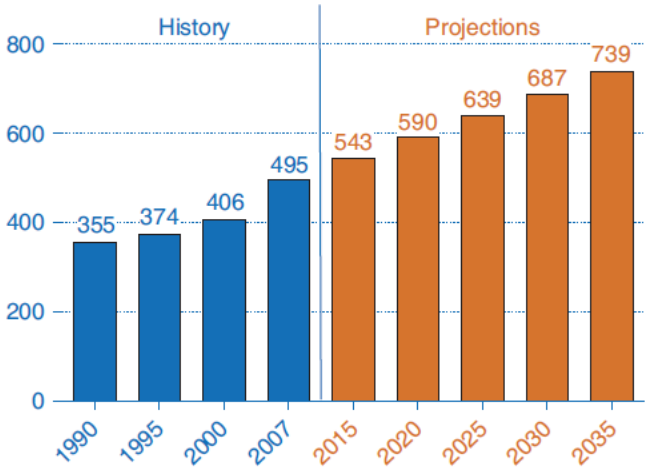

Figure 2.1.1 World marketed energy consumption, 1990-2035 (quadrillion Btu*) (EIA, 2010)

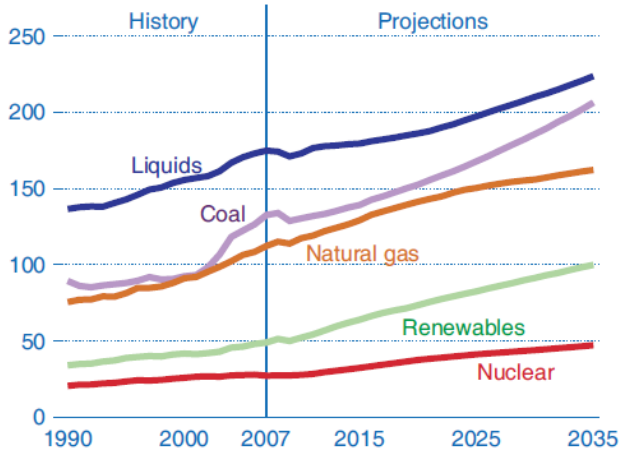

Figure 2.1.2 World marketed energy use by fuel type, 1990-2035 (quadrillion Btu*) (EIA, 2010)

Figure 2.1.2 shows that up to 2035, the share of nuclear and renewable energy will increase but fossil fuels will still have the major share.

The buildings sector, comprising residential and commercial consumers, accounts for about one-fifth of the world's total delivered energy consumption (EIA, 2010). In the residential sector, energy use is defined as the energy consumed by households, excluding transportation uses.

*1 quadrillion Btu = 10^{15} Btu = 1.055 × 10^{18} joules (1.055 exajoules or EJ)

In the IEO2010 Reference case (EIA, 2010), world residential energy use increases by 1.1 percent per year over the projection period, from 50 quadrillion Btu in 2007 to 69 quadrillion Btu in 2035.

The commercial sector - often referred to as the services sector or the services and institutional sector - consists of businesses, institutions, and organizations that provide services. This sector encompasses many different types of buildings and a wide range of activities and energy-related services. In the IEO2010 Reference case, the energy consumption of OECD (Organisation for Economic Co-operation and Development) and non-OECD countries in commercial sector expands by 0.9 and 2.7 percent respectively from 2007 to 2035.

In the UK, domestic sector - with 45.6 million tonnes of equivalent oil - was responsible for 29 percent of the final energy consumption in 2008. The final energy consumed by the service sector - with 19.8 million tonnes of equivalent oil - was 13 percent.

The break down of the domestic energy consumption by fuel type shows that in this sector, fuel usage been shifted by 8%, from solid fuel in 1990 to natural gas in 2007 (Figure 2.1.3).

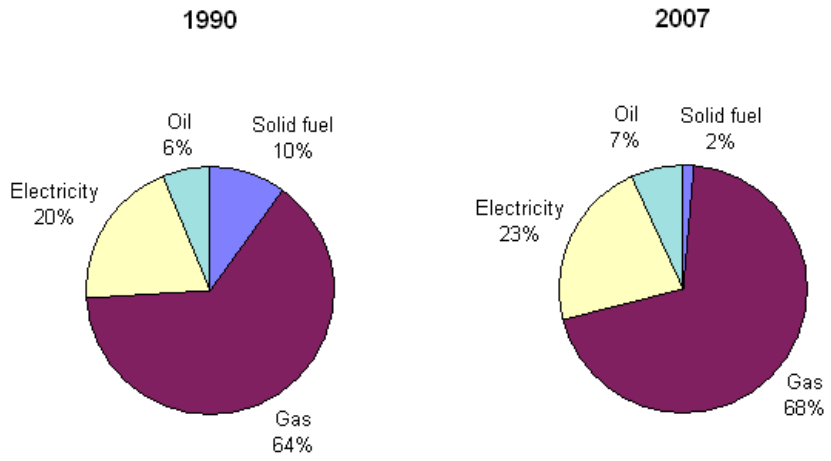

Figure 2.1.3 Domestic sector final energy consumption by end use by fuel in UK, 1990 and 2007 (DECC, 2008)

The break down of the service sector energy consumption by fuel type, as shown in Figure 2.1.4, demonstrates that in this sector gas and electricity were the main energy types in 2007.

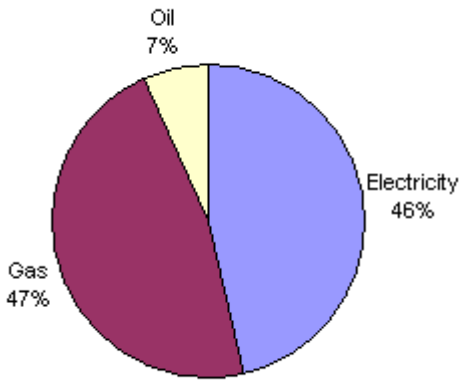

Figure 2.1.4 Service sector final energy consumption by end use by fuel 2007 (DECC, 2008)

Projected trends in the energy demand of the UK by sectors is shown in Figure 2.1.5 (DECC, 2009a). The domestic sector is projected to decrease by 19 percent between 2007 and 2020, despite the government's major programme of house building, which is expected to result in almost three million new houses being built by 2020 (DCLG, 2010). This is driven by energy efficiency measures, microgeneration and renewable heat.

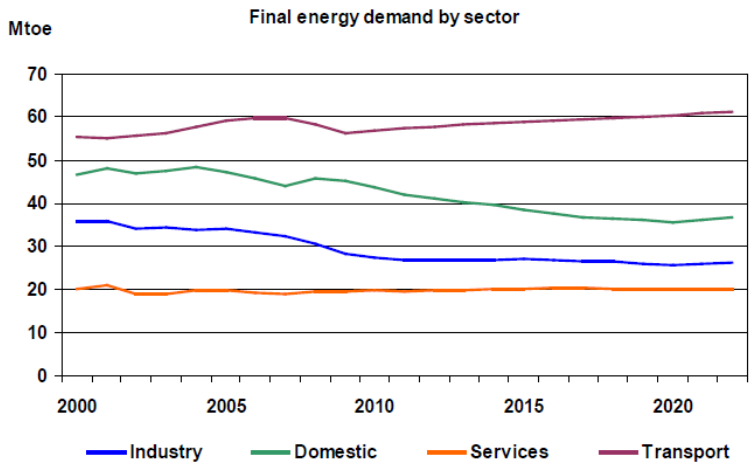

Figure 2.1.5 Final energy demand by sector in UK (DECC, 2009a)

2.1.2 World and UK fossil fuel price

The price of oil like any other commodity, is subject to the law of supply and demand. World oil prices forecast in three oil price cases are shown in Figure 2.1.6 (EIA, 2010). The Reference case projection is a business-as-usual trend estimate, given known technology and technological and demographic trends. The effects of different assumptions about future oil prices with different macroeconomic growth rates are illustrated in IEO2010 by two alternative cases for high and low oil price.

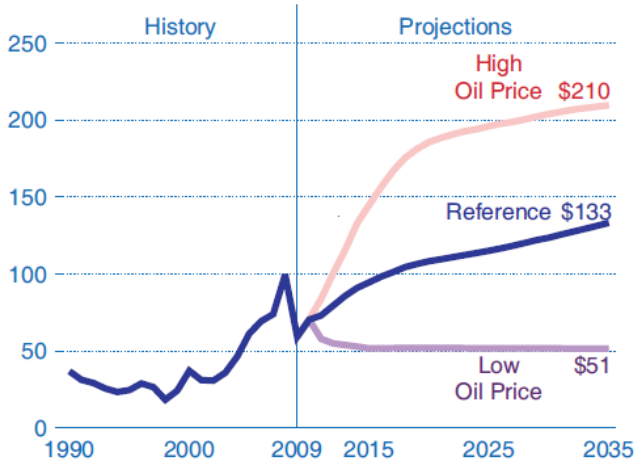

Figure 2.1.6 World oil prices in three Oil Price cases, 1990-2035 (2007 dollars per barrel) (EIA, 2010)

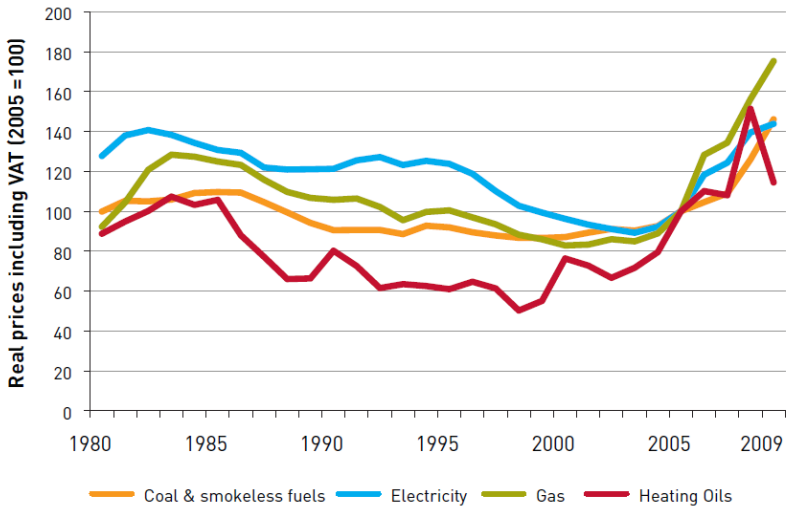

Figure 2.1.7 Fuel price indices for the domestic sector in UK, 1980 to 2009 (DCLG, 2010)

Fuel price in the UK depends on the world's fuel price, and has increased continuously. Figure 2.1.7 shows the fuel price indices for the domestic sector from 1980 to 2009 (DECC, 2010a).

2.1.3 Fuel poverty

An increase in the fuel price causes low-income households to be faced with difficulties in heating their homes. A household is said to be in fuel poverty if it needs to spend more than 10% of its income on energy (DECC, 2009b) in order to heat their home to a "satisfactory level", which is defined as 21˚C in the main living areas and 18˚C in other occupied rooms.

Fuel poverty can be driven by three key factors; energy costs, energy efficiency of the home and the income of the household (SCRI, 2010).

The number of households in fuel poverty in the UK has fallen from around 6.5 million in 1996 to around 2.1 million in 2004. This figure has increased continuously since 2004, so that there were around 3.3 million fuel poor households in England in 2008. This rise is attributable to the higher energy prices experienced in recent years (DECC, 2010b).

2.1.4 Security of supply

As UK (and European) demand for fossil fuel increases and output from the North Sea declines, the UK will rapidly switch from near energy self sufficiency to being a major energy importer in a relatively short space of time. The increased dependence on fossil fuel from relatively politically unstable regions will increase the risk of supply interruptions and fuel price volatility.

In addition the UK has a particular security-of-supply problem looming, known as the "energy gap" (Mackay, 2008). A substantial number of old coal power stations and nuclear power stations will be closed down during the next decade, so

there is a risk that electricity demand will sometimes exceed electricity supply, if adequate plans are not implemented.

2.1.5 Carbon dioxide emission and global warming

World energy use continues to be at the centre of the climate change debate because anthropogenic emissions of carbon dioxide result primarily from the combustion of fossil fuels. In the IEO2010 Reference case, world energy-related carbon dioxide emissions are set to grow from 29.7 billion metric tons in 2007 to 33.8 billion metric tons in 2020 and 42.4 billion metric tons in 2035 (Figure 2.1.8) (EIA, 2010).

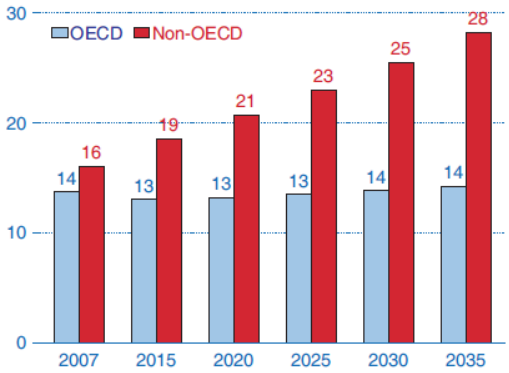

Figure 2.1.8 World energy-related carbon dioxide emissions, 2007-2035 (billion metric tons) (EIA, 2010)

The Kyoto Protocol is an international agreement linked to the United Nations Framework Convention on Climate Change. The major feature of the Kyoto Protocol is that it sets binding targets for 37 industrialized countries and the European Community for reducing greenhouse gas emissions.

Figure 2.1.9 shows the greenhouse gas and CO_2 emissions in the UK from 1990 to 2009. In 2008, UK emissions of the basket of six greenhouse gases covered by the Kyoto Protocol were estimated to be 628.3 million tonnes carbon dioxide equivalent (MtCO2e) (DECC, 2010a).

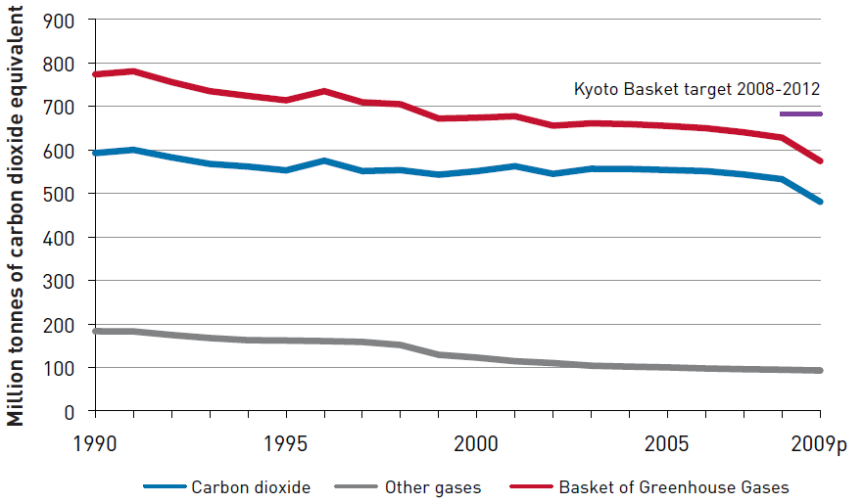

Figure 2.1.9 Greenhouse gas and carbon dioxide emissions, 1990 to 2009 (DECC, 2010a).

CO_2 is the main greenhouse gas, accounting for about 85 per cent of total UK greenhouse gas emissions in 2008, the latest year for which final results are available. In 2008, UK net emissions of CO_2 were estimated to be 532.8 million tonnes carbon (Mt).

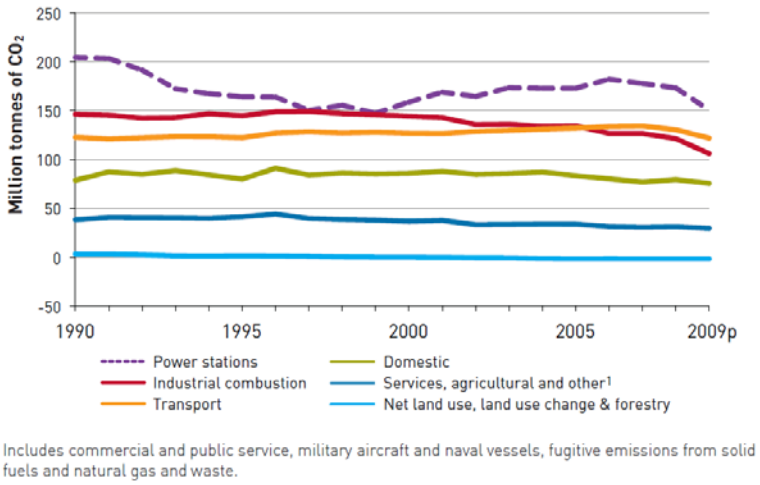

Figure 2.1.10 Emissions by sector, 1990 to 2009 (DECC, 2010a)

Figure 2.1.10 shows the CO_2 emissions by different sectors in the UK from 1990 to 2009. The residential and non-residential sectors account for 23% and 12% of the total UK greenhouse gas emissions respectively.

The UK Committee on Climate Change establishes a long-term framework to tackle climate change by introducing carbon budgets (CCC, 2011). A "carbon budget" is a cap on the total quantity of greenhouse gas emissions emitted in the UK over a specified time. Under a system of carbon budgets, every tonne of greenhouse gas emitted between now and 2050 will count. Where emissions rise in one sector, corresponding falls in another will be achieved. Each carbon budget covers a five-year period, with three budgets set at a time (DECC, 2011a). The first three carbon budgets will run from 2008-12, 2013-17 and 2018-22. The fourth carbon budget, covering the period 2023-2027, was set in law in June 2011 and requires emissions to be reduced by 50% below 1990 levels.

2.1.6 Resource depletion

Resource depletion is an economic term referring to the exhaustion of raw materials within a region. Resources are commonly divided between renewable resources and non-renewable resources. Use of either of these forms of resources beyond their rate of replacement is known as resource depletion.

Fossil fuels are non-renewable resources because they take millions of years to form, so reserves are being depleted much faster than new ones are being made.

2.1.7 Energy efficiency

Energy efficiency means using less energy to provide the same level of energy service. It is therefore one method of reducing fossil fuel consumption and greenhouse gas emissions.

There are a variety of energy efficiency measures available that can reduce the energy consumption in buildings, such as thermal insulation of the building envelope, double glazing, replacing low efficiency boilers and chillers with high efficiency ones and using high efficiency lighting and appliances.

2.1.8 Renewable energy

Renewable energy is energy which comes from natural resources such as sunlight, wind, rain, tides, and geothermal heat, and which are naturally replenished. Obtaining energy from renewable sources does not produce greenhouse gas, and since it replaces the energy obtained by the combustion of fossil fuels, thus using renewable energies reduces the greenhouse gas emission. Most of the renewable energies are dependent on atmospheric conditions, so they might not available on demand. Energy management and storage systems can play a key role in overcoming the intermittency of renewable sources.

In 2008, about 19% of the global final energy consumption of the world came from renewables, with 13% coming from traditional biomass, which is mainly used for heating, and 3.2% from hydroelectricity (REN21, 2010). Figure 2.1.11 shows the renewable energy share of global final energy consumption in 2008.

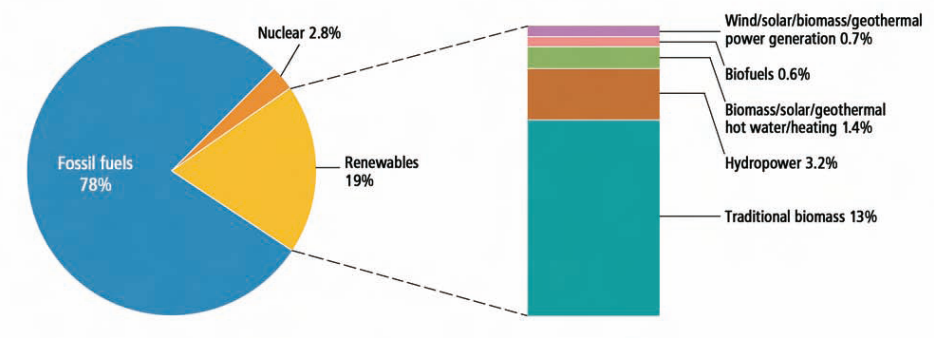

Figure 2.1.11 Renewable energy share of global final energy consumption, 2008 (REN21, 2010)

In the UK, the total use of renewables was 6,874.9 Thousand tonnes of oil equivalent in 2009 (DECC, 2010a). Figure 2.1.12 shows that biomass accounted for 80.7% of the renewable energy sources used in 2009, with most of the remainder coming from large-scale hydro and wind generation. Wind (with an 11.6% share) continues to account for more than large scale hydro (5.8%) in primary input terms. Of the 6.87 million tonnes of oil equivalent of primary energy use accounted for by renewables, 4.90 million tonnes was used to generate

electricity, 1.01 million tonnes was used for road transport, and 0.97 million tonnes was used to generate heat. Renewable energy use grew by 14.6% between 2008 and 2009, and is now more than two and a half times the level it was at in 2000.

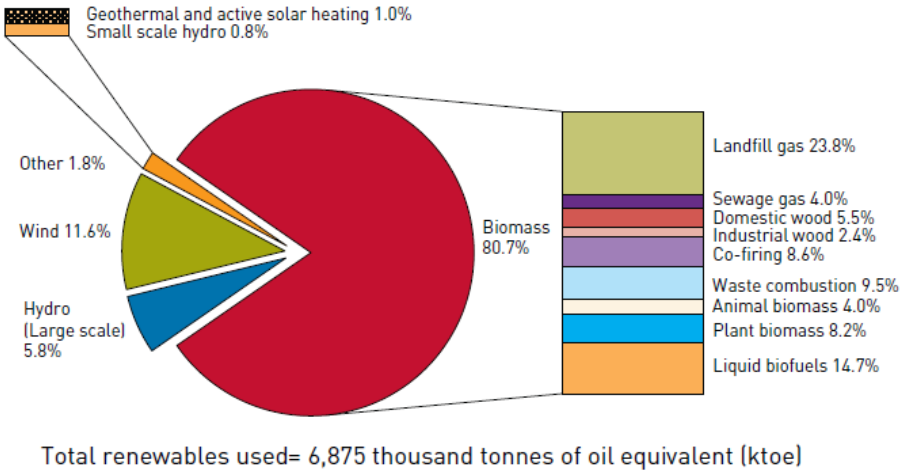

Figure 2.1.12 Renewable energy sources in UK, 2009 (DECC, 2010a)

In March 2007, the European Council agreed to a common strategy for energy security and tackling climate change. One element of this was establishing a target for 20% of the EU's energy to come from renewable sources. During 2008 a new renewable Energy Directive was negotiated on this basis and resulted in agreement of different country "shares" of this target. For the UK, by 2020, 15% of the final energy consumption – calculated on a net calorific basis, and with a cap on fuel used for air transport – should be accounted for by energy from renewable sources.

During 2009, 3.0% of the final energy consumption of the UK was from renewable sources. (DECC, 2010a). The UK's Renewable Energy Strategy (RES) (DECC, 2009c) was launched in July 2009. The strategy outlines how the UK aims to move towards generating 15% of its final energy consumption (including electricity, heat and transport) from renewable sources by 2020.

2.1.9 Incentives, regulations and policies in UK

2.1.9.1 Climate Change Act 2008

The Climate Change Act of 2008 is an Act of the Parliament of the United Kingdom (Crown, 2008a). It received Royal Assent on 26 November 2008. The Act places a duty on the Secretary of State to ensure that the net UK carbon account for all six Kyoto greenhouse gases for the year 2050 is at least 80% lower than the 1990 baseline. The Act aims to enable the United Kingdom to become a low-carbon economy and gives ministers powers to introduce the measures necessary to achieve a range of greenhouse gas reduction targets. An independent Committee on Climate Change (CCC) has been created under the Act to provide advice to UK Government on these targets and related policies.

2.1.9.2 Energy Act 2008

The Energy Act 2008 was given Royal Assent on 26 November 2008 (national archive, 2008) (Crown, 2008b). Along with the Planning Act 2008 and the Climate Change Act 2008, the Energy Act was developed to ensure UK legislation sustains national long-term energy and climate change strategy.

2.1.9.3 Feed-in tariff

Following the Energy Act 2008, the government has introduced a feed-in tariff from April 2010 covering the generation of electricity from renewable sources. This brings the UK into line with many European countries that already have a feed-in tariff. In Germany, Spain, France and Italy the introduction of a feed-in tariff for renewable electricity has resulted in a massive growth in the installation of solar PV, wind and other renewable energy systems both for domestic and commercial systems (Renewable Energy Tariff, 2011). The same effect is anticipated on the UK renewable energy market.

The scheme covers the following electricity-generating technologies, up to an installation size of 5 Mega Watts:

- Solar electricity (PV) (roof mounted or stand-alone)
- Wind turbine (building mounted or free standing)
- Hydroelectricity
- Anaerobic digestion
- Micro combined heat and power (micro CHP) (limited to a pilot at this stage)

The tariffs available and the process for receiving them vary, depending on the technology, scale of installation, when the technology was installed, and whether the system and the installer were certificated. The payment under feed-in tariff happens in 3 ways:

1. Generation tariff – a set rate paid by the energy supplier for each unit (or kWh) of electricity the customer generates. This rate will decrease each year for new entrants to the scheme (except for the first 2 years), but once the customer join he/she will continue on the same tariff for 20 years, or 25 years in the case of solar electricity (PV). Table A-1 in Appendix A shows tariff levels for the installations completed from 1st April 2010 to 31st March 2013 for the lifetime of the tariff.

2. Export tariff – the customer will receive a further 3p/kWh from the energy supplier for each unit he/she exports back to the electricity grid, that is when it is not used on site. The export rate is the same for all technologies.

3. Energy bill savings – the customer will be make savings on his/her electricity bills, because generating electricity to power his/her appliances means he/she does not have to buy as much electricity from the energy supplier. The amount the customer saves will vary dependent on how much of the electricity he/she uses on site.

All generation and export tariffs will be linked to the Retail Price Index (RPI) which ensures that each year they follow the rate of inflation.

2.1.9.4 Renewable heat incentive

Heat production is responsible for around half (49%) of the final energy consumption demand in the UK and roughly half of all the UK's carbon emissions.

Heat generated from renewable energy sources currently meets 1 percent of the UK's total heat demand. To reach the 2020 renewable energy target, around 12 percent of the UK's heat needs to be generated from renewable sources. This will require all parts of society including government to play their role.

The Renewable Heat Incentive (RHI) (DECC, 2011b) is a new payment being introduced in the UK for generating heat from renewable sources. The Renewable Heat Incentive starts in June 2011. However, any suitable system installed from July 15, 2009 will be eligible for the tariffs when they begin.

At the start of the RHI scheme, only non-domestic sectors will be supported. The non-domestic segment includes schools, hospitals, businesses, public sector, charities and not-for-profit organisations, and industry.

The second phase of support is intended to be introduced from 2012, which will establish support for the domestic sector as well as a number of other technologies and fuel uses that are unable to be supported from the outset.

The renewable heat technologies that are eligible under the RHI are:

- Biomass boilers (Including CHP biomass boilers)
- Solar Thermal
- Ground Source Heat Pumps
- Water Source Heat Pumps
- On-Site Biogas combustion
- Deep Geothermal
- Energy from Municipal Solid Waste
- Injection of biomethane into the grid

The renewable heat tariff levels which depend on the renewable heat type and its scale are shown in Table A-2, Appendix A. The tariff life time is between 10 and 23 years depending on which type of renewable heat system is used. The payback time is about five to nine years. According to the Government, which set

the tariff levels, users will earn a return of 12% per annum. This will be tax free for individuals. The equivalent for feed-in tariffs is 5%-8%.

2.1.9.5 Building regulations Part L (2006, 2010)

Part L is the section of the building regulations which deals with the conservation of fuel and energy. In general, Part L states that a building should be designed and constructed so as to ensure that the energy performance of that building limits the CO_2 emissions from the operation of the building by limiting the energy consumption associated to the emission. For compliance it should be proved that the CO_2 emission rate of the complete building does not exceed the target emission rate set by the reference notional building.

Part L does not refer to renewable energy sources anywhere, however to meet the carbon target the most effective method of reducing carbon emissions is on-site renewable electricity generation (photovoltaics, wind turbines, combined heat and power (CHP) or micro-CHP) and renewable heat (solar heat, heat pump, biomass boiler).

2.1.9.6 Code for sustainable homes

The Code for Sustainable Homes is a rating system for the environmental impacts of housing in England & Wales. The Code was officially launched on December 13, 2006, and was introduced as a voluntary standard in England in 2007. The Code is a complement to the Energy Performance Certificates system for new homes introduced in 2008 under the European Energy Performance of Buildings Directive, and is a base for the most recent changes to the Building Regulations in England and Wales.

The Code is a 6 level rating system and considers the performance of 9 sustainability criteria which are combined to assess the overall environmental impact. One of the sustainability criteria is the building energy consumption and resulting emissions of carbon dioxide to the atmosphere.

For energy and emission compliance the code levels require a Dwelling Emission Rate (DER) to be a certain percentage better than the Target Emission Rate (TER) as set in Part L of the Building Regulations. Table 2.1.1 shows these percentages which are better than Part L (2006) for different code levels.

Table 2.1.1 Minimum standard and number of points for each code level (DCLG, 2006b)

Achieving a sustainability rating

	Minimum Standards				
	Energy		Water		
Code Level	Standard (Percentage better than Part L[1] 2006)	Points Awarded	Standard (litres per person per day)	Points Awarded	Other Points[4] Required
1(★)	10	1.2	120	1.5	33.3
2(★★)	18	3.5	120	1.5	43.0
3(★★★)	25	5.8	105	4.5	46.7
4(★★★★)	44	9.4	105	4.5	54.1
5(★★★★★)	100[2]	16.4	80	7.5	60.1
6(★★★★★★)	A zero carbon home[3]	17.6	80	7.5	64.9

Notes
1. Building Regulations: Approved Document L (2006) – 'Conservation of Fuel and Power.'
2. Zero emissions in relation to Building Regulations issues (i.e. zero emissions from heating, hot water, ventilation and lighting).
3. A completely zero carbon home (i.e. zero net emissions of carbon dioxide (CO_2) from **all** energy use in the home).
4. All points in this document are rounded to one decimal place.

2.1.9.7 Building a Greener Future: Policy Statement (2007)

It was proposed that the energy/carbon performance set in the Building Regulations is improved continuously in three steps. Table 2.1.2 summarises the three steps of carbon improvement over time, compared to the 2006 Part L Building Regulations.

Table 2.1.2 Proposed carbon improvements over time (DCLG, 2006a)

Date	2010	2013	2016
Carbon improvement as compared to Part L (BRs 2006)	25%	44%	zero carbon
Equivalent energy/carbon standard in the Code	Code level 3	Code level 4	Code level 6

2.2 Integration of renewable energies in buildings

The application of renewable energies for supplying energy demand for residential and service buildings has two main technical barriers. The first barrier is that renewable energies are mostly not available on demand time. For example PV panels generate electricity during the day-time, while the main electrical demand of a residential building is in the early morning and night-time. The second barrier is that the renewable energy sources are mostly intermittent and depend on the atmospheric conditions. To overcome these barriers, extra renewable energy should be stored and used when the generated renewable energy is not sufficient.

Integration of different renewable sources is another way to overcome the intermittent nature of an individual source. For example PV panels and wind turbine can be integrated to have at least one source of energy when there is enough solar radiation or wind.

It should be noted that the intensity of solar and wind energy is low. In some applications, especially in commercial and high-rise residential buildings the limitation of the available space for the renewable energy system installations and also the installations cost can be a barrier to having a fully stand-alone energy system. In these applications the available dimension of the renewable energy source (like PV panels) can be integrated with a conventional energy system, to supply only part of the energy demand. In this case, the conventional energy system can also be a backup for the renewable energy source.

The integration of renewable energies in buildings and energy storage have been studied in different aspects in much of the literature. These literature studies

include the integration of thermal systems, the integration of electrical systems (hybrid power systems), and the integration of thermal and electrical systems and the role of energy storage in these three categories. In these literature studies the main objectives are the sizing and simulation of the systems, but they also highlight the importance of integrating the renewable and low carbon energy technologies as well as energy storage.

Different types of energy storage devices can be used in the energy systems. Dell, et al. (2001) evaluated the prospects of the candidate storage technologies including pumped-hydro, flywheels, hydrogen (for use in fuel cells) and batteries for application in centralized and distributed electricity supplies, and hybrid electric vehicles. They concluded that there is a very real need for storing generated electricity from most renewable forms of energy. Realistic options for this are pumped-hydro, kinetic energy in flywheels, or chemical energy in batteries. Where the terrain is suitable, pumped-hydro is the way to store large quantities of electricity. By contrast, flywheels and batteries are able to store only comparatively small amounts of electrical energy and are therefore better suited to locally generated or distributed electricity. Flywheels, in particular, have only a small energy-storage capacity but may be charged and discharged at very high rates. They are, in effect, surge-power devices and, as such, are complementary to batteries. Batteries are the best option available for storing small–medium quantities of electricity.

Sontag and Lange (2003) studied the cost effectiveness of a decentralized and integrated energy supply system for the power and heat supply of a residential complex. The system consisted of a power-controlled combined heat and power (CHP) plant, a PV array for power generation as well as a field of solar thermal collectors with a short-term accumulator for water heating and a long-term accumulator for supplying heat for domestic heating purposes. Figure 2.2.1 shows the energy supply system. Simulation results demonstrated the synergetic effects that result from the combination of a CHP plant with wind power and PV plants of varying sizes, which have an effect on the cost effectiveness of the plant as a whole. Different dynamics of energy sources (wind and solar energies) and of the consumption of power and heat were the decisive factors. The power deficits of

wind turbine and PV panels were compensated through the application of a natural gas-operated CHP plant. In almost all variants, the demand for fossil energy carriers was distinctly less than in conventional energy supply plants.

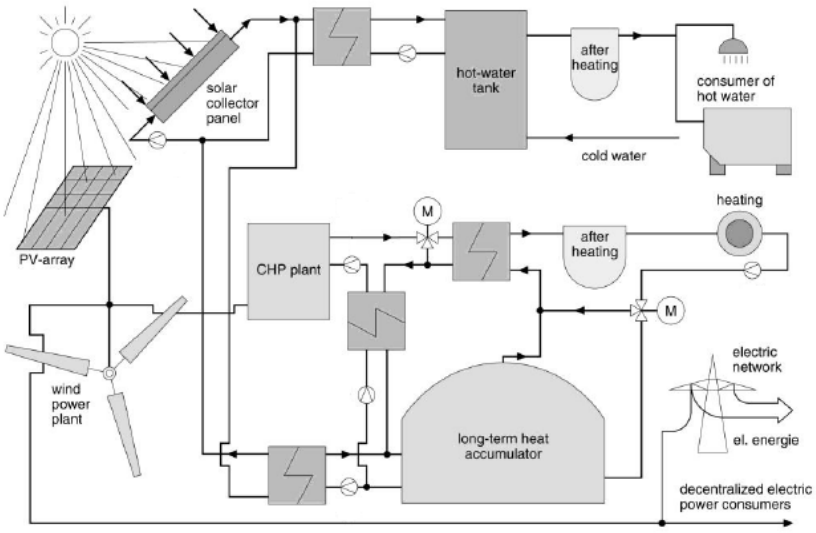

Figure 2.2.1 Decentralized CHP plant system for power and heat supply with different renewable energy generating Components (Sontag and Lange, 2003)

Doherty, et al. (2004) studied the performance of a ground source heat pump that has been installed at the Eco-House, University of Nottingham. The Eco-House is a four bedroom detached dwelling constructed of brick, block, glass and steel. It is connected to the electricity grid and has an 18kW condensing gas boiler. In addition to a 8 kW reversible ground source heat pump installed into the house after construction, several other low energy systems have been installed (Figure 2.2.2). These include integrated PV roof slates (1.5 kWp) on the south side and two tracking PV arrays (1 kWp each) to generate electricity. Two wind turbines are also used to generate additional electrical power. Evacuated solar tube collectors (3 kWth) are used to provide part of the building's requirement for hot water. Each technology makes a contribution to reducing the conventional energy consumption of the house. The heat pump was installed to provide space heating and cooling to the house, with back-up heating supplied by an installed natural gas-fired condensing boiler. The results showed that the design coefficient of performance (COP) of the heat pump can be achieved through proper installation and careful consideration of the operation of the system as a whole.

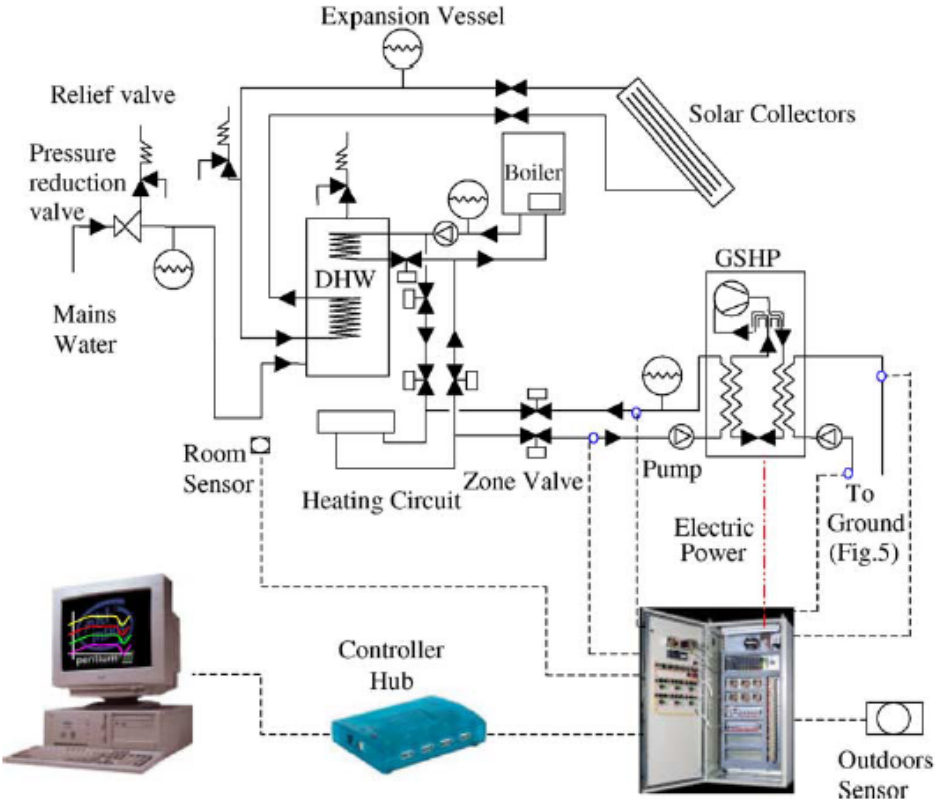

Figure 2.2.2 Schematic representation of the Ground Source Heat Pump installed in the Eco-House (Doherty, et al., 2004)

Trigeneration, also called CCHP (combined cooling, heat and power), is a low carbon technology that simultaneously generates electricity, useful heating and useful cooling from the same original heat source such as fuel or solar energy (Figure 2.2.3). Kavvadias and Maroulis (2010) developed a multi-objective optimization method (see references within this paper) for the design of trigeneration plants. The optimization was carried out on technical, economical, energetic and environmental performance indicators. Both construction (equipment sizes) and discrete operational (pricing tariff schemes and operational strategy) variables were optimized, based on realistic conditions. The problem was solved using a multi-objective evolutionary algorithm. An example of a trigeneration system in a 300 bed hospital was studied in order to demonstrate the design procedure, the economic and energy performance of the plant, as well as the effectiveness of the proposed approach even under fluctuating energy prices. The

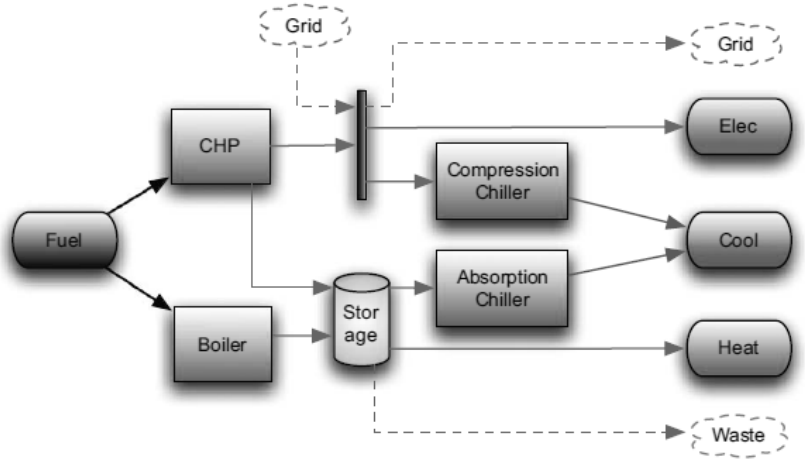

Figure 2.2.3 Energy flow diagram for a trigeneration system (Kavvadias and Maroulis, 2010)

results showed that the trigeneration plants can be more economically attractive, energy efficient and environmental friendly than conventional cogeneration plants. The higher investment needed to approach the energetic optimum costs for buying a bigger prime mover cannot be left to entrepreneurs. Instead some financial incentives should be provided, in order to make the solution which provides the largest energy saving and emission reduction, economically attractive even under fluctuating energy prices. Incentives can be either given in the form of capital or fuel subsidy in order to keep a fixed spark spread price and reduce the uncertainty of energy prices. The latter would promote a more decentralized supply model, which could lower the delivered costs of electricity and reduce the demand of primary fuel while helping to reduce environmental impact.

Table 2.2.1 Summary of the renewable and low carbon heating/cooling systems

Heating system	Cooling system	Electrical system	Reference
Solar collector, CHP and after heating (boiler)	-	PV array, wind turbine, CHP and grid	Sontag and Lange (2003)
Solar collector, heat pump and boiler	-	-	Doherty, et al. (2004)
CHP and boiler	Compression and absorption chillers	CHP and grid	Kavvadias and Maroulis (2010)

Table 2.2.1 shows a summary of the renewable and low carbon heating/cooling systems in the above research studies.

As an application of the hybrid power system Nelson, et al. (2006) performed an economic evaluation of a hybrid wind/PV/fuel cell (FC) generation system for a typical home in the US Pacific Northwest (Figure 2.2.4). In this configuration the combination of an FC stack, an electrolyser, and hydrogen storage tanks was used as the energy storage system. This system was compared to a traditional hybrid energy system with battery storage. The cost of electricity, an overall system cost, and a break-even distance analysis was also calculated for each configuration. This analysis determines how far the site of the stand-alone alternative energy system should be from the existing utility line so that the system is cost effective (breaks even) when compared to using conventional grid power. Cost figures at the date of the research as well as the break-even line distance comparison showed a clear economic advantage for the traditional wind/PV/battery system over the wind/PV/FC/electrolyser system.

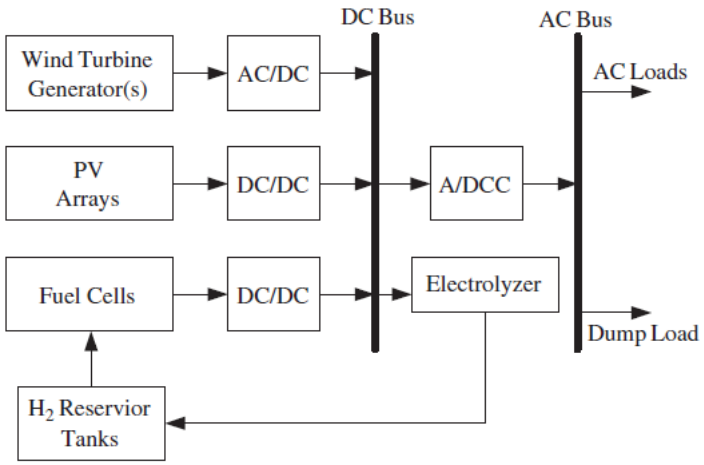

Figure 2.2.4 Proposed wind/PV system with FC/electrolyser storage (Nelson, 2006)

Belfkira, et al. (2011) presented a methodology of sizing optimization for a stand-alone hybrid wind/PV/diesel energy system (Figure 2.2.5). Their approach

used a deterministic algorithm to suggest, among a list of commercially available system devices, the optimal number and type of units ensuring that the total cost of the system was minimized while guaranteeing the availability of the energy. A deterministic algorithm (Jones, et al., 1993) was used to minimize the total cost of the system while guaranteeing the satisfaction of the load demand. Obtained results showed the great impact of the site energetic potential (wind and solar radiation) as well as the load profile on the optimal hybrid system constitution (numbers of wind turbines, of PV panels and of batteries) and the related cost of the hybrid system. Also, conclusions showed that a stand-alone hybrid wind/PV/diesel system with a battery bank seems to be a motivating techno-economic solution to meet the energy demand of remote consumers, where the number of operating hours of the diesel generator has to be reduced.

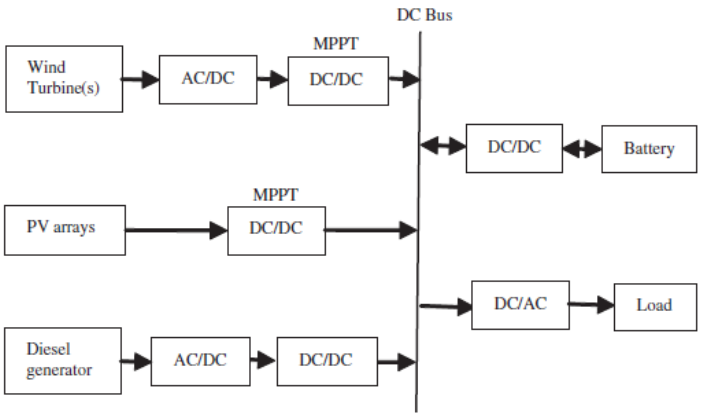

Figure 2.2.5 Block diagram of a hybrid wind/PV/diesel system (Belfkira, et al., 2011)

A stand-alone renewable-energy system employing a hydrogen-based energy store was commissioned within the HaRI project at West Beacon Farm, Leicestershire, UK. Little, et al. (2007) reported on the electrical integration of the renewable energies in this project. Figure 2.2.6 shows that the interconnection of the various generators, loads and storage system is made through a central DC busbar.

The rotating generators, such as the wind turbines, have been connected through standard industrial drives operating in regenerative mode, while the DC devices-

electrolyzer, fuel cell and solar photovoltaic array employ custom DC-DC converters. The main objective of the system control is to maintain the DC voltage on the busbar within the operational limits of the power-electronic converters, under all possible conditions. The energy flow in and out of the hydrogen tanks is determined by controlling the electrolyzer and fuel cell. Likewise, the thermal mass of the buildings provides some flexibility in the operation of the heat pump. The CHP unit has been used to provide additional heat for supplying a genuine heat demand in winter.

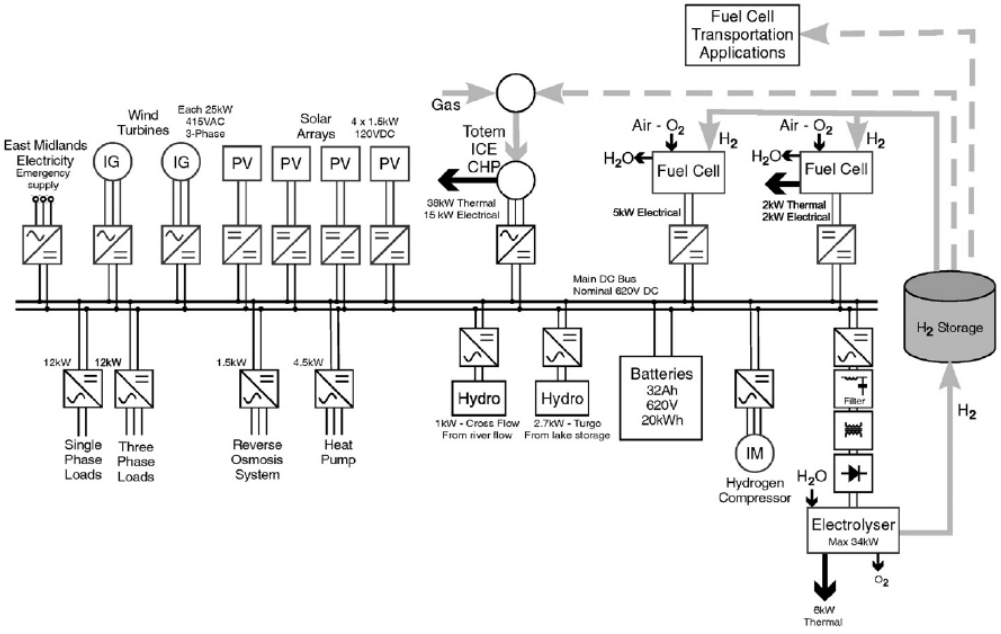

Figure 2.2.6 The West Beacon Farm stand-alone power supply (Little, et al., 2007)

The specifications of the renewable electrical systems in the above research studies are shown in Table 2.2.2.

Study of the current research in building integrated renewable and low carbon energy systems shows that there are numerous applications with different combination of these technologies. These applications can be divided into heating/cooling systems, heating/cooling/electrical systems and electrical systems with storage.

Table 2.2.2 Summary of the renewable electrical systems

Electrical generator	Storage device	Reference
Wind turbine, PV array and Fuel cell	Hydrogen tank (with electrolyzer)	Nelson, (2006)
Wind turbine, PV array and diesel generator	Battery	Belfkira, et al. (2011)
Wind turbine, PV array, hydro turbine, CHP, fuel cell and grid	Battery and hydrogen tank (with electrolyzer and compressor)	Little, et al. (2007)

2.3 Management and control of renewable energy systems in buildings

The intermittency of the available power from renewable sources has a great impact on the related energy system performance. Integration of renewable energy systems and energy storage in these systems has a major role in maximizing the utilization of renewable energies. By integrating different renewable energy sources, energy storage devices, non-renewable systems and grids, a sophisticated supervisory control system is needed for the management of the building energy plant.

There are a number of controllers available in the literature; including heuristic or operational strategy based controllers, Fuzzy Logic based controllers, Artificial Neural Network based controllers, mathematical optimization based controllers, and finally hybrid controllers. These studies show the importance of optimal and reliable supervisory control for the building integrated renewable and low carbon energy systems. In this section a comprehensive study of these controllers is presented.

2.3.1 Fixed control algorithm

The fixed control strategies of hybrid power systems are the operational routines that do not change during different environmental, technical and economical conditions. These methods mainly were used as operational strategy for optimization of the hybrid power system component sizes. Some parameters of the operational strategies could be optimized through the optimization procedure (Dufo-Lo´pez , et al., 2007).

Barley and Winn (1996) set a guideline about the optimal dispatch strategy in a hybrid power system consisting of wind/PV generator(s), diesel generator and battery. These control strategies were frugal discharge, load-following, state of charge (SOC, see Section 4.2.1 for definition) set point and the full power strategy. Frugal discharge is based on critical load, where if the net load is higher than the critical load it is economical to run the diesel generator. In load-following strategy, batteries are not charged by the diesel generator. The diesel operating point is set to match the net load. SOC set point strategy is used to charge batteries to the user defined point, at which the diesel generator should be started. The generator operates at full-power and the excess power is used to charge the batteries without dumping power. In the full power strategy the generator operates at full power for a minimum time period.

The results showed that it is not cost-effective to fully charge batteries with diesel power. Instead, one of the load-following or full power charging strategies should be used. The right choice between these strategies depends on the fuel cost, the battery replacement cost per kWh of its cycle life, the round-trip storage efficiency, the diesel generator size, the diesel fuel curve slope and intercept, and the wind turbine array sizing. Frugal discharge strategy should be used in conjunction with either of the load-following and full power charging strategies.

Ulleberg (2004) presented a control strategy for a PV and battery system with a hydrogen subsystem consisting of an electrolyzer, pressurized hydrogen gas storage, and fuel cell. The battery was used for short term energy storage and

hydrogen storage was used for the long term. The control strategy was based on the battery's state of charge (SOC). When the demand is more than the supply and SOC is going down from its maximum point, first the electrolyzer turns off and then by further reduction of SOC the fuel cell turns on. When the supply is more than demand and SOC is going up from its minimum point, first the fuel cell turns off and by further increase of SOC the electrolyzer turns on. This study demonstrated that the performance of a PV/hydrogen system can be significantly affected by relatively small changes made to the control strategy.

Dufo-Lo´pez , et al. (2007) presented a control strategy, optimized by genetic algorithms, to control stand-alone hybrid renewable electrical systems with hydrogen storage. The strategy optimizes the control of the hybrid system by minimizing the total cost throughout its lifetime. The optimized hybrid system can be composed of renewable sources (wind, PV and hydro), batteries, fuel cell, AC generator and electrolyzer. If the renewable sources produce more energy than the one required by the loads, the spare energy can be used either to charge the batteries or to produce H_2 in the electrolyzer. The control strategy optimizes how the spare energy is used. If the amount of energy demanded by the loads is higher than the one produced by the renewable sources, the control strategy determines the most economical way to meet the energy deficit. The optimization of the various system control parameters was done using genetic algorithms.

The literature review of the fixed control algorithms shows that this control method is a simple control strategy that can be used without the need for complex hardware and software. The control set points can be determined by heuristic methods or they can be obtained during an optimization process. Without this optimization the controller cannot consider the economical parameters like battery wear cost. This method can be used easily in sizing problems. In these problems the time period is normally one year, and includes a large number of time steps, for example 8760 hours. Due to the lack of control variables, or low numbers of static variables, the fixed control algorithm does not cause a huge computational barrier in solving the related sizing optimization problem.

2.3.2 Fuzzy logic control

Fuzzy logic control (FLC) provides a means of converting a linguistic control strategy based on expert knowledge into an automatic control strategy. FLC is derived from fuzzy set theory and fuzzy logic introduced by Zadeh (1965) and (1973) respectively. In fuzzy set theory (Zadeh, 1965), the transition between membership and nonmembership can be gradual. Therefore, boundaries of fuzzy sets can be vague and ambiguous, making it useful for approximate systems. In any fuzzy logic system, the system takes a value and first passes it through a fuzzification process. Then it is processed by an inference engine (or fuzzy rule set). Finally, it goes through a defuzzification process. FLC's are an attractive choice when precise mathematical formulations are not possible. Other advantages of FLC are: 1) it can work with less precise inputs; 2) it doesn't need fast processors; 3) it needs less data storage in the form of membership functions and rules than conventional look up tables for nonlinear controllers; and 4) it is more robust than other nonlinear controllers.

Jeong, et al. (2005) used FLC for the energy management of a hybrid system consisting of a fuel cell and a battery pack. In this system the battery was used to meet the peak power demand; hence, the size of the fuel cell stack can be minimum. A fuzzy logic algorithm was used to determine the fuel cell output power depending on the external power requirement and the battery state of charge (SOC). If the power requirement of the hybrid system is low and the SOC is low, then the greater part of the fuel cell power is used to charge the battery pack. If the power requirement is relatively high and the SOC is also high, then the fuel cell and the battery are concurrently used to supply the required power. These if-then operation rules were implemented by fuzzy logic for the energy management of the hybrid system. Non-linear models for the fuel cell and battery were used. The results showed that the fuzzy logic controller can be used for this non-linear system and with an acceptable load following capacity, the operation efficiency of the hybrid system is improved and the battery state of charge is maintained at a reasonable level, which increases the battery life time.

Boukettaya, et al. (2007) presented the design of a fuzzy logic supervisor for controlling the power flows in a hybrid power system, comprising a photovoltaic panel, a diesel generator and a flywheel storage system that supplies power to a load. The control of the power exchanged between the flywheel energy storage system and the load is achieved with the help of a fuzzy logic based supervisor, with the aim of minimizing the variations of the power generated by the diesel generator and supplying the load as much as possible. The performance of the fuzzy logic controller was confirmed by DC bus voltage. This voltage was kept near to the reference value during the test.

Ben Salah, et al. (2008), Lautier, et al. (2007) and Chaabene, et al. (2007) presented a fuzzy algorithm (an algorithm based on fuzzy logic) for the energy management of a domestic PV panel which makes decision about connecting domestic apparatus on either the electrical grid or a PV panel. The decision is made in real time with respect to multi-energy saving criteria and to the photovoltaic panel maximum available power and apparatus states. The PV panel was considered as a complementary electric source to supply energy to domestic apparatus and to reduce the grid electricity consumption, so there was no need for batteries.

Lautier, et al. (2007) developed a fuzzy logic controller for reducing the operational cost and the environmental impact of diesel power system for an off-grid community. The system uses battery storage in order to supply the grid as a stand-alone power supply during low demand and to operate as a peak shaving and diesel generator load regulation unit during medium and high demand.

Ben Salah and Ouali (2010) presented a control strategy for active energy flow in a hybrid PV system. The method introduced online energy management by a hierarchical fuzzy controller operating between energy sources that consist of PV panels, the battery and the load. The fuzzy logic controller was developed for power splitting between the PV panels and the battery, and it makes decision to choose the switching chain rules and corresponding control action. Simulation test results illustrated improvement in the operation's efficiency of the online state of the switches, and the battery's SOC was maintained at a reasonable level.

Summary of the above research in which the FLC method has been used, are shown in Table 2.3.1.

The review of this research shows that it has been used with nonlinear energy system models or with energy systems that do not have a precise mathematical model. Fuzzy system is an approximate function. The quality of the fuzzy approximation is highly dependent on the experience of the user that sets the rules (Jain and Martin, 1999). Derivation of these rules in a long time horizon, which should be considered in the storage of renewable energies, can be very difficult or impossible. So in the literature FLC is used in relatively simple energy systems which have less flexibility.

Table 2.3.1 Summary of the literature of FLC method

Energy system	Controller characteristic	Reference
Fuel call and battery	Control of Fuel cell to charge battery	Jeong, et al. (2005)
PV, diesel and flywheel storage	Control of exchanged power between flywheel and load	Boukettaya, et al. (2007)
PV	Control of domestic apparatus to connect either PV or grid	Ben Salah, et al. (2008)
Diesel and battery	Control of stored electricity in battery in order to reduce operational cost	Lautier, et al. (2007)
PV and battery	Control of power flow between PV and battery	Ben Salah and Ouali (2010)

2.3.3 Artificial Neural Network (ANN)

An artificial neural network (ANN), usually called neural network is a mathematical model or computational model that is mainly planned to imitate the behaviour of a biological network of neurons. It is developed and meant to overcome the unfavourable circumstances lying in serial computation with the parallel processors computing.

A neural network usually involves a large number of processors operating in parallel, each with its own small sphere of knowledge and access to data in its local memory. Typically, a neural network is initially "trained" or fed large amounts of data and rules about data relationships. A program can then tell the network how to behave in response to an external stimulus or can initiate activity on its own.

In making determinations, neural networks use several principles, including gradient-based training, fuzzy logic, genetic algorithms, and Bayesian methods. Neural networks are sometimes described in terms of knowledge layers, with, in general, more complex networks having deeper layers. In feed forward systems, learned relationships about data can "feed forward" to higher layers of knowledge. Neural networks can also learn temporal concepts and have been widely used in signal processing and time series analysis.

Al-Alawi, et al. (2007) presented a predictive ANN-based prototype controller for the optimum operation of integrated hybrid renewable energy-based water and power supply system consisting of PV panels, a diesel generator, a battery bank for energy storage and a reverse osmosis desalination unit. The electrical load consisted of typical households and the desalination plant. The proposed ANN controller was designed to take decisions on diesel generators on/off status and maintain a minimum loading level on the generator to reduce fuel dependency, engine wear and tear due to incomplete combustion and to cut down on greenhouse gas emissions. Back propagation architecture was used for the neural networks. The statistical analysis of the results indicated that the proposed ANN-based model can predict the power usage and generator status at any point of time with high accuracy.

Jifang, et al. (2010) reported a neural networks control strategy for a grid connected hybrid power system consisting of a wind generator, solar panels and an energy storage device. In order to accelerate the convergence and to prevent oscillation, the Levenberg-Marquardt algorithm (Levenberg, 1944; Marquardt, 1963) was used in the training of neural networks. Simulation showed that the strategy can make the voltage sustained, stable and continuous in the maximum use of renewable energy.

There are few research studies concerning the application of the ANN controller in the control and management of renewable energy systems in buildings. Like FLC, ANN controllers do not use mathematical models of the system. The self-learning and generalization nature of neural networks enable it to be more effectively used in nonlinear and time variant problems. The problem with the ANN controller is the difficulty of determining the proper size and structure of neural networks (Jain and Martin, 1999). Also, neural networks do not scale well. To control a renewable energy system, the manipulation of learning parameters for learning and convergence becomes increasingly difficult.

2.3.4 Multi-period optimization

Multi-period optimization links more than one time period of the operation of a single model. This helps in using the trade-offs of resource allocation over time, such as energy storage, and also in the capture multi time step operation strategies like ramping and start and stop time delays of the units. Optimization models can be solved analytically, with mathematical programming, dynamic programming, or heuristic (global) search techniques such as evolutionary algorithms or combinations of the above. In the following sections, mathematical programming and dynamic programming models are explained.

2.3.4.1 Mathematical programming

Mathematical programming concerns finding the minimum or maximum of a function of one or multiple variables by mathematical methods. The function is called the objective function. The variables can be continuous or integer or a mixture of both. Mathematical programming can be unconstrained or it can be subjected to some constraints. In addition the objective function and the constraints can be linear or nonlinear.

A general mixed-integer optimization model for the multi-period operational optimization problem was given by Iyer and Grossmann (1998):

$$\min \sum_{t=1}^{P} f_t(x_t, \delta_t) \qquad \text{(2-1a)}$$

$$\text{sub. to } h_t(x_t, \delta_t, \theta_t) \le 0, \quad t = 1,..., p \qquad \text{(2-1b)}$$

$$r(x_1, \delta_1, \theta_1, ..., x_p, \delta_p, \theta_p) \le 0 \qquad \text{(2-1c)}$$

$$x_t \in R^q \times R^p, \ \delta \in \{0,1\}^{n \times p}$$

Here x_t is the state and control variables for period t, δ_t is the binary variables that determine the on/off status of units for period t, and θ_t is the parameters (e.g. demands) for period t.

In the above formulation, the objective function includes the operating costs f_t for each period $t = 1,..., p$. Equation (2-1b) represents the state equations for each period of operation and Equation (2-1c) are linking constraints that represent constraints that involve variables for all periods of operation.

In the process industry multi-period mixed integer programming has been used for production planning (Sahinidis and Grossmann, 1991; Zhang and Rong, 2008; Varvarezos, et al., 1995), heat exchanger networks (Floudas and Grossmann, 1986; Floudas and Grossmann, 1987) and the operational optimization of utility systems (Iyer and Grossmann, 1998; Marechal and Kalitventzeff, 2003; Zhang and Hua, 2007).

In the electrical power industry multi-period programming has been used for generation scheduling or unit commitment and dynamic economic dispatch (Xia and Elaiw, 2010; Tao Li and Shahidehpour, 2005; Carrion and Arroyo, 2006, Logenthiran and Srinivasan, 2009; Catalao, et al., 2010). The unit commitment problem determines the combination of available generating units, and the scheduling of their respective outputs to satisfy the forecasted demand with the minimum total production cost under the operating constraints enforced by the system for a specified period that usually varies from 24 hours to one week.

Multi-period programming has been used for the control of hybrid power and CHP systems. In some research it has been called optimal control or model predictive control.

Korpas and Holen (2006) used mathematical optimization for deriving a methodology for the operation planning of a hybrid plant with wind power and hydrogen storage. Hydrogen produced from electrolysis was used for power generation in a stationary fuel cell, and as fuel for vehicles. The methodology was used for plants operating in a power market, but it was demonstrated that the operating principles could also be applied for isolated H_2- based energy systems with a backup generator. The generation scheduling problem for the hybrid plant was formulated as a profit-maximizing function, taking into account the electricity price variations and costs with imported H_2, or without imported H_2. During online operation, the hourly values of the electrolyzer power and the fuel cell power were determined by applying a receding horizon strategy, based on updated generation forecasts and costs for balancing power. It was shown that the fuel cell was used only in cases with large electricity price variations and high balancing costs, since the overall efficiency of the H_2 chain is relatively low. In this literature the optimization problem was solved by linear programming, but the binary variables concerning on/off statuses of the equipment were not included in the optimization problem. The on/off statuses were determined by trail and error.

Geidl and Andersson (2007a) presented a framework for the integrated modelling and optimization of energy systems with multiple energy carriers. Based on the concept of energy hubs, a generic steady state model for describing conversion and storage of multiple energy carriers, such as electricity, natural gas, hydrogen, or district heating, was developed and used for system optimization. In this literature, for the splitting of an energy carrier flow between multiple energy converters a dispatch factor was used, which led to a nonlinear optimization problem. The solution of a nonlinear problem is uncertain, since it is non-convex, and thus may have local optima (Sweeney, et al., 2009). In addition, the solution of a nonlinear problem, specially when integer variables are involved, is difficult. Although the start/stop of the converter and the charging/discharging of the storage

device were modelled by using integer variables, scheduling of complex operations, like sequential start up of the converters (for example cogeneration unit and auxiliary boiler) has not been considered in this literature.

Zervas, et al. (2008) used mathematical programming for the optimal control of a grid connected hybrid power system consisting of a PV array, electrolyzer, hydrogen storage tank and fuel cell. The system was used to cover the energy needs of a typical household located in Athens, Greece. The system could buy electricity from the grid or sell it to the grid. An on-line optimization problem was formulated and solved and was used as a decision making tool regarding the operation of the system. The formulation took into account updated estimations of the PV power generation over a future prediction horizon and a profile of the energy demand over the same time horizon. In this literature, the benefits of using the rolling horizon concept for improving the decision strategy were shown. The system did not include a battery for the storage of electricity. The battery with respect to the hydrogen storage has a higher round trip efficiency and is suitable for short term storage. In this dissertation, both battery storage and hydrogen storage are considered.

Houwing, et al. (2008) showed possible cost advantages of applying mathematical programming to a residential micro-combined heat and power system. The mathematical programming was considered as Model Predictive Control (MPC). Simulation results illustrated that MPC gives better outcomes in terms of daily energy costs when a larger prediction horizon is adopted by the controller. The results also showed that MPC control of distributed energy resources can lead to cost savings, but that these savings were strongly dependent on the controlled physical systems and their surroundings in terms of (regulated) energy tariffs. So it was recommended that the MPC controllers should be designed in such a way that they would be flexible and can be adjusted to evolving systems and system environments. The Stirling engine used in this study can only operate in part load and full load modes. In new micro-CHP products, fully modulating Stirling engines are used for increasing of performance, that are considered in this dissertation.

Collazos, et al. (2009) developed a predictive optimal control system for micro-CHP in domestic applications. The system aimed at integrating stochastic inhabitant behaviour and meteorological conditions as well as modelling imprecision, while defining operation strategies that maximize the efficiency of the system, taking into account the performances, the storage capacities and the electricity market opportunities. Numerical data of an average single family house was taken as a case study. The predictive optimal controller used mixed-integer and linear programming, where energy conversion and energy services models were defined as a set of linear constraints. Start-up and shut-down operations, as well as the load dependent efficiency of the cogeneration unit, were modelled by integer variables. Due to low heating demand in domestic applications, the back-up or auxiliary boiler should operate in sequence (in series) with micro-CHP, which is considered in this dissertation.

Clastres et al. (2010) explained how a PV based multisource system for residential application with co-management of sources and loads could contract to provide ancillary services, particularly the supply of active power services. The mathematical model for calculating the system's optimal operation (sources, load and exchanges of power with the grid) resulted in a linear mixed integer optimisation problem, in which the objective was to maximize the profits achieved by taking part in the electricity market. The results showed that PV electricity producers can gain by taking part in the markets for balancing power or ancillary services despite the negative impact on profit of several types of uncertainty, notably the intermittent nature of the PV source. In this literature, only the battery has been considered for electricity storage, which will become very expensive if it is sized for long term (seasonal) electricity storage in stand-alone (grid independent) applications.

A summary of the research outlined above, in which the mathematical programming method has been used, is shown in Table 2.3.2.

The existing research in the area of the control of renewable energy systems based on multi-period optimization shows that this method is the best candidate for optimal control of building energy systems. The multi-period optimization

based on mathematical programming can use trade-offs of resource allocation over time and capture constraint on the variables. The objective function can handle various types of costs, including economical and emission costs. This method can also consider the on/off inputs that are essential in the planning and scheduling of energy systems. In addition, complex operational strategies can be included in the mathematical model of the energy system. Finally the prediction capability of this method makes it a powerful tool for the optimization of the energy systems with energy storage and time variant energy prices. In this kind of energy system the optimal inputs should be calculated for a long time period (with enough time steps), to include the effects of energy storage and energy price in one time step on the other time steps. This method can be used to consider the uncertainty in weather forecasting and load prediction by stochastic programming. In this method the operation of non-linear energy systems can be optimized by non-linear programming.

Table 2.3.2 Summary of the literature of mathematical programming method

Energy system	Controller characteristic	Reference
Wind power, hydrogen storage and fuel cell	Control of exported electricity, electrolyzer and fuel cell power	Korpas and Holen (2006)
Energy system with multiple energy carriers	Control of exchanged energy with grid , and converters and storage power	Geidl and Andersson (2007a)
PV, electrolyzer, hydrogen storage tank and fuel cell	Control of exchanged electricity with grid, and electrolyzer and fuel cell power	Zervas, et al. (2008)
Micro-CHP, auxiliary boiler and hot water tank	Control of exchanged electricity with grid, and micro-CHP, boiler and hot water storage power	Houwing, et al. (2008)
Micro-CHP, boiler and hot water tank	Control of exchanged electricity with grid, and micro-CHP, boiler and hot water storage power	Collazos, et al. (2009)
PV and battery	Control of sources, load and exchanges of power with grid	Clastres, et al. (2010)

2.3.4.2 Dynamic programming

Dynamic programming usually refers to simplifying a decision, by breaking it down into a sequence of decision steps over time. The method is generally applicable to problems which exhibit the Markovian property (Belegundu and Chandrupatla, 2011). A process exhibits the Markovian property if the decisions for optimal return at a stage in the process depend only on the current state of the system and the subsequent decisions. Dynamic programming relies on the principle of optimality enunciated by Bellman (Bellman, 1957). Bellman's Principle of Optimality states "An optimal policy has the property that whatever the initial state and initial decisions are, the remaining decisions must constitute an optimal policy with respect to the state resulting from the first decision."

Faille, et al. (2007) studied the optimal control of a domestic micro combined heat and power system. The objective function was to reduce the gas and electricity bill of the consumer. The optimizations of a micro-CHP were carried out using mixed integer linear programming and dynamic programming. It was explained that the dynamic programming is more suited to integrate nonlinearity and mixed integer programming can integrate time-dependent constraints. This study showed that dynamic programming compared well with mixed integer linear programming. It was described that the dynamic programming is simpler to implement in real-time application, because it does not need a sophisticated solver and presents a constant computation time. Furthermore, stochastic features of thermal and electrical needs should be better handled in a dynamic programming framework.

Dynamic programming is well suited for solving allocation problems with a few discrete points of control variables and state variables (one or two state variables). If the control and state variables are discretized to have M variables, for N time steps, an order of M^N calls to the system model would be required. Such a computational overhead is sufficient to discount dynamic programming as a viable option for solving the control problem of complex integrated renewable and low carbon energy systems.

2.3.5 Model Predictive Control

Model Predictive Control (MPC) (Camacho and Bordons, 2004; Maciejowski, 2002) is a powerful method of controlling multi-input/multi-output (MIMO) systems that are subject to input and output constraints. The objective of the MPC control calculations is to determine a sequence of control inputs so that the predicted response moves to the set point in an optimal manner.

The basic concept of MPC is shown in Figure 2.3.1. At each sampling time, denoted by k, the future outputs $\{\hat{y}(k+i), i=1,...,P\}$ over the prediction horizon P are predicted. These predictions are based on the process model and future control signals $\{u(k+i), i=0,...,M-1\}$. The input is held constant after the control horizon M. The actual output y, predicted output $\hat{y}$, and manipulated input u are shown in Figure 2.3.1.

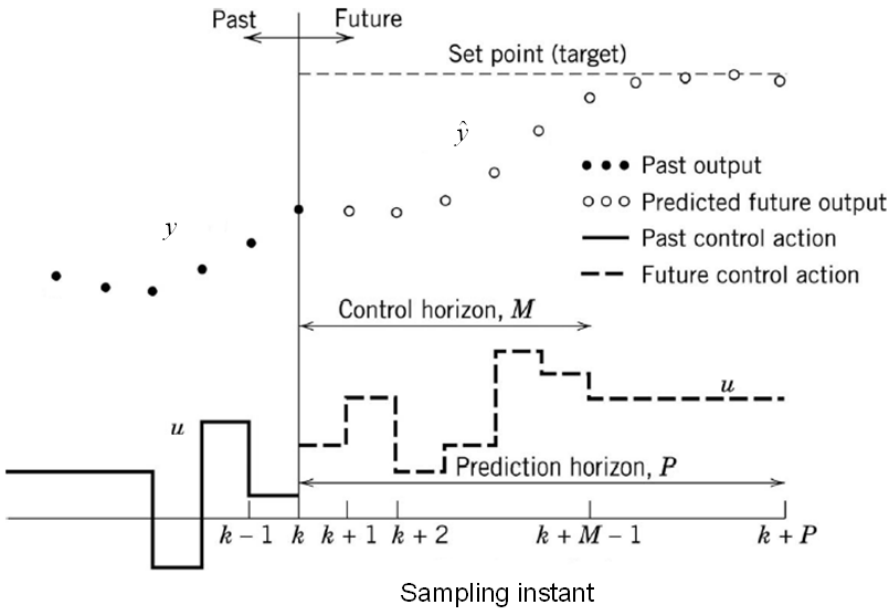

Figure 2.3.1 Basic concept for model predictive control (Seborg, et al, 2004)

After this, the set of future control signals, $\{u(k+i), i=0,...,M-1\}$, for the control horizon M are calculated by solving the following optimization problem:

$$\min_{\{u\}_o^{N-1}} J(\{u\}_0^{N-1}, x(t)) \equiv \sum_{i=1}^{P} \left\| Q_y(\hat{y}(k+i) - y_r) \right\|_p + \sum_{i=0}^{M-1} \left\| Q_u(u(k+i) - u_r) \right\|_p + \\ + \sum_{i=0}^{M-1} \left\| Q_{\Delta u} \Delta u(k+i) \right\|_p \tag{2-2a}$$

$$\text{subj. to} \begin{cases} y_{\min} \le \hat{y}(k+i) \le y_{\max}, & i = 1,...,P \\ u_{\min} \le u(k+i) \le u_{\max}, & i = 0,...,M-1 \\ \Delta u_{\min} \le \Delta u(k+i) \le \Delta u_{\max}, & i = 0,...,M-1 \end{cases} \tag{2-2b}$$

Here y_r and u_r are reference outputs and reference inputs respectively and Q_y, Q_u and $Q_{\Delta u}$ are weighting matrices. P and M are the number of predictions and control inputs which are referred to as the prediction horizon and the control horizon respectively. p is the norm, that can be 2, 1 or infinity.

MPC uses a receding horizon principle. Although at time step k the future control sequence $u(k),\ldots,u(k+M-1)$ is determined, only the first element of optimal sequence $(u(k))$ is applied to the process. At the next time instant the horizon is shifted one step, the model is updated with new information from the measurements, and a new optimization at time step $k+1$ is performed. This procedure is repeated at each sampling time.

The hierarchical, multilayer approach to process automation is a standard in process industries, and a well understood technique able to cope with the complexity and multiple criteria of operation (Tatjewski, 2010). Figure 2.3.2 shows the multilayer control structure. The main control layers include: the regulatory (feedback) control layer, which keeps the process at given operating points and can itself be divided into basic and advanced control layers, and the set-point optimisation layer, which calculates these operating points (Findeisen, et al., 1980; Marlin, 1995; Blevins, et al., 2005; Brdys and Tatjewski, 2005; Tatjewski, 2007). In complex control systems applying advanced control techniques, the regulatory control layer consists typically of two layers (Tatjewski, 2010): the basic (direct) dynamic control layer, usually equipped with PID (proportional-integral-derivative) controllers, and a higher, advanced control layer (also called the

constraint control layer, set-point control layer or the MPC layer), in which MPC algorithms are typically implemented, see, e.g., Blevins, et al. (2005), Qin and Badgwell (2003), Maciejowski (2002), Brdys and Tatjewski (2005) or Tatjewski (2007).

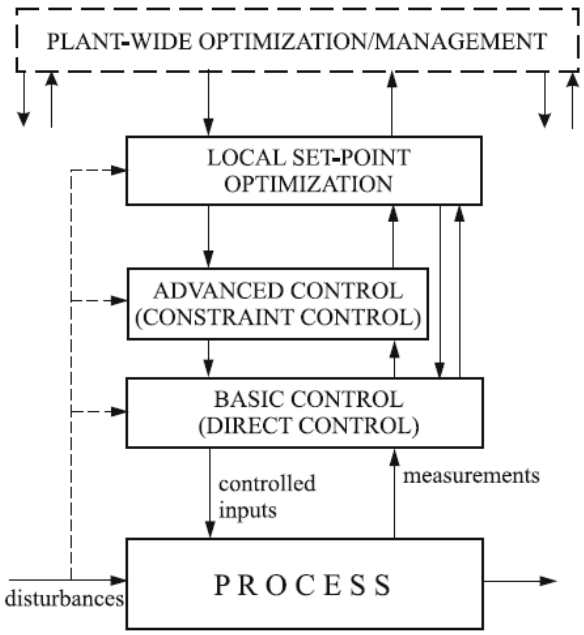

Figure 2.3.2 Multilayer control structure (Tatjewski, 2010)

To maximise economic profits, MPC algorithms cooperate with set-point optimisation, the purpose of which is to calculate online optimal set-points for MPC (Blevins, et al., 2005; Brdys and Tatjewski, 2005; Engell, 2007; Tatjewski, 2007; 2008; Ławryn´czuk, 2011; Maciej, 2011).

It is also possible to integrate set-point optimisation and MPC optimisation into one optimisation problem (Tvrzska de Gouvea and Odloak, 1998; Tatjewski, 2007; Zanin, et al., 2000; 2002). Alternatively, an integrated predictive optimiser and constraint supervisor can be used (Tatjewski, et al., 2009). It provides the control layer with set-points calculated for both optimality and constraint handling.

There has been significant interest recently in using MPC for various aspects of building for controlling primary and secondary HVAC systems. A primary HVAC

system is associated with the plant and a secondary HVAC system is associated with distribution and end use.

The evaluation of optimal controllers for active and passive building thermal storage has been studied by several researchers (Henze, et al., 2004a; Liu and Henze, 2006 ; Henze, et al. 2007 ;Henze, et al., 2003). In particular in Liu and Henze (2006) the optimal controller was implemented in a receding horizon fashion.

The controller that minimizes cooling costs by regarding the time-varying electrical energy price was presented by Yudong Ma, et al. (2009). The aim was to take advantage of night-time electricity rates and to lower the ambient temperature while precooling the chilled water tank.

Ma, et al. (2011) developed a model-based multi-variable controller for building cooling systems equipped with thermal energy storage by using the prediction of weather conditions and buildings loads. Real-time implementation and feasibility issues of the MPC scheme were addressed by using a simplified hybrid model of the system, a periodic robust invariant set as terminal constraints, and a moving window blocking strategy.

Optimal zone temperature and ventilation set-points (load-side analysis) have been studied by Henze, et al. (2004b) and Kolokotsa, et al. (2009).

Yuan and Perez (2006) and Huang, et al. (2009) focused on optimal operating strategies in the context of VAV systems by considering the optimization of air flow rate and air temperature set-points.

Yudong Ma, et al. (2011) worked on Model Predictive Control (MPC) of heating, ventilation, and air conditioning (HVAC) over networks of thermal zones. The control objective is to keep zone temperatures within a comfort range while consuming the least energy by using predictive knowledge of weather and occupancy.

Siroky, et al. (2011) focused on the analysis of energy savings that can be achieved in a building heating system by applying Model Predictive Control (MPC) and using weather predictions.

In the electrical power system, the MPC method has recently been studied. Le Xie and Ilic, (2009) presented potential benefits of applying MPC to solving the multi-objective economic/environmental dispatch problem in electric power systems with many intermittent resources. They showed that the proposed MPC approach could lower the generation costs by directly dispatching the generator output from the renewable resources in order to compensate temporal load variations over pre-defined time horizon. Furthermore, the multi-objective economic/environmental cost function provided a formulation to study the trade-off of efficiency and environmental impact in future energy systems.

Xiaohua Xia, et al. (2009) proposed an MPC approach to the dynamic dispatch problem by the optimal control dynamic dispatch framework. They showed that the MPC approach provides solutions converging to the optimal solution and the MPC algorithm is also robust under certain disturbances and uncertainties.

The above studies highlight the importance and novelty of MPC for the supervisory control of building integrated renewable and low carbon energy systems.

2.3.6 Hybrid methods

In last 20 years, a lot of work has been done for the further improvement of the optimization algorithms in the industry. On one side, an algorithm may be simple but suboptimal and on the other, complex but accurate. To achieve further advancements over the existing algorithms, one must complement the different algorithms. So in the main, more than one algorithm has been merged together which forms a hybrid model to meet the industry requirement.

Ohsawa, et al. (1993) used hybrid artificial neural networks-dynamic programming for the operation control of the photovoltaic/diesel hybrid power generation system. The optimal operation patterns of the diesel generator were calculated by dynamic programming under the known insulation and load demand, which minimize the fuel consumption of the diesel generator. These optimal patterns were learned by a three layers neural network, and it was tested for the different insulation and demand data from those used in the learning.

Fung (2000) used a combined fuzzy-logic and genetic algorithm technique for the short term generation scheduling of a system consisting of diesel generators, a PV array and a battery bank. The fuzzy logic algorithm based on the heuristic knowledge about the proposed hybrid energy system was developed and was used to determine the preliminary diesel generator schedule and the battery charge/discharge strategy. A genetic algorithm was then used to optimise the initial schedule by working on the rule base of the fuzzy logic algorithm.

Welch and Venayagamoorthy (2007) presented a particle swarm optimization method for optimizing an FLC for a grid independent system consisting of a PV collector array, a storage battery, and loads (critical and non-critical loads). Particle swarm optimization was used to optimize both the membership functions and the rule set in the design of the fuzzy logic controller. Optimizing the PV system controller yielded improved performance, allowing the system to meet more of the loads and keep a higher average state of battery charge. The potential benefits of an optimized controller included lower costs through smaller system sizing and a longer battery life.

Venayagamoorthy and Welch (2010) presented an energy dispatch controller for use in a grid-independent PV system. The controller was an optimal energy dispatch controller based on a class of Adaptive Critic Designs (ACDs) called Action Dependent Heuristic Dynamic Programming (ADHDP). This class of ACDs uses two neural networks to evolve an optimal control strategy over time. The first neural network or ‘‘Action’’ network dispenses the actual control signals while the second network or ‘‘Critic’’ network uses these control signals along with the system states to provide feedback to the action network, measuring

performance using a utility function. This feedback loop allows the action network to improve behaviour over time. The optimal energy dispatcher placed emphasis on always meeting the critical load, followed by keeping the charge of the battery as high as possible so as to be able to power the critical load in cases of extended low output from the PV array, and lastly to power the non-critical load in so far as not interfering with the first two objectives.

As mentioned in Sections 2.3.2 and 2.3.3, every intelligent technique has particular computational properties (e.g. ability to learn, explanation of decisions) that make them suitable for particular problems and not for others. The literature review shows that by combining the intelligent techniques together, or with other techniques, the limitations are reduced. However, hybrid methods have still not been used in complex energy systems, and it is very difficult to generalize their application in building energy systems.

2.4 Optimization problems

In this section a comprehensive review of the basic optimization problems, which is used in the proposed approaches to the design of a supervisory MPC (Chapters 5 and 6), is presented.

2.4.1 General formulation

The general optimization problem is a determination of the optimum (minimum or maximum) of an objective function under certain constraints. It can be generally stated as:

$$\min_{\mathbf{x}} f(\mathbf{x}) \tag{2-3a}$$

$$\text{subj. to} \quad h_i(\mathbf{x}) = \mathbf{0}, \qquad i = 1,2,...,m_{eq} \tag{2-3b}$$

$$g_i(\mathbf{x}) \le \mathbf{0}, \qquad i = 1,2,...,m \tag{2-3c}$$

$$\mathbf{x} \in S \subseteq X$$

Here the vector $\mathbf{x} \in R^n$ denotes the optimization variable, $f(\mathbf{x}) : R^n \mapsto R$ is the objective function, $h_i(\mathbf{x}) : R^n \mapsto R$ and $g_i(\mathbf{x}) : R^n \mapsto R$ are equality and inequality constraints, respectively. The set S is a subset of n-dimensional space. X is the domain of the decision variables and $S \subseteq X$ is the set of feasible or admissible decisions.

Optimization problems which are maximization problems can be cast in the form of (2-3) through the simple transformation (Fletcher, 2000):

$$\max_{\mathbf{x}} f(\mathbf{x}) = \min_{\mathbf{x}} - f(\mathbf{x}) \qquad (2\text{-}4)$$

The function $f(\mathbf{x})$ has a local (relative) minimum at $\mathbf{x}^*$ if $f(\mathbf{x}^*) \le f(\mathbf{x})$ holds for all $\mathbf{x}$ in a small neighbourhood N of $\mathbf{x}^*$ in the feasible design space S (Arora, 2011). If strict inequality holds then $\mathbf{x}^*$ is called a strong (strict) local minimum; otherwise it is called a weak local minimum.

Neighbourhood N of the point $\mathbf{x}^*$ is defined as the set of points:

$$N = \{\mathbf{x} \,|\, \mathbf{x} \in S \text{ with} \left\| \mathbf{x} - \mathbf{x}^* \right\| < \delta\} \qquad (2\text{-}5)$$

for some small $\delta > 0$. Geometrically, it is a small feasible region around the point $\mathbf{x}^*$.

The function $f(\mathbf{x})$ has a global (absolute) minimum at $\mathbf{x}^*$ if $f(\mathbf{x}^*) \le f(\mathbf{x})$ for all $\mathbf{x}$ in the feasible design space S. If strict inequality holds for all $\mathbf{x}$ other than $\mathbf{x}^*$, then $\mathbf{x}^*$ is called a strong (strict) global minimum; otherwise it is called a weak global minimum.

2.4.2 Convex optimization

A set $S \in R^s$ is convex if

$$\lambda x_1 + (1-\lambda) x_2 \in S \text{ for all } x_1, x_2 \in S, \lambda \in [0,1].$$

A function $f : S \mapsto R$ is convex if S is convex and

$$f(\lambda x_1 + (1-\lambda)x_2) \le \lambda f(x_1) + (1-\lambda) f(x_2)$$

$$\text{for all } x_1, x_2 \in S, \lambda \in [0,1].$$

A function $f : S \mapsto R$ is strictly convex if S is convex and

$$f(\lambda x_1 + (1-\lambda)x_2) \le \lambda f(x_1) + (1-\lambda) f(x_2)$$

$$\text{for all } x_1, x_2 \in S, \lambda \in (0,1).$$

A function $f : S \mapsto R$ is concave if S is convex and $-f$ is convex. The standard optimization problem (2-3) is said to be convex if the cost function f is convex on X and S is a convex set. A fundamental property of convex optimization problems is that local optimizers are also global optimizers.

2.4.3 Linear Programming

The Linear Program (LP) is a convex optimization problem where the objective function and constraints are linear functions. LPs are usually formulated in the so-called inequality form as follows:

$$\min_{\mathbf{x}} \mathbf{c}^T \mathbf{x} \qquad \text{(2-6a)}$$

$$\text{subj. to } \mathbf{A}\mathbf{x} = \mathbf{b} \qquad \text{(2-6b)}$$

$$\mathbf{A}_{eq}\mathbf{x} = \mathbf{b}_{eq} \qquad \text{(2-6c)}$$

with $\mathbf{c} \in R^n$, $\mathbf{A} \in R^{m \times n}, \mathbf{b} \in R^n, \mathbf{A}_{eq} \in R^{m_{eq} \times n}$, and $\mathbf{b}_{eq} \in R^{m_{eq}}$. Here, m and m_{eq} denote, respectively, the number of inequality and equality constraints.

An optimal solution of a linear programming must lie on the boundary of the feasible region. Algebraically, this says that an optimal solution must satisfy the boundary equation for one or more of the constraints (Winston and Goldberg, 2004).

There are two fundamentally different types of algorithms for solving LPs: simplex and interior-point methods (Vanderbi, 2008). The runtime for the simplex method is exponential in the worst case, while interior-point algorithms have a worst-case polynomial bound. However, this worst-case bound has little relevance for practical problems and both schemes are competitive in practice.

2.4.4 Mixed Integer Linear Programming

If in a linear programming problem, the vector of variables is composed of a real and a binary part, i.e. $\mathbf{x} = [\mathbf{x}_r^T, \mathbf{x}_b^T]^T$ with $\mathbf{x}_r \in R^{n_r}$ and $\mathbf{x}_b \in \{0,1\}^{n_b}$, problem (2-6) is referred to as a Mixed Integer Linear Program (MILP). Formally it can be stated as:

$$\min_{\mathbf{x}} \mathbf{c}_r^T \mathbf{x}_r + \mathbf{c}_b^T \mathbf{x}_b \qquad \text{(2-7a)}$$

$$\text{subj. to} \quad \mathbf{A}_r \mathbf{x}_r + \mathbf{A}_b \mathbf{x}_b \le \mathbf{b} \qquad \text{(2-7b)}$$

$$\mathbf{A}_{eq,r} \mathbf{x}_r + \mathbf{A}_{eq,b} \mathbf{x}_b \le \mathbf{b}_{eq} \qquad \text{(2-7c)}$$

$$\mathbf{x}_b \in \{0,1\}^{n_b}$$

A Mixed Integer Linear Program (MILP) is a non-convex optimization problem. Although the objective function and constraints are linear, the non-convexity comes from the fact that the optimized variables $\mathbf{x}_r$ and $\mathbf{x}_b$ belong to the real set R and binary set $\{0, 1\}$, respectively. The non-convexity makes solving MILP more difficult for obtaining a global optimum.

In a native brute-force way of solving an MILP problem, all feasible combinations of binary variables are enumerated and then an LP problem for each condition is solved. The binary variables which lead the best value of the objective function are selected as optimum values. As there are n_b binary variables, this would require 2^{n_b} LP problems to be solved, in the worst case. So the complete enumeration approach is inefficient for large-scale problems (Sarker and Newton, 2008). Fortunately, if the binary variable is fixed or relaxed, a convex set is attained and the problem can be solved using methods for convex optimization.

This principle is deployed in the branch and bound and the cutting plane methods. The details of these methods can be found in Nemhauser and Wolsey (1999). The combination of these techniques is known as the branch and cut method (Hillier and Lieberman, 2005). It should be noted that even with these methods, the algorithms have exponential complexity depending on the cardinality of binary vector $\mathbf{x}_b$.

2.5 Conclusions

The literature review showed that from environmental, economical and energy security points of view, utilization of the renewable and low carbon energy systems in buildings is desirable and inevitable.

Review of the regulations, policies and incentives showed that there are enough incentives and enforcements for using renewable and low carbon energy systems in buildings, so the use of these systems will be increased in the future.

The literature review of the sample integrated renewable and low carbon energy systems showed that a wide range of technologies have been studied for sizing and optimization. Integration of different renewable energies gives more reliability for the utilization of them. For example by the integration of a PV and a wind turbine in a building, at night-time when the PV arrays cannot generate electricity, wind speed may be high enough for the wind turbine to generate electricity. The renewable energy technologies that have been proposed in building applications are mostly PV cell, solar collector, wind turbine and biomass. Low carbon technologies in building applications are CHP, heat pump and fuel cells. Storage devices used in building energy systems are the battery, the hydrogen tank, the hot water tank and the phase change material.

A literature review of the various control methods showed that each control method has its advantages and disadvantages. The methods based on multi-period optimization and MPC have been recognised as the best method for supervisory

control and operational management of the integrated renewable and low carbon energy systems.

Although the multi-period optimization has been used in some of the literature, there is not a unified method for the utilization of this technique in various types of building integrated renewable and low carbon energy systems. In addition, some of the complicated operational strategies have not been studied in the literature; for example, the operational sequence of the subsystems, e.g. the operation of the auxiliary boiler after reaching the full capacity of the cogeneration unit, or the maximizing of the stored energy in a multi-storage energy system (e.g. battery and hydrogen).

The MPC method has been used in chemical process engineering, electrical power networks, and in building primary and secondary HVAC systems, but it has not been used in the building integrated renewable and low carbon energy systems. In addition, there are no studies for designing explicit MPC in this research area.

A review of the related mathematical programming methods revealed that although there are efficient methods for the solution of linear and mixed integer linear programming, the number of binary variables (a binary variable represents an event which either does/does not occur, e.g. start/stop or charge/discharge in this research) in the mixed integer linear programming can be a computational barrier in the solving of large scale problems.

Chapter 3

Building energy system

In this chapter the building integrated renewable and low carbon energy system is described. This is the basis of the building energy system model which is obtained in Chapter 5. Input energies to the system and output energies from the system are explained in this chapter. In addition, the input data which are necessary for the operation of the supervisory controller are described in this chapter. These data include the predicted weather data and the building energy demand.

3.1 Building energy system

A system is a collection of connected components that is characterized by the interrelation between the components and system boundaries. The boundary separates the components of the system from the outside environment.

The components of the building energy system are energy converters, energy storage devices and on site renewable energy generators. These components have interaction with each other, and are surrounded by the building energy system boundaries.

Input and output energies cross the boundary of the system. The input energies bring different kinds of energies from distribution grids to the inside of the system. The available grids depend on the geographical location of the building. These grids are discussed in Section 3.2. The output energies can be divided into two parts. One part is delivered to the building to supply different kinds of energy

demands including electricity, heating and cooling loads and the other part is delivered to the grid. The amount of energy that is delivered to the grid depends on the energy price, the contract with the grid operator and governing regulations.

For each energy carrier an energy bus is considered. This bus can enter the system and/or exit from the system, or just be placed inside the system. All of the energy converters, storage devices and renewable energies are connected to the associated energy buses.

Renewable energies that enter the system are characterised in terms of their intensity; for instance, solar energy in terms of solar radiation per unit area (W/m^2), wind energy in terms of wind velocity (m/s) and biomass energy in terms of mass flow rate (kg/h). The harvested renewable energies are added to the related energy buses inside the system.

The system boundary, system inputs and outputs, energy buses and system components are shown in Figure 3.1.1.

In a building energy system there are other types of equipment, like pumps, fans and controllers. Although these consume energy, they have no direct role in the conversion or storage of the energy carriers, and usually their energy consumption is negligible. This equipment is excluded from the modelling of the system, but their electricity consumption can be included in the building electrical load.

The data that is needed for the optimal control of the system includes current and forecasted energy prices, weather data and building energy demand. These data are discussed in Section 3.4.

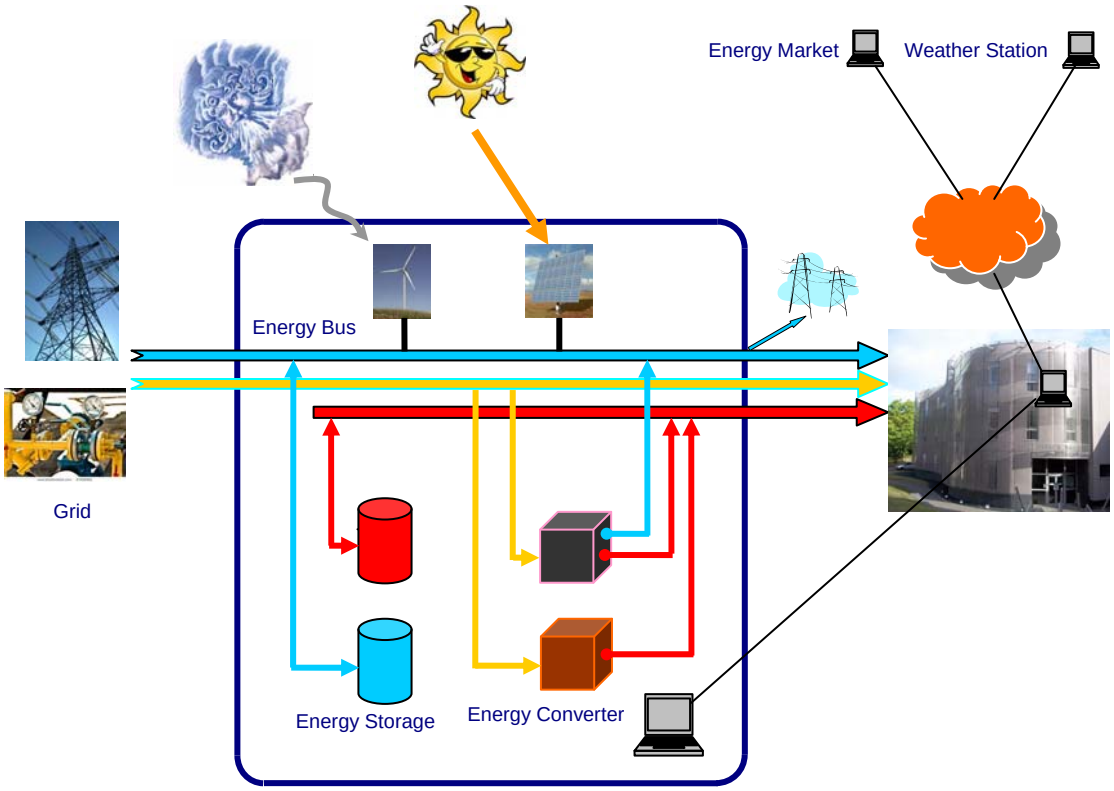

Figure 3.1.1 Building energy system concept

3.2 Energy infrastructures

Energy infrastructures are large distribution networks that connect energy sources to the energy consumers including the building energy system. These networks are called national grids, and each country has different types of them in different parts of the country. Some of the grids can be extended to several countries. The building energy system can buy energy from the grid or sell energy to the grid (Chapter 5).

3.2.1 Electricity grid

For the distribution of electrical energy from generating power plants to the consumers, it is first transmitted to the substations located near to the consumers. For this purpose electricity is transmitted at high voltages (110 kV or above) to

reduce the energy losses in long distance transmission. In the UK, the interconnected high voltage transmission lines are typically referred to as the national grid, while in the US, they are called power grids or just the grid. In the substation, voltage is reduced and electricity is distributed to the consumers. Figure 3.2.1 shows that the electricity grid in the UK has been spread all around the country and supplies the electricity to buildings and industries. In addition, distributed renewable generators can easily be connected to the grid.

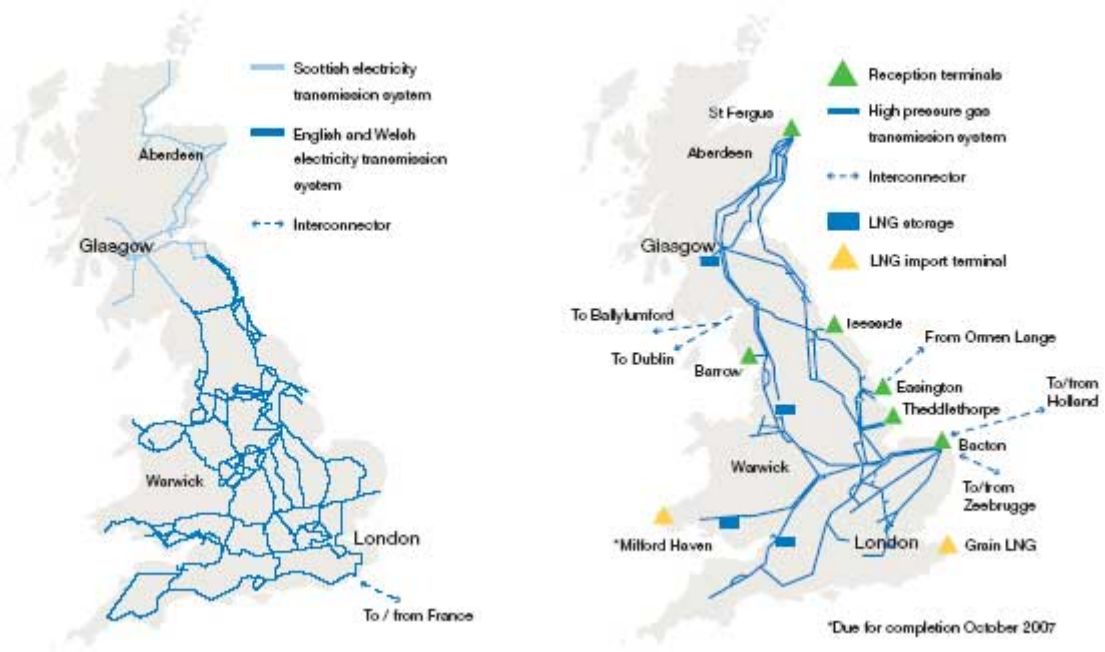

Figure 3.2.1 Gas and electricity grids in UK (National Grid, 2011)

3.2.2 Gas grid

Gas is transmitted with high pressure from gas terminals to the local distribution points. At these points gas is taken from the high pressure transmission system and distributed through low pressure networks of pipes to industrial complexes, offices and homes.

In the UK, National Grid is the owner, operator and developer of the majority of Britain's gas transportation system. National Grid receives gas from six coastal reception terminals around Great Britain (National Grid, 2011).

There are eight Gas Distribution Networks (GDNs), which each cover a separate geographical region of Britain. In addition there are a number of smaller networks owned and operated by Independent Gas Transporters (IGTs) - most but not all of these networks have been built to serve new housing. Figure 3.2.1 shows that UK has an advanced gas grid which can supply gas to the boilers and micro-CHP systems in buildings.

3.2.3 District heating grid

District heating requires central heating plants or combined heating and power (CHP) plants and a highly insulated heat main of supply and return pipes distributing hot water (or steam) to the buildings which might be connected (ASHRAE, 2008). At a junction point, heat is transferred from the mains to the building heating circuits by a heat exchanger.

District heating is widely used in regions with large fractions of multi-family buildings, providing as much as 60% of the heating and hot water energy needs for 70% of the families in Eastern European countries and Russia (OECD/IEA, 2004). In UK, the Pimlico District Heating Undertaking (PDHU), located just north of the River Thames in London, first became operational in 1950 and continues to expand to this day (Energy Saving Trust, 2005). Two other large municipal district heating schemes are in Nottingham and Leicester (Ove Arup, 2008). The Nottingham district heating scheme has been running since the 1970s. It provides heat and power to 4,600 homes, civic buildings, schools and Nottingham Trent University. Leicester district heating scheme has CHP units at four council sites, serving 17 council buildings and 4,000 residential premises.

3.2.4 District cooling grid

District cooling is the production and distribution of chilled water or other cooling media from a central source, for the cooling of multiple buildings (ASHRAE, 2008). This is done by producing chilled water at a central plant by vapour compression or absorption chillers and then piping the water, through underground insulated pipes to customers. The main benefits of district cooling are reduced energy and maintenance costs because the buildings that employ it eliminate the need for expensive water chillers. District cooling is suitable for nearly all kind of densely built-up areas like downtown business districts and institutional settings such as college campuses where cooling demand exists.

3.2.5 Hydrogen grid

A hydrogen infrastructure is the infrastructure of pipes and stations for the distribution and sale of hydrogen fuel (Ball and Wietschel, 2009). This infrastructure connects the point of hydrogen production or delivery of hydrogen, with the point of demand. Mostly hydrogen is produced at the place of demand, with every 50 to 100 miles (80 to 160 km) having an industrial production facility. As of 2004 there are 900 miles (1450 km) of low pressure hydrogen pipelines in the USA and 930 miles (1500 km) in Europe (Hephaestus Books, 2011).

3.3 On grid and off grid energy systems

The building energy system can be connected to one or more grids, or it can be stand-alone, without any connection to the regional or country energy infrastructures.

3.3.1 On grid building energy system

An on grid building energy system is connected to the energy infrastructures. The common energy infrastructures were discussed in the Section 3.2. The on grid building energy system can produce energy locally by renewable resources. It can convert one form of energy to other form(s), and store it for later consumption. Also a grid connected building energy system can buy energy from the grid and/or sell energy to the grid.

3.3.2 Off grid building energy system

An off grid or stand-alone building energy system does not have any connection to the energy grids. The energy supply from this system is onsite energy harvested from renewable resources. In this system, the extra energy can be stored and used later. For emergency cases, when there is no renewable energy available, a diesel generator is normally considered. If different kinds of renewable energy resources are used, the system is called a hybrid system. Remote rural area electrification and summer house electrification are examples of the off grid energy system.

3.4 Renewable energies

The renewable energies which are used mostly in the building energy systems are solar energy, wind energy, ground source energy and biomass energy. In the following sections, a brief description of these energy sources is given. The related renewable energy harvesting equipment is described and modelled in Section 4.1 and Appendix A.

3.4.1 Solar energy

Almost all of the energy that drives the various systems (climate systems, ecosystems, hydrologic systems, etc.) found on the Earth originates from the Sun.

Solar energy is created at the core of the Sun when hydrogen atoms are fused into helium by nuclear fusion. The radiative surface of the Sun, or photosphere, has an average temperature of about 5800 Kelvin. Most of the electromagnetic radiation emitted from the Sun's surface lies in the visible band centred at 0.5 μm. The total quantity of energy emitted from the Sun's surface is approximately 63,000,000 W/m^2.

The energy emitted by the Sun passes through space until it is intercepted by planets and other celestial objects. The power density of solar radiation measured just outside Earth's atmosphere and over the entire solar spectrum is called the solar constant. According to the World Meteorological Organization, the most reliable (1981) value for the solar constant is 1370 ± 6 W/m^2. Of this power, 8% is in the ultraviolet wavelengths, 47% in the visible spectrum, and 45% in the infrared region. The solar constant is actually not a true constant, but is subject to a small continuous variation due to the shape of the Earth's orbit, amounting to −3.3% from the average at about July 5, when the Earth is at its greatest distance from the Sun, and +3.4% at about January 3, when the Earth is closest to the Sun.

Solar radiation is attenuated before reaching Earth's surface by an atmosphere that removes or alters part of the incident energy by reflection, scattering, and absorption. Radiation scattered by striking gas molecules, water vapour, or dust particles is known as diffuse radiation. Clouds are a particularly important scattering and reflecting agent, capable of reducing direct radiation by as much as 80 to 90%. Because cloud distributions and types are highly variable, these reductions are quite unpredictable. The radiation arriving at the ground directly from the Sun is called direct or beam radiation. Global radiation is all the solar radiation incidents on the surface, including direct and diffuse.

The map in Figure 3.4.1 shows variations in annual mean values of global solar irradiation on a south facing $30°$ inclined plane in the UK in kWh/m^2. The map shows that utilization of solar energy in the southern part of the UK is more feasible.

Solar energy can be converted directly to thermal and electrical energy, by solar collector and by PV cell respectively, and can be used in buildings.

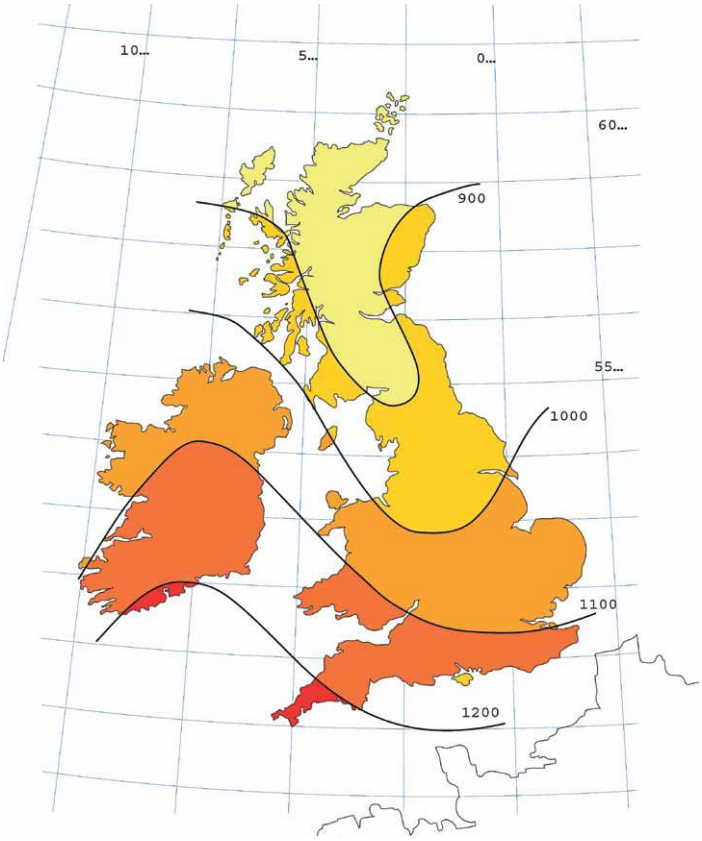

Figure 3.4.1 UK annual mean values of global solar irradiation on a south facing 30 ° inclined plane in kWh/m^2 (Source: Solar Trade Association).

3.4.2 Wind energy

Wind energy is energy from moving air, caused by temperature (and therefore pressure) differences in the atmosphere. Irradiance from the sun heats up the air, forcing the air to rise. Conversely, where temperatures fall, a low pressure zone develops. Winds (i.e. air flows) balance out the differences. Hence, wind energy is solar energy converted into the kinetic energy of moving air.

Figure 3.4.2 shows that the UK has a great wind resource, however the wind speed depends on the terrain, bodies of water and vegetative cover, and careful

consideration of the exact location is required prior to deployment of a wind turbine.

The wind energy, when harvested by modern wind turbines, can be used to generate electricity.

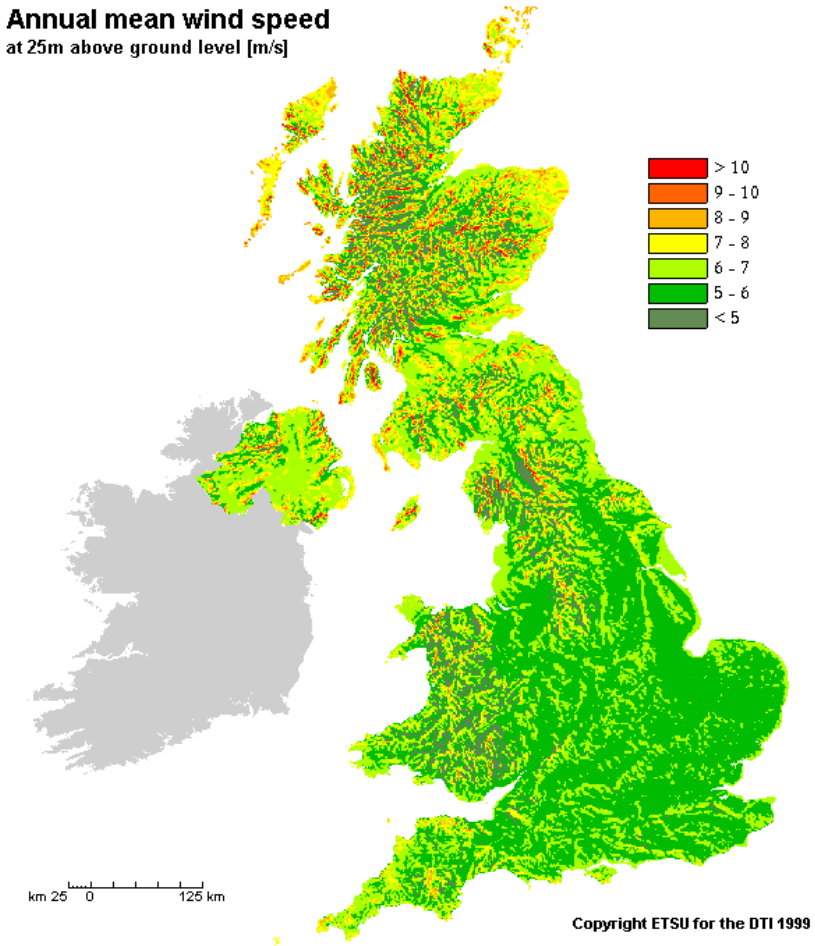

Figure 3.4.2 Annual mean wind speed in different part of the UK (Source :UK Wind speed Database/BERR)

3.4.3 Ground source energy

Ground source energy is a type of solar energy as it relies on the Sun warming the ground. As a result, the ground temperature shows seasonal fluctuations to depths of about 15 m where the temperature is relatively constant and approximately equal

to the mean annual air temperature (8 - 11°C in the UK). The ground source energy can be taken from the ground itself or from groundwater. Due to the low temperature of the source, a heat pump should be used for exploiting this energy.

3.4.4 Biomass energy

The UK Biomass Strategy (DTI and DEFRA, 2007) define biomass as "any biological material, derived from plant or animal matter, which can be used for producing heat and/or power, fuels including transport fuels, or as a substitute for fossil fuel-based materials and products". Biomass is considered a carbon neutral resource because the carbon dioxide (CO_2) emitted during energy production is reabsorbed during the growth of the crop. Emissions released during the establishment, harvesting, production, supply and transport phases however, result in a slight positive overall contribution to CO_2 emissions.

Raw materials that can be used to produce biomass fuels are widely available across the UK and come from a large number of different sources, including virgin wood, energy crops, agricultural residues, food waste and industrial waste and co-products. Different sources of biomass fuel have different characteristics such as moisture content and size. These characteristics can be affected by transportation and storage.

The simplest way of using many forms of biomass for energy is simply burning it in a biomass boiler. Three types of biomass most commonly used in building applications are logs, wood chips and wood pellets. Wood pellets are made from compressed sawdust and wood shavings and other biomass products and are uniform in size and shape. They have higher energy content and so take up less storage space than logs or wood chips. Stove and boiler manufacturers specify the size, shape and moisture content their products need to perform well. Wood pellet systems are the smallest, neatest and the most like a mainstream boiler and require the least input from the user.

Wood chips are cheaper and more abundant. They allow for more mechanisation than logs, but are not as efficient as wood pellets. It is important that they are pretty uniform in size in order to work smoothly in an automated domestic system.

3.5 Predicted data

Weather prediction and building energy demand prediction are the data that enter the supervisory controller. The weather forecasted data is received online from the weather station for the next few hours up to the next few days. This data can be modified by some statistical models locally and then used for prediction purposes. The predicted data are used for prediction of available renewable energies and building loads. The detail of prediction methods is not considered in this research, so in Chapter 6 it is assumed that the solar radiation and building load values are predicted values.

3.5.1 Prediction of weather data

Forecasted weather data are used for the prediction of building heating, cooling and electrical loads, as well as for the prediction of available renewable energy in the future hours. The forecasted data include solar radiation, wind speed, dry bulb temperature and the relative humidity of the outdoor air. These data can be obtained online from the weather stations. The forecasts are usually not perfect, however in this research the prediction errors are disregarded.

The approaches used in modern weather forecasting mainly include traditional synoptic weather forecasting, numerical weather prediction, and statistical methods.

Synoptic weather forecasting was the primary method for making weather predictions until the late 1950s, and involved the analysis of synoptic weather charts, employing several empirical rules.

Numerical weather prediction, used extensively in modern weather forecasting, is based on the fact that the gases of the atmosphere obey fluid dynamics and thermodynamics principles. Ideally, these physical laws can be used to predict the future state of the atmosphere, when the current conditions are known. Numerical weather prediction uses a number of highly refined computer models that attempt to mimic the behaviour of the atmosphere.

Statistical methods, using past weather data to predict future events, are often used in conjunction with numerical weather predictions. One statistical approach, the analog method, examines past weather records to find those that come close to duplicating current conditions.

3.5.2 Prediction of building loads

The building energy demand includes electricity, heating and cooling demands which are dependent on the weather condition, occupancy schedule and temperature set points. If electricity or hydrogen is used for refuelling cars, in the building or in the home, the required energy should be considered in the building load. The predicted heating, cooling and electrical loads of the building should be available online for the controller.

There are several methods for the prediction of heating and cooling loads, which fall into three categories: physical models, black-box models and grey-box models. The physical models use the building simulation tools, like EnergyPlus, for the building heating and cooling load calculations. However these models have a large number of parameters to tune and need a lot of building and system data. The black-box models (including time-series models, Fourier series models, regression models, Artificial Neural Network (ANN) models and fuzzy logic models) are easier to implement, but it is more difficult to find the optimum parameters. The

gray-box models are similar to the black-box models, except that they use a simplified thermal model of the building in the calculations.

Similar to the building heating and cooling load prediction methods there are some methods for the prediction of building electrical load. Most of the current research has focused on the ANN method.

In this study it is assumed that the building heating, cooling and electrical loads have been predicted and are available for the controller.

3.5.3 Prediction of available Renewable energy

The output power from the renewable sources can be forecasted by using the related predicted weather data. For this purpose the controller uses the forecasted weather data in the mathematical model of the renewable energy equipment (Chapter 4) and determines the predicted output power for the future hours.

3.6 Conclusions

In this chapter a general building energy system was explained. It was shown that this system consists of three groups of components: energy converters, energy storage devices and on site renewable energy generators. Depending on the building energy system component and building location, different energy carriers can enter the system. Also, depending on the building energy demands, different energy carriers exit from the system. In addition, surplus electricity generated by the renewable and low carbon energy equipment can be exported to the grid.

It was shown that for the supervisory control of the building energy system, short term prediction of the weather data and building electrical, heating and cooling loads are necessary. The forecasted weather data are used for the prediction of available renewable energy, as well as for the prediction of heating and cooling loads of the building.

Chapter 4

Modelling of energy conversion and storage equipment

A building energy system usually consists of energy converters and energy storage devices. Each of these components is a subsystem of the whole energy system. Energy converters convert energy from one form to another in order to supply building electricity, heating and cooling demands. For example, a boiler is an energy converter which transforms chemical energy of the natural gas into heat. In energy storage devices, energy can be directly stored, for example storage of heat in the hot water tank, or it can be converted to another form of energy and stored, similar to the storage of electrical energy in chemical energy form as in batteries and hydrogen tanks.

In this chapter, mathematical models of the subsystems are derived. A mathematical model is an abstract model that uses appropriate equations to describe the behaviour of a system. In deriving the mathematical models it is assumed that the subsystems are in steady state. With long time steps, the transient behaviour of the subsystem, which may take place in a short portion of the time step, can be neglected. In addition, it is assumed that the subsystems are linear and their models are expressed by linear equations. In fact most of the energy converters and storage devices have nonlinear behaviour. However, the error resulting from assuming a linear model for these components - in comparison with the uncertainties which exist in the building energy demand and available renewable energy predictions - is negligible.

4.1 Energy conversion equipment

In a building energy system various pieces of mechanical and electrical equipment are used for energy conversion. The selection and sizing of these pieces of equipment are out of the scope of this research. In the following sections, a brief description of the equipment is given, and their mathematical models are described. The equipment that is considered in the following sections are: the boiler, the CHP, the PV cell, the electrolyzer, the fuel cell and the diesel generator. These are used in the applications described in Chapter 6. Mathematical models of other conventional energy converters, which are not used in the applications, are presented in Appendix B.

4.1.1 Boiler

Boilers convert energy from fossil fuels, biomass or electricity to heat. There are several different types of boilers. The efficiency of fuel-burning boilers is defined in three ways: combustion efficiency, overall efficiency, and seasonal efficiency.

The combustion efficiency of a boiler is defined as input minus stack (chimney) loss, divided by input, and ranges from 75 to 86% for most noncondensing mechanically fired boilers. The combustion efficiency of condensing boilers is in the range of 88 to over 95% (ASHRAE, 2008).

Overall efficiency of the boiler is gross output divided by input. Gross output is measured from the steam or water leaving the boiler, and depends on the installation characteristic. Overall efficiency is lower than combustion efficiency by the percentage of heat lost from the outside surface of the boiler (this loss is usually called radiation loss), and by off-cycle energy loses (for applications where the boiler cycles on and off). Overall efficiency can be precisely determined only under laboratory test conditions, directly measuring the fuel input and the heat absorbed by the water or steam of the boiler. The overall efficiency of electric boilers is in the 92 to 96% range.

Most of the boilers operate at part load during the heating season. Part load efficiency of the boiler is normally less than full load efficiency. In addition, the boiler is off sometimes in the heating season. Seasonal efficiency is the actual operating efficiency of the boiler considering losses during part load operation of the boiler and heat losses when the boiler is off.

For the purpose of this research, the seasonal efficiency is used. If the seasonal efficiency of the boiler is known, then output heat from the boiler can be determined from the following equation (ASHRAE, 2008):

$$P_b(t) = \eta_b LHV_{fuel} \dot{m}_{fuel}(t) \qquad (4\text{-}1)$$

Here P_b is the output heat from the boiler, η_b is the seasonal boiler efficiency, LHV_{fuel} is the lower heating value of fuel and $\dot{m}_{fuel}$ is fuel rate. For condensing boilers the higher heating value of the fuel (HHV_{fuel}) should be used.

4.1.2 Cogeneration or Combined Heat and Power (CHP)

Cogeneration or combined heat and power (CHP) is the use of a heat engine or a thermal power plant to simultaneously generate electricity and useful heat.

According to the second law of thermodynamics it is impossible to convert heat completely into work. That is, it is impossible to extract energy by heat from a high-temperature energy source and then convert all of the energy into work. At least some of the heat must be passed to a low-temperature heat sink. Thus, a heat engine with 100% efficiency is thermodynamically impossible.

The rejected heat in large power plants is carried to the users by district heating pipelines. Micro-combined heat and power (or micro-CHP) is an extension of the application of cogeneration to the single/multi family home or small office building.

For a cogeneration plant having electric and thermal efficiency, electrical and heat power outputs are calculated as below (ASHRAE, 2008):

$$P_{e\ chp}(t) = \eta_{e\,chp}\ LHV_{fuel}\ \dot{m}_{fuel}(t) \qquad (4\text{-}2)$$

$$P_{h\ chp}(t) = \eta_{h\ chp}\ LHV_{fuel}\ \dot{m}_{fuel}(t) \qquad (4\text{-}3)$$

Here $P_{e\ chp}$ and $P_{h\ chp}$ are the output electricity and output heat from the CHP respectively, $\eta_{e\,chp}$ and $\eta_{h\,chp}$ are the electrical and thermal efficiencies of the CHP respectively, LHV_{fuel} is the lower heating value of the fuel and $\dot{m}_{fuel}$ is the fuel consumption rate.

In a cogeneration system the Alfa value is defined as the ratio of electrical output to thermal output:

$$Alfa\ value = \frac{P_{e\,chp}}{P_{h\,chp}} \qquad (4\text{-}4)$$

In the UK, the heat to power ratio is conventional, and is the ratio of output heat power from the CHP unit to output electrical power.

Table 4.1.1 compares some of the important performance characteristics of the various types of small scale cogeneration systems (Kreith and Goswami, 2007).

Natural gas is the preferred fuel for the spark engines, but they can also run on propane or gasoline. Compression-ignition engines can operate on diesel fuel or heavy oil, or they can be set up in a dual-fuel configuration that burns primary natural gas with a small amount of diesel fuel. The engines used for micro-CHP units are normally designed as packaged units. The size of micro-CHP units, which use internal combustion engines as a prime mover, varies from 10 to 200 kW.

Table 4.1.1 Technical Features of small- Scale CHP Devices (Kreith and Goswami, 2007)

	Reciprocating Engine	Microturbine	Stirling Engines	PEM Fuel Cells
Electric power(kw)	10 – 200	25 – 250	2-50	2-200
Electric efficiency, full load (%)	24 – 45	25 – 30	15 – 35	40
Electric efficiency, half load (%)	23 – 40	20 – 25	35	40
Total efficiency (%)	75 – 85	75 – 85	75 – 85	75 - 85
Heat/electrical power Ratio	0.9 – 2	1.6 – 2	1.4 – 3.3	0.9 – 1.1
Output temperature Level (C)	85 – 100	85 – 100	60 – 80	60 - 80
Fuel	Natural or biogas, diesel fuel oil	Natural or biogas, diesel, gasoline, alcohols	Natural or biogas, LPG, several liquid or solid fuels	Hydrogen, gases including hydrogen methanol
Interval between Maintenance (h)	5000 – 20,000	20,000-30,000	5,000	N/A
Investment cost ($/kw)	800 – 1500	900 – 1500	1300 – 2000	2500 - 3500
Maintenance costs (c/kw)	1.2 – 2.0	0.5 – 1.5	1.5 – 2.5	1.0 – 3.0

The microturbine is a newly developed small-sized gas turbine with power generation from 25 to 250 kW. Like the large gas turbines, the microturbine generator consists of a compressor, a combustion chamber, a one-stage turbine, and a generator. The rotating speed of the generator can be up to 10,000 rpm. The high-frequency electricity output is first rectified and then converted to 60 Hz. The advantages of microturbine CHP are low noise and relatively low NO_x emission. Its disadvantages are low electricity efficiency and high initial cost. Micro turbine CHPs are suitable for taking a base-load of electricity, heating, and cooling because of their inflexibility in handling load changes.

The Stirling engines are small-scale engines from 2 to 50 kW that are targeting the future residential CHP needs (Kreith and Goswami, 2007). The Stirling engine uses the Stirling cycle and is a reciprocating engine. However, unlike the internal-combustion engine, the Stirling engine is an external-combustion engine. The combustion takes place outside the cylinder. The piston is driven by compression or expansion of working gases due to the alternating heating and cooling of the cylinder by the external heat source. The engine converts thermal energy to

mechanical energy and drives the generator. The Stirling engine can run on various fuels, both gas fuels and solid fuels, due to its external combustion. As it has been shown in Table 4.1.1 the advantages of Stirling engines are its quiet operation, little maintenance, and low NO_x emission. Its disadvantage is its relative lower electrical efficiency, typically 25-30%.

4.1.3 PV Cell

Photovoltaic cells (PV cells) produce direct current electricity from light. Photovoltaic systems are designed around the photovoltaic cells. Since a typical photovoltaic cell produces less than 3 watts at approximately 0.5 volt dc, cells must be connected in series-parallel configurations to produce enough power for high-power applications. Figure 4.1.1 shows how cells are configured into modules, and how modules are connected as arrays.

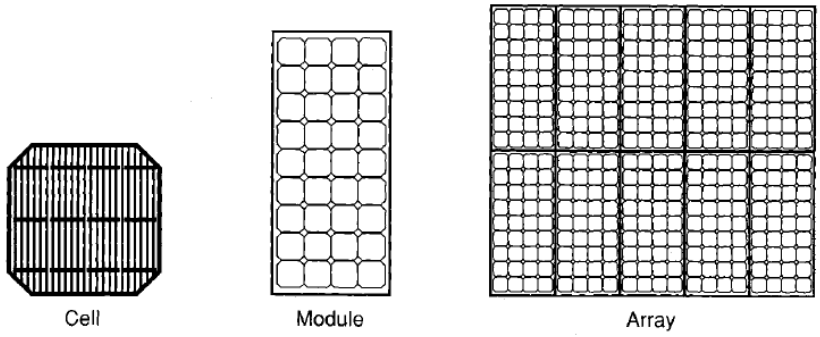

Figure 4.1.1 Several PV cells make a module and several modules make an array

The actual power output from a PV cell depends on several factors including ambient temperature, operating voltage and current, wind speed, shadows and dirt. For calculating the output powers some literatures like Senjyu, et al. (2007) and Bernal-Agustín, et al. (2010) have assumed that the output power is proportional to the hourly solar irradiation on the photovoltaic generator surface. The coefficient of proportionality is called efficiency, which depends on the above factors. Kolhe, et al. (2003) have derived the efficiency analytically and Yang, et al. (2009) have

considered the PV cell temperature, voltage and current directly to obtain output power. If the PV generator has a Maximum Power Point Tracking (MPPT) system, the efficiency is multiplied by the MPPT system efficiency (Yang, et al., 2009). In this research the following equation is used to estimate the PV array power from the estimated average hourly beam and the diffuse irradiation on the tilted PV surface (NREL, 2008).

$$P_{PV} = f_{PV} Y_{PV} (\frac{I_T}{I_S}) \qquad (4\text{-}5)$$

Here f_{PV} is the PV derating factor, Y_{PV} is the PV array capacity, I_T is the global solar radiation incident on the PV array, and I_S is 1 kW/m2, which is the standard amount of radiation used to rate the capacity Y_{PV} of PV modules. The PV derating factor accounts for losses/discrepancies between the rated and the actual performance of the PV array due to factors such as the soiling of the panels, operating temperature, wiring losses and shading. NREL (2008) recommends a derating factor of 90% in temperate climates, and between 70% and 80% in warmer climates.

4.1.4 Electrolyzer

Electrolysis of water is the decomposition of water molecules (H_2O) into oxygen (O_2) and hydrogen gas (H_2) caused by an electric current being passed through the electrodes and water. One important use of the electrolysis of water is to produce hydrogen. The hydrogen can be stored and used in a fuel cell to produce electricity and it can also be used for fuelling of cars.

All electrolysers consist of an anode and a cathode separated by an electrolyte. However, different electrolysers function in slightly different ways (HMGS, 2011).

In a Proton Exchange Membrane (PEM) electrolyser the electrolyte is a solid plastic material. The water reacts at the anode to form oxygen and positively charged hydrogen ions (protons). These hydrogen ions migrate across the PEM to

the cathode, where they combine with electrons from the external circuit to form hydrogen gas.

Anode Reaction: $2H_2O \rightarrow O_2 + 4H^+ + 4e^-$

Cathode Reaction: $4H^+ + 4e^- \rightarrow 2H_2$

In Alkaline electrolysers the PEM is replaced with an alkaline solution (typically sodium or potassium hydroxide) that acts as the electrolyte.

Solid oxide electrolysers use a solid ceramic material as the electrolyte. This selectively transmits negatively charged oxygen ions at elevated temperatures and therefore generates hydrogen in a slightly different way:

- Water at the cathode combines with electrons from the external circuit to form hydrogen gas and negatively charged oxygen ions;
- The oxygen ions pass through the membrane and react at the anode to form oxygen gas and give up the electrons to the external circuit.

Table 4.1.2 shows the electrolyte, operating temperature and technology status for the above three types of electrolyzers.

Table 4.1.2 Electrolyte, operating temperature and technology status of the electrolyzers (HMGS, 2011)

	Electrolyte	**Temperature**	**Technology Status**
PEM	Solid plastic	80-100°C	Pre-commercial - at a similar stage as hybrid vehicles.
Alkaline	KOH, NaOH	100-150°C	Has been commercial for decades. A well mature technology that can be installed tomorrow - similar to the familiar ICE engine.
Solid Oxides	Solid ceramic	500-800°C	Still under research

A number of mathematical models for electrolyzers are available in the literature. Most of these models use empirical coefficients to describe the current-voltage relationship for the electrochemical reactions occurring at the electrolyzer stack. In some cases the power draws of ancillary equipment are ignored. Empirical relationships are used to characterize the water consumption, auxiliary

power requirements, the efficiency of converting electrical power at the stack to hydrogen, and the oxygen production.

The electrical conversion efficiency of the electrolyzer is defined as the energy content (based on higher heating value) of the hydrogen produced divided by the amount of electricity consumed (NREL, 2008). With this definition, electrolyzer efficiency can be expressed by the following equation:

$$\eta_{ely} = \frac{\dot{m}_{h_2} HHV_{h_2}}{P_{ely}} \qquad (4\text{-}6)$$

Here P_{ely} is input power to the electrolyzer, $\dot{m}_{h_2}$ is mass flow rate of the produced hydrogen and HHV_{h_2} is higher heating value of hydrogen. The higher heating value of hydrogen is 142 MJ/kg, which is equal to 9.4 kWh/kg (NREL, 2008). Electrolyzer efficiency is a function of the power supply and the electrolyzer's temperature, but in this research the working condition and then electrolyzer efficiency is considered to be a constant average value. With this assumption, the electrical power consumed by the electrolyzer can be derived from the equation:

$$P_{ely} = \frac{\dot{m}_{h_2} HHV_{h_2}}{\eta_{ely}} \qquad (4\text{-}7)$$

4.1.5 Fuel Cell

A fuel cell is an electrochemical cell that produces electricity from a fuel and consists of an anode, a cathode, and an electrolyte. The fuel (hydrogen) is fed to the anode and releases electrons and hydrogen ions (protons). The electrons are conducted to the cathode via an external circuit. The electron current can be utilized to generate electricity. The hydrogen protons move through the electrolyte material to the cathode. Oxygen or air passes through the cathode in the fuel cell, where oxygen is reacted with the hydrogen proton to form water and release heat. A typical fuel cell system consists of three parts: a fuel reformer section, a power

generation section, and a power conditioning section. The heat rejected from the fuel reformer and the power generation section can be recovered and used to drive absorption chillers and heat exchangers to supply hot water and chilled water for building air conditioning systems.

The fuel cell technologies can be classified as Polymer Electrolyte Membrane Fuel Cell (PEMFC), Alkaline Fuel Cell (AFC), Phosphoric Acid Fuel Cell (PAFC), Solid Oxide Fuel Cell (SOFC), and Molten Carbonate Fuel Cell (MCFC), according to their types of electrolyte (EEA, 2008). Characteristics of major fuel cell types are shown in Table 4.1.3. Although solid oxide fuel cells have been used recently in residential applications, PEM fuel cells seem to be the most suitable for residential applications and are the type used in most of the building energy systems currently under development. This is largely due to their relatively low operating temperatures (under 100° C; 212° F) and favourable price (EEA, 2008).

Table 4.1.3 Characteristic of major fuel cell types (EEA, 2008)

	PEMFC	AFC	PAFC	MCFC	SOFC
Type of Electrolyte	H^+ ions (with anions bound in polymer membrane)	OH^- ions (typically aqueous KOH solution)	H^+ ions (H_3PO_4 solutions)	$CO_3^=$ ions (typically, molten $LiKaCO_3$ eutectics)	$O^=$ ions (Stabilized ceramic matrix with free oxide ions)
Typical construction	Plastic, metal or carbon	Plastic, metal	Carbon, porous ceramics	High temp metals, porous ceramic	Ceramic, high temp metals
Internal reforming	No	No	No	Yes, Good Temp Match	Yes, Good Temp Match
Oxidant	Air to O_2	Purified Air to O_2	Air to Enriched Air	Air	Air
Operational Temperature	150- 180°F (65-85°C)	190-500°F (90-260°C)	370-410°F (190-210°C)	1200-1300°F (650-700°C)	1350-1850°F (750-1000°C)
DG System Level Efficiency, percent HHV	25 to 35%	32 to 40%	35 to 45%	40 to 50%	45 to 55%
Primary Contaminate Sensitivities	CO, Sulfur, and NH3	CO, CO_2, and Sulfur	CO < 1%, Sulfur	Sulfur	Sulfur

The advantages of fuel cell technology are its high electrical efficiency, which can be as high as 45% - 55 %, and low emission. Fuel cells are applicable for various purposes, based on the operating temperature levels of the cell. The major disadvantage of a fuel cell is the high price.

A number of system-level PEMFC models are available in the literature. However, many of these focus upon the electrochemical reactions occurring within the stack and neglect the power draws of ancillary devices such as pumps, fans, and controls. In contrast, the lumped parameter model has been derived to facilitate calibration and considers the performance of the coherent unit (Beausoleil-Morrison, et al., 2006). The unit's steady-state electrical and thermal output is characterized by empirical correlations in response to H_2 consumption, cooling water temperature and flow rate.

The heat and power produced by a fuel cell stack are calculated from the electrical and thermal efficiencies.

The electrical and thermal efficiencies of fuel cell are defined based on the lower heating value (LHV) of hydrogen (NREL, 2008). The electrical efficiency of the fuel cell is defined as the electrical power generated divided by the amount of hydrogen consumed :

$$\eta_{e\,fc} = \frac{P_{e\,fc}}{\dot{m}_{h_2} LHV_{h_2}} \tag{4-8}$$

Here $\eta_{e\,fc}$ is the fuel cell's electrical conversion efficiency, $\dot{m}_{h_2}$ is mass flow rate of the consumed hydrogen and LHV_{h_2} is lower heating value of hydrogen. The lower heating value of hydrogen is 120 MJ/kg, which is equal to 33.3 kWh/kg (NREL, 2008). Fuel cell efficiency is a function of the power output and fuel cell's temperature, but in this research the working condition and then the fuel cell's efficiency is considered to be a constant average value. With this assumption the electrical power output from the fuel cell can be derived from the equation:

$$P_{e\,fc} = \eta_{e\,fc} \dot{m}_{h_2} LHV_{h_2} \tag{4-9}$$

Similarly, the thermal efficiency of the fuel cell is defined as the heating power output divided by the amount of hydrogen consumed:

$$\eta_{h\,fc} = \frac{P_{h\,fc}}{\dot{m}_{h_2} LHV_{h_2}} \qquad (4\text{-}10)$$

Here $\eta_{h\,fc}$ is the fuel cell's thermal conversion efficiency. The other variables are the same as expressed above. The electrical power output from the fuel cell can be derived from the equation:

$$P_{h\,fc} = \eta_{h\,fc} \dot{m}_{h_2} LHV_{h_2} \qquad (4\text{-}11)$$

4.1.6 Diesel generator

The conventional diesel generator normally consists of an internal combustion engine, directly coupled to a synchronous generator. A diesel engine converts the chemical energy of the fuel into mechanical energy, which rotates the generator. In the generator, mechanical energy is converted to electrical energy.

The fuel of the engine is normally diesel fuel, but other kind of fuels such as gas, biogas, and hydrogen can be used in the engine.

Skarstein and Uhlen (1989) proposed a linear equation for the diesel generator's fuel consumption:

$$F = F_o + F_i P_{dsl} \qquad (4\text{-}12)$$

Here F (litres/h) is the diesel generator fuel consumption and P_{dsl} (kW) is the diesel generator output power. F_i is a constant and equal to 0.246 (litres/kWh). F_o is proportional to the rated power of the diesel generator (P_{dslr}):

$$F_o = B\, P_{dslr} \qquad (4\text{-}13)$$

Here B is equal to 0.08415 (litres/kWh).

4.2 Energy storage devices

Energy storage in the building integrated energy system includes electrical energy storage, hydrogen storage, heat storage and cool storage. Storage of each type of energy can be based on different technologies. The selection and sizing of the energy storage devices is out of the scope of this research. Some of the technologies that are used in the applications in Chapter 6, including the battery, the hot water tank and the hydrogen tank will be modelled in the following sections. Cooling energy storage, which is used in chilled water systems in order to use cheap night-time electricity, is presented in Appendix B.

4.2.1 Battery

Extra electricity generated in the building energy system from renewables and CHP, and also electricity from the grid (when it is cheaper), can be stored in the building energy system in different ways. Battery (normally a lead-acid battery), the ultracapacitor and the flywheel are used for short term electricity storage. For long term storage of electricity, electricity is used for hydrogen production and then the hydrogen is compressed and stored in cylinders. The stored hydrogen can be converted to electricity by a fuel cell. In the following, the battery energy storage model is derived.

The battery is a device that stores electrical energy in electrochemical form. There are different type of battery on the market including lead-acid, Lithium-Ion, and Nickel–Cadmium. Lead-acid batteries are normally used in buildings and stationary applications.

Different mathematical modelling of batteries has been reported in many studies. Among them, the KiBaM model (Manwell and McGowan, 1993) and the Ampere-hour (Ah) model (like Diaf, et al., 2007 and Ai, et al., 2003) are mostly used. In this research the ampere-hour model is used. In this model, the energy stored in the battery in time step $(t + \Delta t)$ is determined by the following equation:

$$E_{bat}(t+\Delta t) = E_{bat}(t)(1-\sigma) + eP_{bat}\Delta t \qquad (4\text{-}14)$$

Here E_{bat} is the energy stored in the battery, σ is the self discharge rate of the battery, P_{bat} is the power charged to the battery $(P_{bat} > 0)$ or discharged from the battery $(P_{bat} < 0)$ and e is calculated from the following equations:

$$e = \begin{cases} \eta_{bat,ch} & (P_b > 0) \\ \dfrac{1}{\eta_{bat,dch}} & (P_b < 0) \end{cases} \qquad (4\text{-}15)$$

Here the $\eta_{bat,ch}$ and $\eta_{bat,dch}$ are battery charging and discharging efficiency respectively.

The maximum charging power of the battery depends on the energy stored in the battery. In this research, the maximum charging power recommended by the battery manufacturer will be used.

Sometimes the stored energy of the battery is expressed by state of charge (SOC) value. The state of charge of the battery is the ratio (often expressed in %) between the currently stored amount of electricity Q_{bat} and the battery capacity:

$$SOC_{bat} = \frac{Q_{bat}}{Q_{bat,\max}} \qquad (4\text{-}16)$$

Here $Q_{bat,\max}$ (Ah) is the battery capacity, the maximal charge which can be reversibly extracted from the battery.

4.2.2 Hot water tank

Thermal energy can be stored as a sensible heat, latent heat and chemical reaction (adsorption). For sensible heat storage, normally the media is water and a hot water tank is used. The hot water tank can be modelled as a fully-mixed tank and fully-stratified tank (TRNSYS). Thermal performance of a real hot water tank is between these two ideal models.

The fully-mixed hot water tank model is used in this research. In this model, the entire liquid in the tank is assumed to have a uniform temperature which changes with time as a result of the net energy addition or withdrawal during the charge or discharge processes, or due to heat loss to the surrounding. The energy balance for the tank can be written as:

$$E_h(t+\Delta t) = E_h(t) + P_h(t)\Delta t - P_{hloss}\Delta t \qquad (4\text{-}17)$$

Here $E_h(t)$ and $E_h(t+\Delta t)$ are the energy stored in the tank at the end of time steps t and $t+\Delta t$ respectively, $P_h(t)$ is the thermal power charged to or discharged from the tank at the end of time step t, P_{hloss} is the heat loss rate form the tank and Δt is the time step length.

4.2.3 Hydrogen tank

Hydrogen produced by the electrolyser should be stored for later use in the fuel cell, or for fuelling of hybrid vehicles and etc. The mass of hydrogen stored in the tank is calculated by:

$$M_{h_2}(t+\Delta t) = M_{h_2}(t) + (\dot{m}_{h_2 in} - \dot{m}_{h_2 out})\Delta t \qquad (4\text{-}18)$$

Hydrogen can be stored in tanks as compressed gas or cryogenic liquid, in solids (metal hydrides, carbon materials) and in liquid H_2 carriers (methanol, ammonia). Compressed gas storage is common in a large scale stationary application.

If a high pressure electrolyzer is used, the outlet hydrogen could be directly stored in the tank, otherwise a compressor is needed to compress the hydrogen. In addition, the fuelling of vehicles by hydrogen requires higher pressure than the hydrogen storage tank and normally a separate compressor is used for this purpose. Reciprocating compressors or centrifugal compressors are used for hydrogen compression. The power consumption of a compressor depends on the pressure

ratio (between the outlet and inlet of compressor) so with a high pressure electrolyzer this power can be reduced.

The power consumption of the compressor is derived from:

$$P_c = SEC\,\dot{V}_{h_2} \qquad (4\text{-}19)$$

Here SEC is the specific energy consumption of the compressor between the electrolyzer and the H_2 storage tanks (Korpas and Holen, 2006). It is assumed that using an average value for SEC is sufficient, since compressed hydrogen will only require 5%-10% of the total energy consumption of the hydrogen production process.

4.3 Conclusions

In this chapter the mathematical models of several energy converter and energy storage devices were described. These models are steady state and linear models, and these have been used in the modelling of the energy systems in Chapters 5 and 6. The renewable energy and conventional converters can be used for electricity, heating and cooling generation. The need for the electricity for lighting and electrical appliances is common between all buildings. But the heating and cooling of the buildings depends on the climatic conditions. In some climates only heating or only cooling are required, and in some climates both heating and cooling are required. For heat storage, using hot water tanks is common but other kinds of heat storage devices like phase change material can be used. For electricity storage in buildings, the lead acid battery and hydrogen are more suitable. Due to the higher round trip efficiency of batteries they are used for short term storage (one or two days) and hydrogen is used for seasonal electricity storage.

Chapter 5

Supervisory controller design

In this chapter two methods are used for building the energy system modelling and Model Predictive Controller (MPC) design. The first method is based on the multi-period optimization and the second method is based on hybrid model predictive control. The designed controller in the second method can work in implicit or explicit form. In the explicit form inputs are obtained by searching a look up table, therefore an online optimization is not required. In each method, initially the building energy system model is derived and then the controller is designed. These methods are used to develop and validate the supervisory controller (Chapter 6).

The models of the building energy system include multiple energy carrier flows from the grid to the system, renewable energies generated on site, energy conversion, energy storage and multiple energy carrier flows from the system to the building and possibly from the system to the grid. The energy converter models used here are steady-state linear models, since the considered time steps are large enough that the dynamics and transient behaviour of the energy converter during the time step are neglected.

The controller can be designed based on a cost, primary energy or emission objective function but, as it was discussed in Chapter 1, the main aim of the controller is to reduce the cost or the CO_2 emission.

The designed controllers are deterministic controllers, so that renewable energies and building loads are completely predictable. Usually to account for

uncertainty in the predicted values stochastic controllers could be used, however this is out of the scope of this research.

5.1 Concept of supervisory controller

It was explained in Section 2.2 that due to the weather conditions, most of the renewable energies are intermittent. So the extra energy from these renewable sources should be stored and used at a later time when the renewable sources are not available.

In addition, in a multiple energy converter, since the demands for output energies are different, operation set point of the equipment should be determined. For example, in cogeneration systems normally the output heat to power ratio is not the same as the heat to power ratio of the building.

Different energy carriers which are bought from the grids can have different prices at different time of day. For example electricity is cheaper at night. So the energy converters that use electricity for conversion, can use cheaper electricity at night-time and store the converted energy for the next day time. Examples of these kind of converters are the heat pump and the vapour compression chiller.

In a building energy system each of the subsystems that was explained in Chapter 4 has its own local control. The supervisory controller determines the operation set points of these local controllers. If a time period is divided into time steps, according to the above reasons, at each time step the duty of the supervisory controller is to determine:

- How much energy should be charged or discharged from the energy storage device
- Which ones of the low carbon and conventional energy converters should be operated and the appropriate output capacity of the converters
- How much energy should be imported from or exported to the grid

For this purpose at each time step, the supervisory controller measures the current states of the system, and based on a specific objective function, the model of the energy system and its constraints, an optimization problem is solved inside the controller and the optimal control sequence for the next finite number of time steps are determined. The concept of the supervisory controller is shown in Figure 5.1.1.

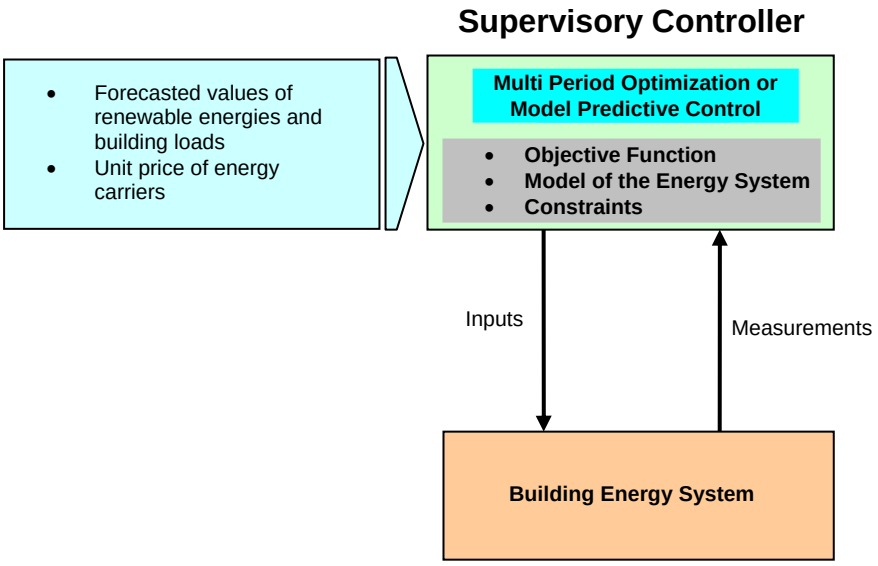

Figure 5.1.1 Concept of supervisory controller

Since the behaviour of the building energy system cannot be exactly predicted by the system's model, and considering the uncertainties in forecasted profiles of the renewable energies and building loads, from the calculated sequence of control inputs only the first time step's inputs are applied to the system. The rest of the control inputs sequence is disregarded. The system then moves to the next time step with evolved states. Based on the new system measurements and updated forecasts, the whole procedure is repeated and a new control inputs sequence is determined. This procedure is repeated in the next time steps.

5.2 Receding horizon multi-period optimization approach

In this approach, a generic model for the system's elements are first derived. Then these models are integrated into the energy buses' model to obtain the whole energy system model. Finally the system model is used for controller design.

5.2.1 Modelling of the energy system

Combined modelling and analysis of energy systems including multiple energy carriers have been studied widely by a research team of the Power Systems and High Voltage Laboratories at the ETH Zurich in the framework of a project named Vision of future energy networks (Favre-Perrod, 2005). The key approach in this project is the so-called energy hub (Geidl, et al., 2007b). An energy hub is considered to be a unit where multiple energy carriers can be converted, conditioned, and stored.

Regarding the dispatch factors that have been used in the energy hub model, this model is a nonlinear mathematical model (Geidl and Andersson, 2007a). So when the model is used for the controller design, the associated optimization problem is a nonlinear and non-convex problem. In nonlinear and non-convex optimization problems, there is uncertainty in finding a global optima (Sweeney, et al., 2009). In addition, solving nonlinear problems is normally difficult and time consuming, which puts a limitation on the online application of the controller.

In this section a linear mathematical model for the building energy system is derived.

The following definitions and notations will be used in the development of the mathematical model of the system, which some of them are based on the research carried out by Geidl and Andersson (2007a).

A set of energy carriers which are entered/exited from the system are considered whose members are denoted by:

$\{\alpha, \beta, \gamma, ..., \omega\} = \{\text{electricity, natural gas, hydrogen,...}\}$

For each energy carrier, an energy bus B is considered, to which all the related system elements are connected:

$B \in \{B_\alpha, B_\beta, B_\gamma, ..., B_\omega\}$

The building energy system has a set of N_{con} numbers of energy converters. Each converter C belongs to this set:

$C \in \{C_1, C_2, ..., C_i, ...C_{N_{con}}\}$

From each energy bus B_α the power that goes to the energy converter is denoted by $P_{\alpha c}$, and the power that comes from the converter to the energy bus is denoted by $Q_{\alpha c}$.

For each energy bus the power that is delivered from the grid is denoted by $P_{\alpha d}$.

For each energy bus the renewable energy power of the same types can be entered. These energies are denoted by R_α and their number is $N_{ren\alpha}$:

$R_\alpha \in \{R_{\alpha 1}, R_{\alpha 2}, ..., R_{\alpha i}, ..., R_{N_{ren\alpha}}\}$

From each energy bus the energy that goes to supply the corresponding building load is shown by $P_{\alpha l}$ and the power that is exported to the grid is shown by $P_{\alpha x}$.

For each energy bus charging/discharging power to/from the storage devices is shown by $P_{\alpha s}$ and the amount of stored energy and storage rate (power) are shown by E_α and $\dot{E}_\alpha$ respectively.

5.2.1.1 Energy converter model

In the following sections a generic model for energy converters is developed. First a converter with single input and single output is modelled. Then the model is generalized for multiple inputs and multiple outputs converters.

5.2.1.2 Single input and single output converter

A single input, single output converter C_i that converts an energy type α to another energy type β is shown in Figure 5.2.1. Steady state power input and power output are indicated by $P_{\alpha ci}$ and $Q_{\beta ci}$ respectively. If the conversion efficiency of the converter is denoted by $\eta_{\alpha\beta}$, the equation between the input and output powers is:

$$Q_{\beta ci} = \eta_{\alpha\beta}^{c_i} P_{\alpha ci} \qquad (5\text{-}1)$$

Figure 5.2.1 Converter with single input and output

As it was stated in Chapter 4, the efficiency of the converter devices are not constant and depend on the input power:

$$\eta_{\alpha\beta}^{c_i} = f(p_{\alpha ci}) \qquad (5\text{-}2)$$

So, in general, the equation (5-1) is a non linear equation. In this research, an average constant efficiency for the converters will be considered; hence the equation (5-1) is a linear equation.

5.2.1.3 Multiple inputs and multiple output converter

A multiple input, multiple output converter system is shown in Figure 5.2.2. An example for this type of converter is a combined heat and power (CHP) unit. In this converter natural gas is normally the input energy carrier and the output energies are electricity and heat.

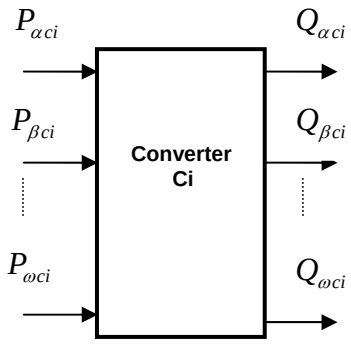

Figure 5.2.2 Converter with inputs $P_\alpha, P_\beta, ..., P_\omega$ and outputs $Q_\alpha, Q_\beta, ..., Q_\omega$.

Similar to equation (5-1), the relation between all inputs and all outputs can be shown by the following matrix equation:

$$\begin{bmatrix} Q_{\alpha ci} \\ Q_{\beta ci} \\ \vdots \\ Q_{\omega ci} \end{bmatrix} = \begin{bmatrix} \eta_{\alpha\alpha}^{c_i} & \eta_{\beta\alpha}^{c_i} & \cdots & \eta_{\omega\alpha}^{c_i} \\ \eta_{\alpha\beta}^{c_i} & \eta_{\beta\beta}^{c_i} & \cdots & \eta_{\omega\beta}^{c_i} \\ \vdots & \vdots & \ddots & \vdots \\ \eta_{\alpha\omega}^{c_i} & \eta_{\beta\omega}^{c_i} & \cdots & \eta_{\omega\omega}^{c_i} \end{bmatrix} \begin{bmatrix} P_{\alpha ci} \\ P_{\beta ci} \\ \vdots \\ P_{\omega ci} \end{bmatrix} \qquad (5\text{-}3)$$

In matrix notation form the above equation can be written as:

$$\mathbf{Q} = \mathbf{\Psi P} \qquad (5\text{-}4)$$

Here $\mathbf{Q}$, $\mathbf{P}$ and $\mathbf{\Psi}$ are the output power vector, the input power vector and the conversion efficiency matrix respectively.

Remark 1

For the converters that were modelled in Section 4.1, in addition to the input power to the converter for the main process, some power is normally needed for the lateral devices inside the converter like the pumps, the control panel and so on. This power is called ancillary or parasitic power and can be considered in the model as energy input with zero output efficiency in the time steps that the energy converter status is on. For simplicity the parasitic power is ignored in the small capacities.

Remark 2

Some thermal equipment like high temperature hot water boilers, steam boilers, combined heat and power units, diesel generators and high temperature fuel cells, especially in large capacities, need to remain on for a minimum number of hours after they started being on. This period is sometimes called the warm up time. During this period the equipment consumes fuel at warm up rate, while the output power from the equipment is zero. In addition, this type of equipment cannot be started again immediately after shutdown. They need some time to stay in shutdown mode, before they can restart again. These conditions can be mathematically modelled, but are not considered in this research.

Remark 3

The diesel generator equation (4-12) shows that the input fuel is the sum of a constant value and a value that is proportional to the output power from the diesel generator. So we use the following model for the fuel consumption:

$$F(t) = F_o \delta(t) + F_i P_{dsl}(t) \qquad (5\text{-}5)$$

Here $\delta(t)$ is a binary variable for each time step that indicates the on status of the diesel generator.

Remark 4

If the input/output powers of the converter are connected to the energy buses through a power conditioner(s), the efficiency of the converter will be multiplied by the efficiency(s) of the interface(s).

5.2.1.4 Renewable energy

A general model for a renewable energy source is shown in Figure 5.2.3. The renewable energy is considered to be connected to the related energy bus through an interface.

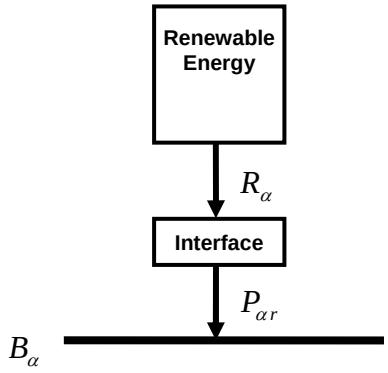

Figure 5.2.3 Model of a renewable energy device.

Through the interface, power may be conditioned and/or converted into another energy carrier (for example from AC to DC). In addition the interface may include a Maximum Power Point Tracking (MPPT) system for the PV panel and wind turbine generators. In the interface, some of the energy is lost due to the efficiency. If we denote the interface efficiency by r_α, the power delivered to the bus is:

$$P_{\alpha r} = r_\alpha R_\alpha \qquad (5\text{-}6)$$

Here R_α is the generated power from the renewables, as described in Chapter 4.

5.2.1.5 Energy Storage

The energy storage device can store energy in one time step and deliver it in other time steps. The amount of energy that is stored in the energy storage device is not equal to the amount of energy that is obtained from it. These losses are due to the physical or chemical processes that take place during the charging and discharging of energy. An energy storage device is shown in Figure 5.2.4. If the charging efficiency is denoted by $\eta_{\alpha ch}$ the amount of energy that is added to the storage in a time step Δt is:

$$E_\alpha(t) - E_\alpha(t-\Delta t) = \int_{t-\Delta t}^{t} \eta_{\alpha ch} P_{\alpha s} dt \qquad (5\text{-}7)$$

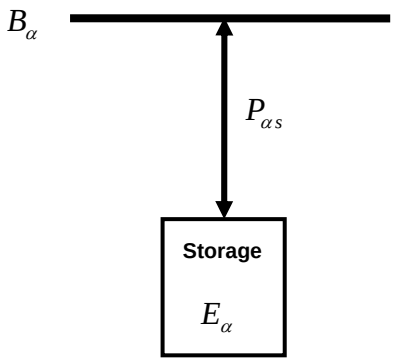

Figure 5.2.4 Model of an energy storage device

In the discharging case if the discharging efficiency is denoted by $\eta_{\alpha dch}$, the amount of stored energy reduction inside the storage device is:

.

$$E_\alpha(t) - E_\alpha(t-\Delta t) = \int_{t-\Delta t}^{t} \frac{1}{\eta_{\alpha dch}} P_{\alpha s} dt \qquad (5\text{-}8)$$

The charging and discharging is a dynamic process and the efficiencies depend on the current energy stored level in the device, E_α, and the rate of charging or discharging, $P_{\alpha s}$. In this study a steady state storage process is assumed, and

average constant values for the charging and discharging efficiencies are used. With this assumption the change of the energy level in the storage device is:

$$E_\alpha(t) - E_\alpha(t-\Delta t) = e_\alpha P_{\alpha s}\Delta t \qquad (5\text{-}9)$$

where :

$$e_\alpha = \begin{cases} \eta_{\alpha ch} & \text{if } P_{\alpha s} \geq 0 \quad \text{(charging/standby)} \\ 1/\eta_{\alpha dch} & P_{\alpha s} < 0 \quad \text{(discharging)} \end{cases} \qquad (5\text{-}10)$$

Remark 1

If the storage device is connected to the energy bus through an interface the charging and discharging efficiencies should be multiplied by the interface efficiencies in the charging and discharging directions respectively. An example for this interface is the charge controller for connecting a lead acid battery to a DC electricity bus.

5.2.1.6 Energy bus model

A general energy bus is shown in Figure 5.2.5. In this figure $\sum_{i=1}^{N_{con}} P_{\alpha ci}$ represents the sum of all power flows from the energy bus B_α to the different energy converters and $\sum_{\forall \alpha}^{\omega}\sum_{i=1}^{N_{con}} Q_{\alpha ci}$ is the sum of all power flows from different energy converters, that convert any type of energy β to the energy type of α, to the energy bus B_α. For this energy bus the energy balance is:

$$P_{\alpha d} = P_{\alpha s} + \sum_{i=1}^{N_{con}} P_{\alpha ci} - \sum_{\forall \alpha}^{\omega}\sum_{i=1}^{N_{con}} Q_{\alpha ci} - \sum_{i=1}^{N_{ren\alpha}} P_{\alpha ri} + P_{\alpha l} + P_{\alpha x} \qquad (5\text{-}11)$$

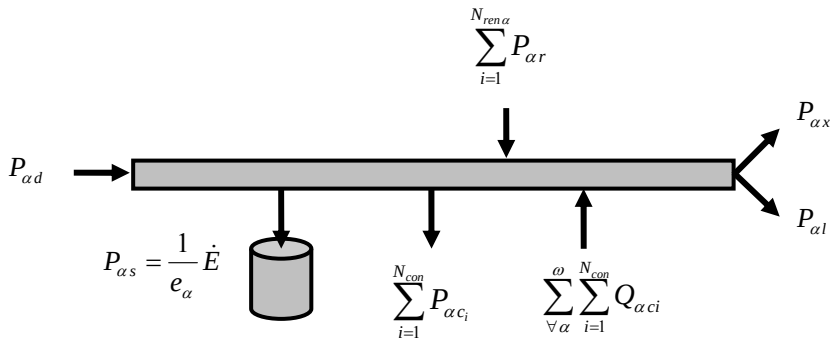

Figure 5.2.5 Energy bus inputs and outputs

By substitution of the different elements from equations (5-3), (5-6) and (5-9) in the equation (5-11) we have:

$$P_{\alpha d}(t) = \frac{E_\alpha(t) - E_\alpha(t-\Delta t)}{e_\alpha \Delta t} + \sum_{i=1}^{N_{con}} P_{\alpha ci}(t) - \sum_{\forall\alpha}^{\omega}\sum_{i=1}^{N_{con}} \eta_{\beta\alpha}^{c_i} P_{\beta ci}(t) - \sum_{i=1}^{N_{ren\,\alpha}} r_\alpha R_{\alpha i}(t) + P_{\alpha l}(t) + P_{\alpha x}(t)$$

(5-12)

Equation (5-12) is a general equation for an energy bus in the system. For modelling of the whole energy system this equation is written for each energy bus. In matrix form the equation is:

$$\mathbf{P_d} = \Phi\dot{\mathbf{E}} + \sum_{i=1}^{N_{con}} \mathbf{P_{c_i}} - \sum_{\forall\alpha}^{\omega}\sum_{i=1}^{N_{con}} \Psi\mathbf{P_{c_i}} - \sum_{i=1}^{N_{ren}} \Omega\mathbf{R}_i + \mathbf{P_l} + \mathbf{P_x} \qquad (5\text{-}13)$$

Here Φ and Ω are the storage efficiency and renewable energies conversion matrices.

Remark 1

If we assume that the time step is one hour and the power unit is kWh then the equation (5-12) is written as:

$$P_{\alpha d}(t)=\frac{E_\alpha(t)-E_\alpha(t-1)}{e_\alpha}+\sum_{i=1}^{N_{con}}P_{\alpha ci}(t)-\sum_{\forall\alpha}^{\omega}\sum_{i=1}^{N_{con}}\eta_{\beta\alpha}^{c_i}P_{\beta ci}(t)-\sum_{i=1}^{N_{ren\alpha}}r_\alpha R_{\alpha i}(t)+P_{\alpha l}(t)+P_{\alpha x}(t)$$

(5-14)

Example:

In the energy system shown in Figure 5.2.6 there are four energy buses namely electricity, natural gas, hot water and hydrogen buses. A PV panel is connected to the electricity bus. A combined heat and power unit (CHP), a boiler, an electrolyzer and a fuel cell are the energy converters. Energy can be stored in hot water and hydrogen storage tanks in the system. Electricity supplies the electrical load of the building, and surplus electricity is converted to hydrogen in the electrolyzer.

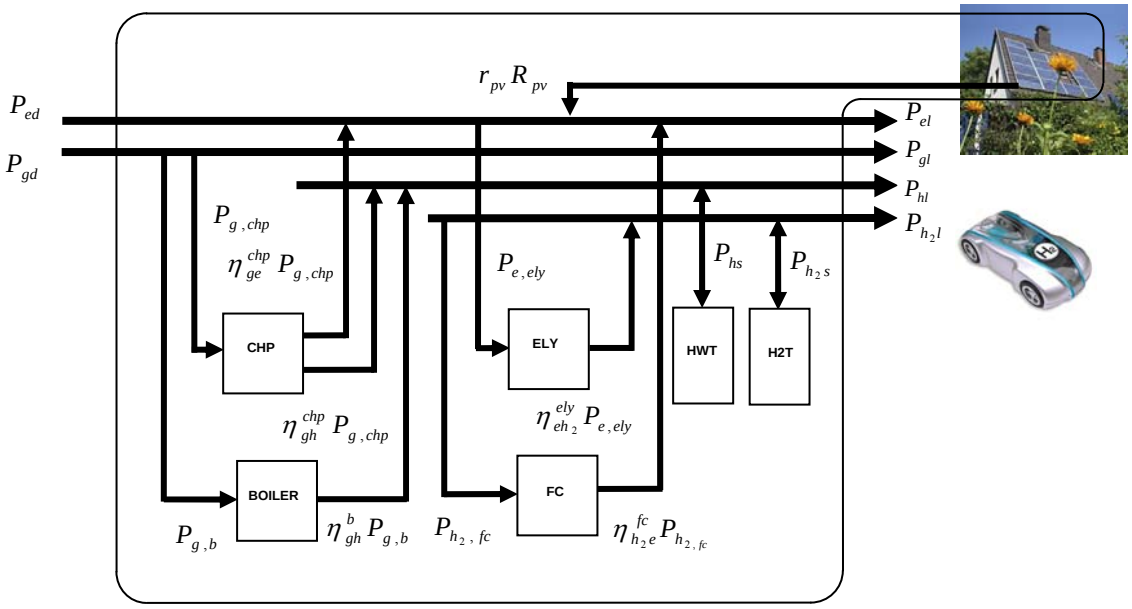

Figure 5.2.6 An example of energy system

Natural gas can be converted to the electricity and heat (hot water) in the CHP unit. In the auxiliary boiler, natural gas is used to prepare hot water. Hot water from the CHP and the boiler supply the heating load of the building including the

space heating load and the domestic hot water demand. Hydrogen can be converted to electricity in the fuel cell, or it can be used for refuelling a hydrogen car.

Equation (5-12) for each of the energy buses is:

For the electricity bus:

$$P_{e\,d}(t) = 0 + P_{e,ely}(t) - [\eta_{ge}^{chp} P_{g,\,chp}(t) + \eta_{h_2 e}^{fc} P_{h_2,\,fc}(t)] - r_{pv} R_{pv}(t) + P_{el}(t) + 0$$

$$P_{e\,d}(t) = P_{e,ely}(t) - [\eta_{ge}^{chp} P_{g,\,chp}(t) + \eta_{h_2 e}^{fc} P_{h_2,\,fc}(t)] - r_{pv} R_{pv}(t) + P_{el}(t)$$

For the gas bus:

$$P_{g\,d}(t) = 0 + P_{g,\,chp}(t) + P_{g,\,b}(t) - 0 - 0 + P_{g\,l}(t) + 0$$

$$P_{g\,d}(t) = P_{g,\,chp}(t) + P_{g,\,b}(t) + P_{g\,l}(t)$$

For the hot water bus:

$$0 = \frac{E_h(t) - E_h(t-\Delta t)}{e_h \Delta t} + 0 - [\eta_{gh}^{chp} P_{g,\,chp}(t) + \eta_{gh}^{b} P_{g,\,b}(t)] - 0 + P_{hl}(t) + 0$$

$$\frac{E_h(t) - E_h(t-\Delta t)}{e_h \Delta t} - [\eta_{gh}^{chp} P_{g,\,chp}(t) + \eta_{gh}^{b} P_{g,\,b}(t)] + P_{hl}(t) = 0$$

For the hydrogen bus:

$$0 = \frac{E_{h_2}(t) - E_{h_2}(t-\Delta t)}{e_{h_2} \Delta t} + P_{h_2,\,fc}(t) - \eta_{eh_2}^{ely} P_{e,\,ely}(t) - 0 + P_{h_2 l}(t) + 0$$

$$\frac{E_{h_2}(t) - E_{h_2}(t-\Delta t)}{e_{h_2} \Delta t} + P_{h_2,\,fc}(t) - \eta_{eh_2}^{ely} P_{e,\,ely}(t) + P_{h_2 l}(t) = 0$$

5.2.2 Control problem formulation

The optimal supervisory controller works based on constrained optimization techniques. A constrained optimization problem has one or multiple objective functions and a set of constraints (Section 2.4). In controlling an energy system,

several objective functions can be regarded. In this research three types of objective function are explained, which are minimized by the optimization for control purposes: the economic objective function, the emission objective function and the primary energy objective function.

Due to the linear model of the system components, the optimization problem is a Mixed Integer Linear Problem (MILP) (Section 2.4.4). The integer (binary) variables are associated with start/stop or charge/discharge modes of the operation of the system components. In addition, the occurrence of events in the system is linked by integer (binary) variables; for example, reaching a maximum output of a CHP unit is linked to the sequential operation of auxiliary boiler. The results of the optimization are the optimal power flows and optimal energy storage levels in the system in time steps.

In the online operation the controller works according to the receding horizon strategy. At each time step k, the controller initially evaluates the current states of the system. Then it calculates the optimal power flows in the system for the next N-1 time steps. Only the control variables computed for the first time step are then applied to the system and the remaining are disregarded. The system then transfers to the next time step (k+1), after which the cycle is repeated.

5.2.2.1 Economic objective function

The economic objective function is the total sum of running costs and profits. The running costs include the energy carriers' costs, the operation and maintenance (O&M) costs and the replacement cost.

The energy carrier costs depend on the various energy suppliers charging tariffs. In the UK the main six energy suppliers (British Gas, EDF, E.on, NPower, Scottish Power and SSE) have different tariffs for electricity and gas. Generally a household is charged one level (unit 1 price) until they reach a pre-specified consumption level (split level), and then the rate switches to a lower level (unit 2 price). However, some tariffs have a fixed daily rate instead which must be paid regardless of how much energy is consumed (standing charge). An electricity tariff

may also consider different prices for night and day times. Table A.3 in Appendix A shows the prices of electricity and gas in the UK which have been used in this research.

There are different tariffs for the district heating price. Normally the price includes a fixed part which is depend on the heating power required by the consumer and a varying part which is dependent on consumption in various months of the year. The district heating price is given to the supervisory controller according to the contract between the supplier and the consumer.

The operation and maintenance (O&M) costs and the replacement costs of the equipment depend on the number of hours that the equipment are in operation. The hourly O&M cost can be obtained from the manufacturer's specification. The hourly replacement cost is equal to the replacement cost divided by the lifetime of the equipment.

The power from the renewable energy generators is free. The maintenance cost of these generators is low, and it is neglected in this research. The replacement cost is normally constant and is independent of the operation of the generator, so it can be omitted from the economical objective function.

The profits are the revenue obtained from selling off the energy to the grid. In small applications only electricity can be sold to the grid. The price of the exported electricity is determined based on the contract.

Considering the above costs and profits, the objective function that should be minimized is the sum of the costs minus the profits in N time periods:

$$J = \sum_{\forall \alpha}^{\omega} \sum_{t=1}^{N} C_{\alpha d} P_{\alpha d}(t) - C_{\alpha x} P_{\alpha x}(t) + \sum_{i=1}^{N_{con}} \sum_{t=1}^{N} (C_{O\&Mci} + \frac{C_{repci}}{LT}) \delta_{onCi}(t) \qquad (5\text{-}15)$$

Here $C_{\alpha d}$ and $C_{\alpha x}$ are the unit price of energy carrier bought from the grid and the unit price of the energy sold to the grid respectively. $C_{O\&M}$, C_{rep} and LT are the

hourly O&M cost, the replacement cost and the lifetime (hours) of the energy converter respectively.

Remark 1

The O&M and replacement costs are normally small in comparison with the energy consumption cost, so for simplicity they are omitted:

$$J = \sum_{\forall \alpha}^{\omega} \sum_{t=1}^{N} C_{\alpha d} P_{\alpha d}(t) - C_{\alpha x} P_{\alpha x}(t) \qquad (5\text{-}16)$$

Remark 2

According to the feed-in tariff and the renewable heat incentive, there are payments for the consumption of electricity and heat which are generated by microgeneration and renewable sources, which should be considered in equation 5-15 as profits.

Remark 3

The replacement cost of the energy storage device is normally very small in comparison with the other costs, except in the case of electricity storage by battery. If there is a battery in the energy system, its wear cost should be added to the economic objective function.

The battery life depends on the number of charging-discharging cycles and how deeply the battery is discharged.

Assume that during the lifetime of a battery a fixed amount of energy can be cycled through the battery before it needs replacing. This amount of energy is called "lifetime throughput" in NREL (2008). The battery wear cost C_{bw} (£/kWh) is the degradation cost that is caused by the cycling of a unit energy through the battery and can be calculated as:

$$C_{bw} = \frac{C_{rep,bat}}{N_{bat} Q_{lifetime} \sqrt{\eta_{rt}}} \qquad (5\text{-}17)$$

Here $C_{rep,bat}$ is the replacement cost of the battery bank, (£), N_{bat} is the number of batteries in the bank and η_{rt} is the battery roundtrip efficiency (fractional). $Q_{lifetime}$ is the lifetime throughput of a single battery, (kWh), and is calculated by converting the maximum capacity of the battery from Ah to kWh and multiplying it by the depth of discharge and the number of cycles to failure (NREL, 2008):

$$Q_{lifetime} = f_i \left(\frac{d_i}{100} \right) \left(\frac{Q_{bat,\max} V_{nom}}{1000} \right) \qquad (5\text{-}18)$$

Here f_i is the number of cycles to failure, d_i is the depth of discharge, (%), $Q_{bat,\max}$ is the maximum capacity of the battery, (Ah) and V_{nom} is the nominal voltage of the battery, (V).

5.2.2.2 Emission objective function

The emission objective function is the sum of CO_2 emissions related to the different energy carrier consumption. The emission of CO_2 for each energy carrier is determined by the multiplication of the energy consumption by the emission coefficient. In the case of onsite energy production and exportation to the outside of the site, the equivalent emission should be subtracted.

$$J = \sum_{\alpha}^{\omega} \sum_{t=1}^{N} K_{\alpha d} P_{\alpha d}(t) - K_{\alpha x} P_{\alpha x}(t) \qquad (5\text{-}19)$$

Here $K_{\alpha d}$ and $K_{\alpha x}$ are the CO_2 emission factors for delivered and exported energy of type α respectively. These coefficients are not necessarily the same. The emission factor of some fuels are shown in Table A.3 in Appendix A. For the net electricity exported to the grid the factor is that for grid-displaced electricity (SAP 2009).

5.2.2.3 Primary energy objective function

Primary energy is the energy from natural resources such as coal, crude oil, natural gas, uranium, sunlight and wind which has not yet undergone any conversion and

transmission to the end user (building). Primary energy is subdivided into renewable/non renewable or into fossil/non-fossil primary energy.

Primary energy is converted in the power plants to electricity and transmitted by power lines. Natural gas is pressurized by a compressor and transmitted in pipe lines. The amount of end used energy can be converted to the equivalent primary energy by multiplying by the primary energy factor. This factor is ratio of input primary energy to the delivered energy to the end user (SAP 2009). The primary energy factor for electricity is dependent on the type of electricity generation in each country. If transmission losses, or the energy required for transmission is considered, the boundary of the system (buses) will be extended to the power plants or terminals and we should add the equivalent primary energy of the transmission as well. In case of onsite energy production and exportation to the outside of the site, the related primary energy equivalent should be subtracted.

The primary objective function can be written as:

$$J = \sum_{\alpha}^{\omega} \sum_{t=1}^{N} f_{\alpha d} P_{\alpha d}(t) - f_{\alpha x} P_{\alpha x}(t) \qquad (5\text{-}20)$$

Here $f_{\alpha d}$ and $f_{\alpha x}$ are the primary energy factors for delivered and exported energy of type α respectively. These coefficients are not necessarily the same. For example in the case of electricity, the exported electricity may be considered to be in competition against other new (high efficiency) electricity plants and/or may be considered as saving off-peak load rather than base load, while the delivered electricity in most countries is regarded as the national mix of existing plants that deliver to the grid. Primary energy factors of the UK's energy sources are shown in Table A.3 in Appendix A.

5.2.2.4 Constraints

The equality constraint of the optimization problem is the energy balance for each energy bus as described by equation (5-13).

The inequality constraints are the upper ($\bar{}$) and lower ($\underline{}$) limit of the power flows and storage levels:

$$\underline{\mathbf{P}_{\mathbf{d}}} \le \mathbf{P}_{\mathbf{d}} \le \overline{\mathbf{P}_{\mathbf{d}}} \quad (5\text{-}21a)$$

$$\underline{\mathbf{P}_{\mathbf{x}}} \le \mathbf{P}_{\mathbf{x}} \le \overline{\mathbf{P}_{\mathbf{x}}} \quad (5\text{-}21b)$$

$$\underline{\mathbf{P}_{\mathbf{c}_i}} \le \mathbf{P}_{\mathbf{c}_i} \le \overline{\mathbf{P}_{\mathbf{c}_i}} \quad (5\text{-}21c)$$

$$\underline{\dot{\mathbf{E}}} \le \dot{\mathbf{E}} \le \overline{\dot{\mathbf{E}}} \quad (5\text{-}21d)$$

$$\underline{\mathbf{E}} \le \mathbf{E} \le \overline{\mathbf{E}} \quad (5\text{-}21e)$$

5.3 Hybrid Model Predictive Control (MPC) approach

In this approach, a general model for the hybrid dynamic system is initially explained. Then a Constrained Finite-Time Optimal Control (CFTOC) problem is described in order to find the optimal input sequence, which minimizes the performance criteria and satisfies the constraints. The CFTOC problem is solved in each time step and the controller works in a receding horizon manner.

5.3.1 Modelling of renewable and low carbon energy system

In hybrid dynamic system approach the building renewable energy system is described by a combination of Linear Time Invariant (LTI) differential and algebraic equations. In this section a state space model for the building integrated renewable and low carbon energy system is considered.

In the building integrated energy system usually continuous and discrete dynamics exists together. For example the charging and discharging of a battery is a continuous dynamic but switching between charging and discharging modes is a discrete event. For this reason the state space model is extended to the hybrid dynamic model.

5.3.1.1 State Space Model

The behaviour of continuous dynamic systems can be described by the following state space equations:

$$\begin{aligned} \dot{x}(t) &= f(x(t), u(t)) \\ y(t) &= g(x(t), u(t)) \end{aligned} \qquad (5\text{-}22)$$

For the linear time invariant systems the above equations can written as:

$$\begin{aligned} \dot{x}(t) &= Ax(t) + Bu(t) \\ y(t) &= Cx(t) + Du(t) \end{aligned} \qquad (5\text{-}23)$$

For the model predictive control, the system equations are often used in the discretized form:

$$\begin{aligned} x(k+1) &= Ax(k) + Bu(k) \\ y(k) &= Cx(k) + Du(k) \end{aligned} \qquad (5\text{-}24)$$

In the building energy system the inputs are the operation set points of the energy converters and the charging/discharging power of the energy storage devices. The states are the energy stored, and the outputs are the building's loads.

5.3.1.2 Hybrid Dynamic Model

Hybrid dynamic systems are systems consisting of continuous-time and discrete-event components that interact with each other. In the model of hybrid dynamic systems the continuous-time component is related with physical first principles and the discrete-event component with logic devices, such as switches, mode selectors and digital circuitry.

Discrete Hybrid Automata (DHA) (Torrisi and Bemporad, 2004) is one of the general modelling formats for hybrid systems. In DHA a finite state machine and a

switched linear dynamic system are interconnected through a mode selector and an event generator, Figure 5.3.1.

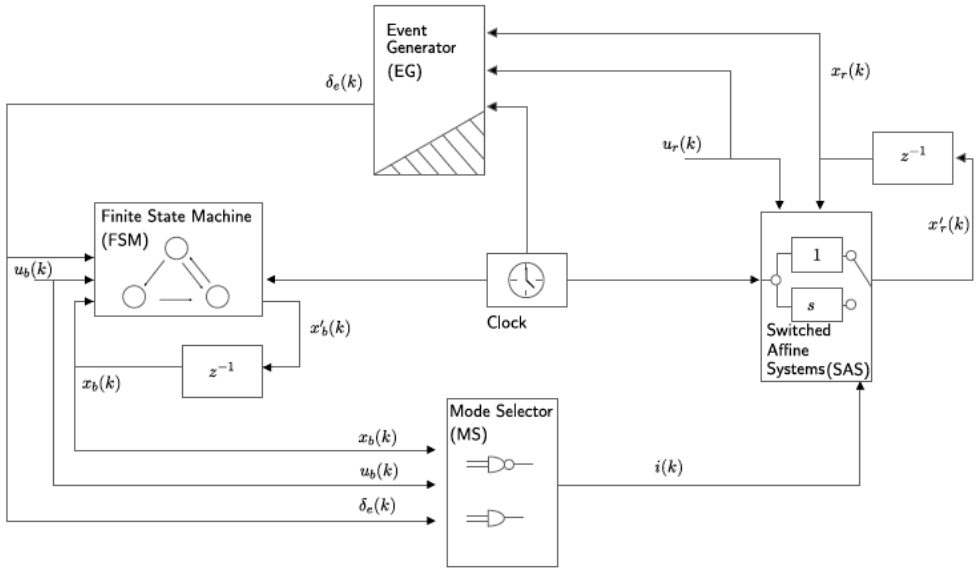

Figure 5.3.1 A discrete hybrid automaton (DHA) (Torrisi and Bemporad, 2004)

A switched affine system (SAS) is a collection of linear affine systems:

$$\begin{aligned} x_r(k+1) &= A_{i(k)}x_r(k) + B_{i(k)}u_r(k) + f_{i(k)} \\ y_r(k) &= C_{i(k)}x_r(k) + D_{i(k)}u_r(k) + g_{i(k)} \end{aligned} \tag{5-25}$$

An event generator (EG) is an object that generates a logic signal according to the satisfaction of a linear affine constraint of states and inputs:

$$\delta_e(k) = f_H(x_r(k), u_r(k), k) \tag{5-26}$$

A finite state machine (FSM), which is also called an automaton, is a discrete dynamic process, where the logical states evolve based on a logical state update function:

$$x_b(k+1) = f_B(x_b(k), u_b(k), \delta_e(k)) \tag{5-27}$$

A FSM can also have an associated Boolean output:

$$y_b(k) = g_B(x_b(k), u_b(k), \delta_e(k)) \tag{5-28}$$

The mode selector (MS) selects the dynamic mode $i(k)$ of the SAS according to a Boolean function consisting of the logic state $x_b(k)$, the Boolean inputs $u_b(k)$, and the events $\delta_e(k)$. The output of this function:

$$i(k) = f_M(x_b(k), u_b(k), \delta_e(k)) \tag{5-29}$$

is called the active mode.

Analysis and control design based on the DHA model often results in computationally complex and difficult problems. Therefore the DHA models are transferred to two special hybrid formats. These formats are Piecewise Affine and Mixed Logical Dynamic system formats.

Piecewise Affine (PWA) systems (Sontag, 1981) are defined by partitioning the state space into polyhedral regions. In each region, the system is associated with a distinct linear affine state-update equation:

$$\begin{aligned} x(k+1) &= A_{i(k)}x(k) + B_{i(k)}u(k) + f_{i(k)} \\ y(k) &= C_{i(k)}x(k) + D_{i(k)}u(k) + g_{i(k)} \\ i(k) &\text{ such that } H_{i(k)}x(k) + J_{i(k)}u(k) \le K_{i(k)} \end{aligned} \tag{5-30}$$

Here $H_{i(k)}x(k) + J_{i(k)}u(k) \le K_{i(k)}$ is a polyhedral partition.

The discrete part of hybrid systems is considered as logical statements. The logical statements can be transformed into mixed integer linear non equalities. The combination of these linear non equalities and LTI state space equations can be

described by the following equalities and non equalities, and this is called the Mixed Logical Dynamic (MLD) format (Bemporad and Morari, 1999):

$$x(k+1) = Ax(k) + B_1u(k) + B_2\delta(k) + B_3z(k) \quad (5\text{-}31a)$$

$$y(k) = Cx(k) + D_1u(k) + D_2\delta(k) + D_3z(k) \quad (5\text{-}31b)$$

$$E_2\delta(k) + E_3z(k) \le E_1u(k) + E_4x(k) + E_5 \quad (5\text{-}31c)$$

Here $x(k) = \begin{bmatrix} x_c(k) \\ x_b(k) \end{bmatrix}$ is the state vector, $x_c(k) \in \mathrm{R}^{n_c}$ and $x_b(k) \in \{0,1\}^{n_b}$, $y(k) = \begin{bmatrix} y_c(k) \\ y_b(k) \end{bmatrix} \in \mathrm{R}^{p_c} \times \{0,1\}^{p_b}$ is the output vector, $u(k) = \begin{bmatrix} u_c(k) \\ u_b(k) \end{bmatrix} \in \mathrm{R}^{m_c} \times \{0,1\}^{m_b}$ is the input vector, $z(k) \in \mathrm{R}^{r_c}$ and $\delta(k) \in \{0,1\}^{r_b}$ are auxiliary variables, A, B_i, C, D_i, and E_i denotes real constant matrices, E_5 is a real vector, $n_c > 0$ and p_c, $m_c, r_c, n_b, p_b, m_b, r_b \ge 0$.

5.3.2 Hybrid MPC design

Model predictive control theory (Section 2.3.5) can be used to control hybrid systems (Bemporad and Morari, 1999). In this case, controller tries the output $y(t)$ to track a reference output signal y_r. The corresponding references for the state, input, and auxiliary variables are denoted by x_r, u_r, z_r respectively. The current time step is represented by t, and the current state is represented by $x(t)$. The following CFTOC problem is defined:

$$\min_{\{u,\delta,z\}_o^{N-1}} J(\{u,\delta,z\}_0^{N-1}, x(t)) \equiv \left\|Q_{xN}(x(N|t) - x_r)\right\|_p + \sum_{k=1}^{N-1}\left\|Q_x(x(k) - x_r)\right\|_p + \\ + \sum_{k=0}^{N-1}\left\|Q_u(u(k) - u_r)\right\|_p + \left\|Q_z(z(k|t) - z_r)\right\|_p + \left\|Q_y(y(k|t) - y_r)\right\|_p \quad (5\text{-}32a)$$

$$\text{subj. to}\begin{cases} x(0|t) &= x(t) \\ x(k+1|t) &= Ax(k|t)+B_1u(k)+B_2\delta(k|t)+B_3z(k|t) \\ y(k|t) &= Cx(k|t)+D_1u(k)+D_2\delta(k|t)+D_3z(k|t) \\ E_2\delta(k|t) &+ E_3z(k|t) \le E_1u(k)+E_4x(k|t)+E_5 \\ u_{\min} &\le u(t+k) \le u_{\max},\ k=0,1,...,N-1 \\ x_{\min} &\le x(t+k|t) \le x_{\max},\ k=0,1,...,N \\ y_{\min} &\le y(t+k) \le y_{\max},\ k=0,...,N-1 \\ S_x x(N|t) &\le T_x \end{cases} \qquad \text{(5-32b)}$$

Here N is the optimal control interval, $x(k|t)$ is the state predicted at time $t+k$ resulting from input u to the system (5-31) starting from the initial state $x(0|t)=x(t)$. $u_{\min}$, $u_{\max}$, $y_{\min}$, $y_{\max}$ and $x_{\min}$, $x_{\max}$ are hard bounds on the inputs, outputs, and states respectively, and $\{x : S_x x \le T_x\}$ is the final target polyhedral subset of the state space R^n. Q_{xN}, Q_x, Q_u, Q_z and Q_y are weighting matrices. For the control of the building integrated renewable and low carbon energy system Q_u is determined by fuel costs or emission factors (Sections 5.2.2.1 and 5.2.2.2), and other weighting matrices are determined by appropriate penalty values. N is predictions horizon and p is norm, that can be 2, 1 or infinity.

It is assumed that for the current time $k=0$ and the initial state of the building integrated renewable and low carbon energy system, $x(0|t)=x(t)$, the optimal solution $\{u_t^*(0),\ldots,u_t^*(N-1),\delta_t^*(0),\ldots,\delta_t^*(N-1),z_t^*(0),\ldots,z_t^*(N-1)\}$ exists. According to the receding horizon idea, the first series of inputs are applied to the system:

$$u(t)=u_t^*(0) \qquad \text{(5-33)}$$

and the subsequent optimal inputs $u_t^*(1),\ldots,u_t^*(N-1)$ are ignored. By repeating the above optimization procedure at time step $t+1$, the control problem (5-32)-(5-33) will provide an extension of MPC to the hybrid model of the building integrated renewable and low carbon energy system.

5.3.3 Explicit MPC

By parametrically solving the CFTOC problem (5-32) we can obtain an explicit solution of the optimal control inputs sequence $U_N^*(x_0) = [u_0^*,...,u_{N-1}^*]$ as a PWA function of the form (Kvasnica, et al., 2004):

$$U_N^*(x_0) = F_r x_0 + G_r \text{ if } x_0 \in P_r \text{ for } P_r = \{x_0 \,|\, H_r x \le K_r\},\ r = 1,...,R \qquad (5\text{-}34)$$

Here P_r is a polyhedral region and R defines the total number of active regions i.e. the region contains the given state x_0, over which such a function is defined.

So for a given state measurement $x_0 = x(t)$, the actual $U_N^*(x_0)$ is obtained by evaluating the PWA function (5-34) and no additional optimization is required. Such a function evaluation can usually be implemented using simple control hardware rather than using a computer, which is normally required for the optimization. Once $U_N^*(x_0)$ is obtained it can be used to perform the MPC in a receding horizon manner in real time.

5.4 Net present value of the supervisory controller

The net present value (NPV) method converts the excess of benefits over costs occurring at different times, where all amounts are discounted for their present value (Kreith and Goswami, 2007). When this method is used for evaluating a cost-reducing investment, the cost savings are the benefits, and it is often called the Net Saving method.

The NPV from an investment, like a new supervisory control system, is calculated by the following equation:

$$NPV_{A1:A2} = \sum_{t=0}^{N} \frac{(B_t - C_t)}{(1+d)^t} \qquad (5\text{-}35)$$

Here $NPV_{A1:A2}$ is the net present value of benefits (benefits or savings net of present value costs) for the alternative A1 as compared with the alternative A2, B_t is the benefits in year t, which may be defined to include energy savings, C_t is the cost in year t associated with the alternative A1 as compared with a mutually exclusive alternative A2, and d is the discount rate.

For the supervisory controller, the alternatives A1 and A2 are the optimal and non-optimal supervisory control system respectively, so the benefit is determined by the total reduction of the operational cost of the building energy system, which is achieved by the utilization of the optimal controller instead of a non-optimal controller.

The non-optimal controller depends on the application. For each application a different control system has been studied in the literature; some of these were explained in Section 2.3.

To calculate the benefits of the supervisory controller in year t, the operation of the controller is simulated based on the weather data and the load profiles of a typical year. The difference of the operational cost of the system with two alternative controllers is the benefit of utilization of the optimal controller. The initial benefits ($t = 0$) are zero.

The cost in year t is the maintenance cost of the two alternative control systems. This cost for $t = 0$ is the difference of the initial cost of the two control systems.

For simplicity, in the applications 1 and 2 in Chapter 6 only the value of the supervisory controller is calculated in a typical day. The yearly value of the controller can be calculated with a whole-year simulation or roughly by multiplying the typical day value by the number of typical days in the year.

Although the direct implication of using the optimal supervisory controller is the reduction of the operational cost of the system, the indirect implications can be

the decrease in CO_2 emission at the national and international level and an increase in the job market in the related industries.

5.5 Conclusions

In this chapter two methods for the modelling of a general building integrated renewable and low carbon energy system were derived. The first method was based on the mathematical modelling of the energy system by assuming a steady state model of the components. The second method was based on the hybrid dynamical model of the energy system. A separate controller was designed based on each modelling approach. Using the first modelling method, the control problem was solved with the multi-period optimization and using the second modelling method, the control problem was solved based on the hybrid MPC. In both approaches it was assumed that the weather data and building load are completely predictable for the time horizon in which the control problem is solved.

Both of the modelling methods and controller designs are unified (generic), and can be used in different building integrated renewable and low carbon energy applications.

Chapter 6

Applications

In this chapter, three applications of the supervisory controller for building energy systems are considered. These applications are selected from different applications of the building integrated renewable and low carbon energy systems to represent three categories: a low carbon energy system, a hybrid renewable power system and a stand-alone hybrid power system. In application 1, the building energy system consists of a micro combined heat and power (micro-CHP), a boiler (or auxiliary heat) and a hot water storage tank. In application 2, the building energy system consists of PV panels, a diesel generator and a battery bank. In application 3, the building energy system consists of PV panels, a battery bank, an electrolyzer and a fuel cell. For comparison of the controllers' performance, in application 1 the controller has been designed based on the multi-period optimization and hybrid MPC methods. For brevity, in applications 2 and 3 the controller has been designed only by the multi-period optimization method.

6.1 Application 1

In this application, a 3 bedroom detached house is considered which is located in the UK. The energy system of the house consists of a modulating micro-CHP and a modulating supplementary boiler, which are connected in series and located in one package. The package is connected in parallel with a hot water storage (buffer) tank. Figure 6.1.1 shows a simplified diagram of the system. The auxiliary boiler gets started sequentially if the heating output from the micro-CHP is in maximum limit, and there is more heat demand. Figure 6.1.2 shows the sequence of operation of the micro-CHP system (BAXI, 2010). Heat from the micro-CHP unit and the

boiler is delivered to the storage tank. For space heating, hot water is supplied from the storage tank with a pump and supply and return pipes. Domestic hot water is supplied with a heat exchanger that transfers heat from the hot water tank to the cold water coming from the water mains. It is assumed that heat loss from the hot water storage tank is negligible and the charging and discharging efficiency of the tank is 100%. The system is connected to the electricity grid with a two-way electrical meter, and can buy electricity from the grid or sell electricity to the grid.

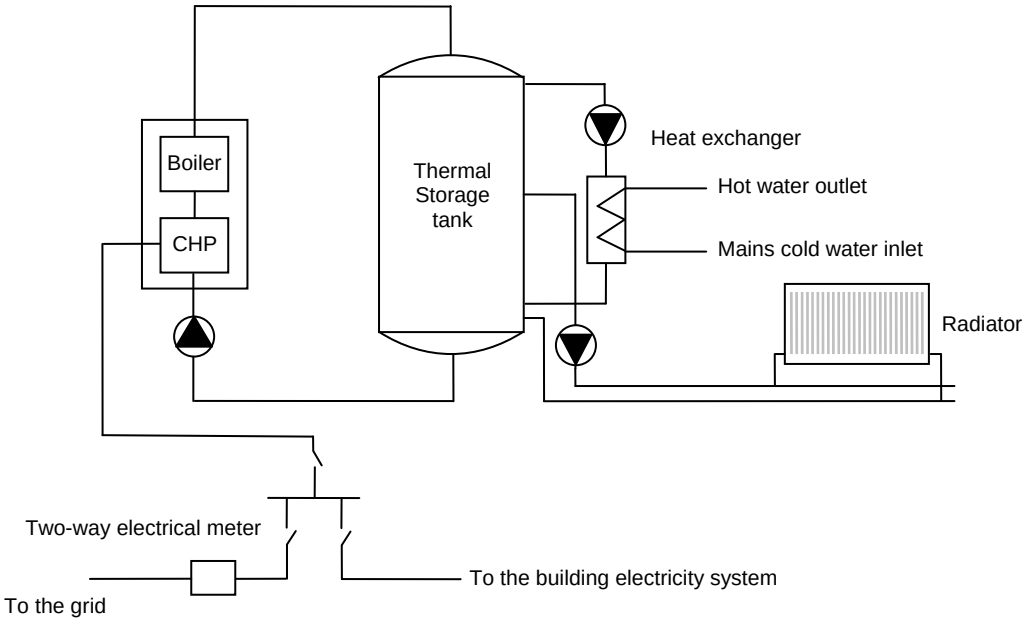

Figure 6.1.1 Diagram of the micro-CHP system

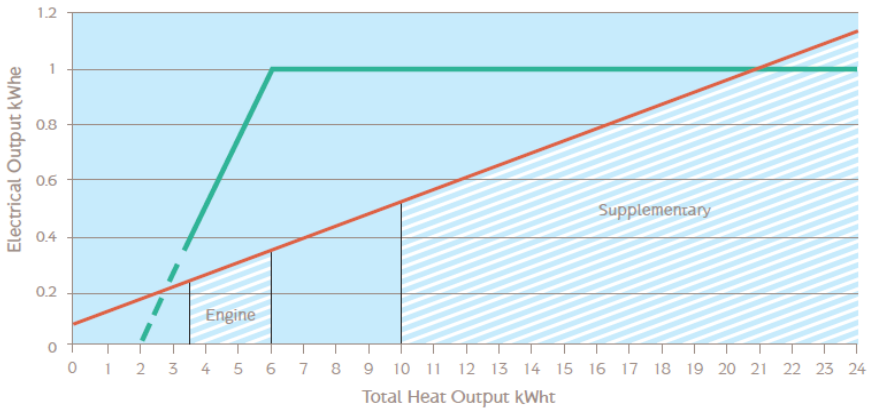

Figure 6.1.2 Relationship between heat and electrical outputs (BAXI, 2010)

The main specifications of the pieces of equipment are shown in Table-6.1.1. The electrical and thermal efficiencies of the micro-CHP and the thermal efficiency of the boiler depend on the operation point, but in this application average efficiency values are used.

Table 6.1.1 Specifications of the equipment in Application 1

Micro-CHP	
Thermal performance	
Engine min heat input (net)	3.7 kW
Engine max heat input (net)	7.7 kW
Engine electrical efficiency (average)	0.1
Engine thermal efficiency (average)	0.8
Auxiliary boiler min heat input (net)	3.8
Auxiliary boiler max heat input (net)	18
Auxiliary boiler efficiency	1.0
Electrical performance	
Electric output min	0.3 kW
Electric output max	1.0 kW
Hot water storage tank	
Hot water tank min energy storage	0
Hot water tank max energy storage	4 kWh
Charging rate max	3 kW
Discharging rate max	3 kW

The water temperature in the hot water storage tank is between 60 and 80 °C, so for storing 4kWh thermal energy a net volume of 176 litres is needed.

Electrical, space heating and domestic hot water heating loads of the 3 bedroom detached house for a typical winter's day are shown in Figures 6.1.3 and 6.1.4 respectively (Abu-Sharkh, et al., 2006).

According to the feed-in tariff in the UK, the payment for the generated electricity with micro-CHP which is consumed in the house is 10.2 p/kWh, and the payment for the generated electricity with micro-CHP which is sold to the grid is 3.1 p/kWh (Table A.1).

The price of the electricity which is bought from the grid is 11.46 p/kWh and the price of the natural gas is 3.1 p/kWh (based on higher heating value).

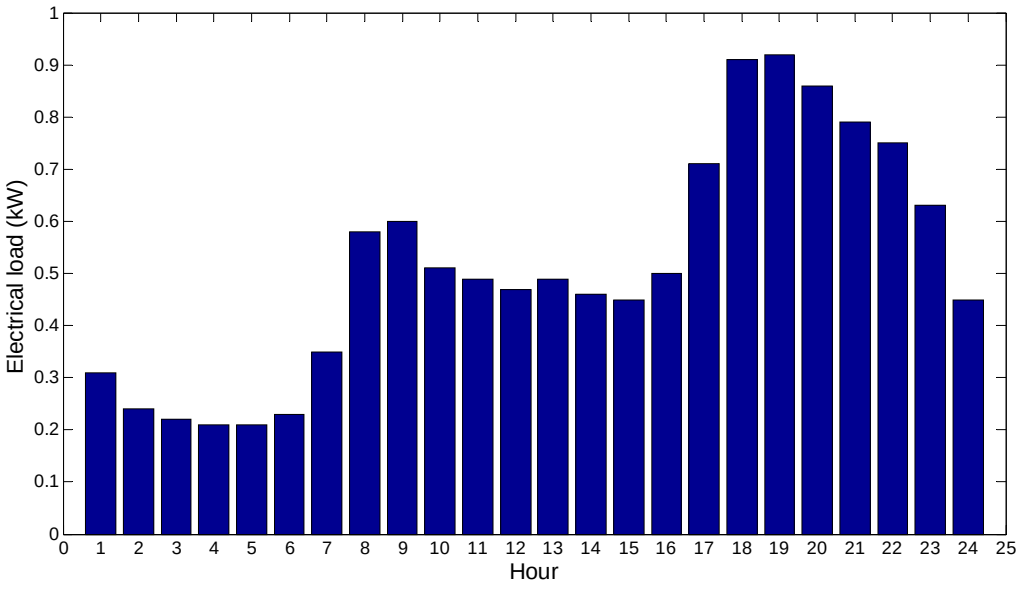

Figure 6.1.3 Electrical load of the house

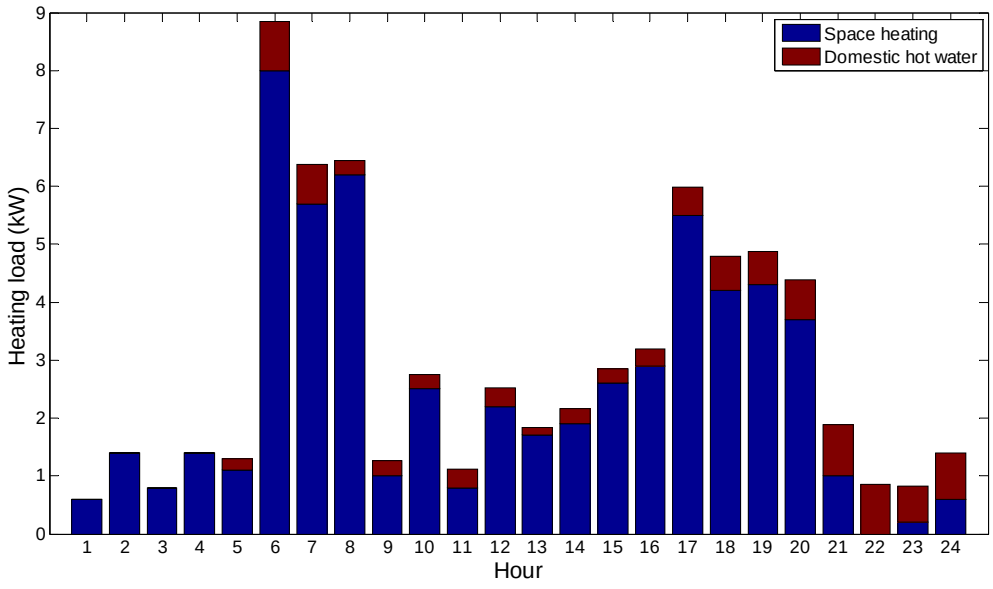

Figure 6.1.4 Space heating and domestic hot water load of the house

For designing the supervisory model predictive controller for this energy system, the following two approaches, explained in Chapter 5, are used:

6.1.1 Multi-period optimization approach

The diagram of the system (Figure 6.1.1) has been redrawn based on the unified modelling method explained in Section 5.2 and is shown in Figure 6.1.5. There are three energy buses in the system. These buses are the electricity bus, the natural gas bus and the hot water bus. The electricity bus starts from the grid and ends in the building and grid. The natural gas bus starts from the grid and ends in the energy system. The hot water bus starts from the energy system and ends in the building.

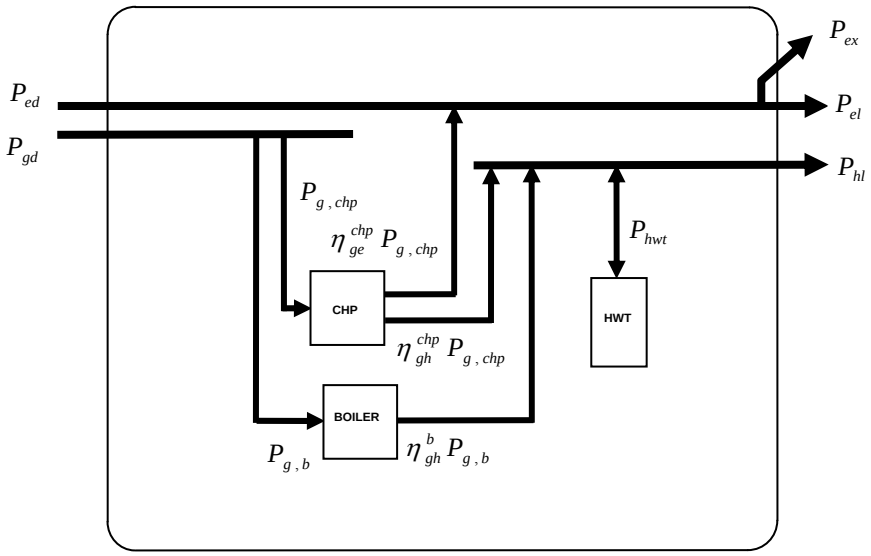

Figure 6.1.5 Diagram of the system in Application1

For the modelling of the energy system five binary variables are considered, which indicate the operating states of the equipment. Table 6.1.2 shows the related equipment states which are indicated by these variables.

The aim is to control the system during one day. The day is divided into 24 time steps, so each time step is equal to one hour.

Table 6.1.2 Auxiliary binary variables in Application 1

δ_1	1= system buys electricity from grid, 0= does not buy
δ_2	1= system sells electricity to the grid, 0= does not sell
δ_3	1= micro-CHP is on, 0= micro-CHP is off
δ_4	1= auxiliary boiler is on, 0= auxiliary boiler is off
δ_5	1 if $P_{g\,chp} \geq P_{g\,chp,\max}$, 0 if $P_{g\,chp} < P_{g\,chp,\max}$

The model of the energy system components in Chapter 4 and the modelling method in Section 5.2.1 are used to obtain the mathematical model of the system.

The energy balance equation (5-12) for the electricity bus is:

$$\delta_1 \cdot P_{ed}(t) + \delta_3 \cdot \eta_{ge}^{chp} \cdot P_{g,chp}(t) = P_{el}(t) + \delta_2 \cdot P_{ex}(t)$$

The system cannot import and export electricity at the same time so:

$$\delta_1 + \delta_2 \leq 1$$

The energy balance equation (5-12) for the gas bus is:

$$P_{gd}(t) = \delta_3 \cdot P_{g,chp}(t) + \delta_4 \cdot P_{g,b}(t)$$

The energy balance equation (5-12) for the hot water bus is:

$$\delta_3 \cdot \eta_{gh}^{chp} \cdot P_{g,chp}(t) + \delta_4 \cdot \eta_{gh}^{b} \cdot P_{g,b}(t) = E_{hwt}(t) - E_{hwt}(t-1) + P_{hl}(t)$$

The constraint for the boiler operation is:

$$\delta_4 - \delta_5 \leq 0$$

It is assumed that the amount of initial and final energy stored in the storage tank is zero in this application:

$$E_{hwt}(0) = E_{hwt}(24) = 0$$

The other constraints are the minimum and maximum values of the imported and exported electricity as well as the minimum and maximum values of the gas input to the micro-CHP and boiler. These values are shown in the Table 6.1.1.

The objective function is the total cost of running the system during the 24 hour period:

$$J = \sum_{t=1}^{24} C_{ed} \cdot P_{ed}(t) - C_{ex} \cdot P_{ex}(t) - C_{econ} \cdot P_{econ}(t) + C_{gd} \cdot P_{gd}(t) \qquad (6\text{-}1)$$

Here C_{ed} is the cost of delivered electricity and C_{ex} is the payment for the exported electricity to the grid. P_{econ} is the consumed electricity in the house and C_{econ} is the payment for the consumed electricity. C_{gd} is the cost of delivered natural gas.

The above optimization problem is converted to a mixed integer linear programming problem, and is solved. The imported and exported electricity are shown in Figure 6.1.6. The generated electricity by micro-CHP and the consumed part of this electricity are shown in Figure 6.1.7. The heat generated by the micro-CHP and auxiliary boiler and stored heat in the storage tank is shown in Figure 6.1.8.

Figure 6.1.7 shows that in hours 1 and 2 the micro-CHP is in operation and generates heat and electricity. The extra generated electricity is exported to the grid. In hour 2 the stored heat in the storage tank reaches its maximum limit, so in hours 3 and 4 the micro-CHP stops running and the heat demand is supplied by the storage tank and the electrical load is supplied by the grid. In hours 5 until 8, where there is a high heating demand, the micro-CHP runs and supplies the heating load, and the extra electricity is sold to the grid. In hour 9 all the electricity generated by the micro-CHP is consumed. In addition, in this hour the electricity deficit is supplied from the grid. In hours 10, 12, 15, 21, 23 and 24 the micro-CHP is off and the electricity is supplied from the grid, and the heating is supplied from the storage tank. In the remaining hours the operation of the system is similar to hour 9.

Figures 6.1.6 and 6.1.7 show that the controller tracks the electrical load fluctuations effectively. For example in hour 6, the generated electricity is 0.73 kWh and the consumed electricity is 0.23 kWh, which is equal to the electrical load

in hour 6 (Figure 6.1.3). Figure 6.1.6 shows that at this hour the exported electricity is 0.5 kWh, which is equal to the difference of generated electricity and consumed electricity (0.73 – 0.23=0.5 kWh).

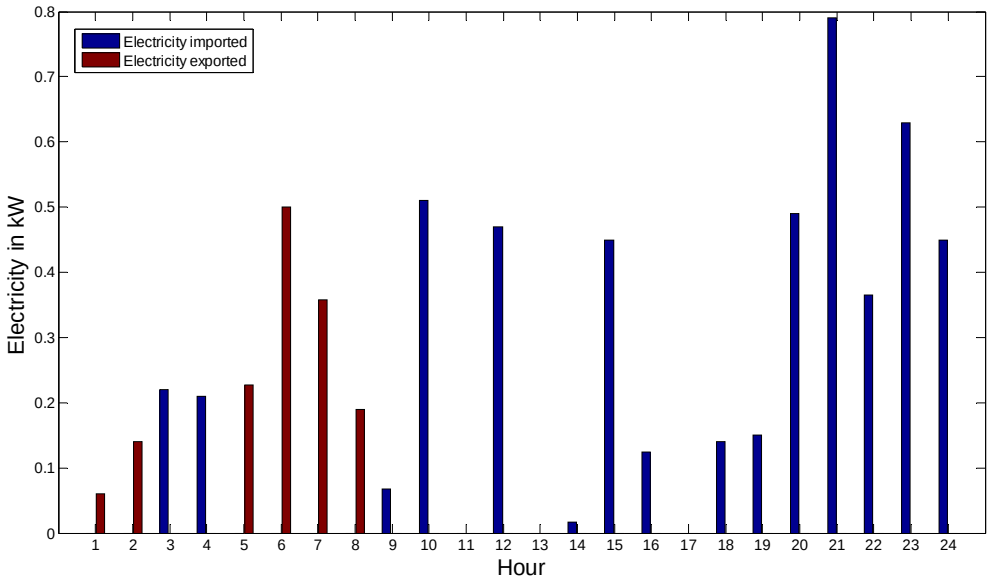

Figure 6.1.6 Imported and exported electricity

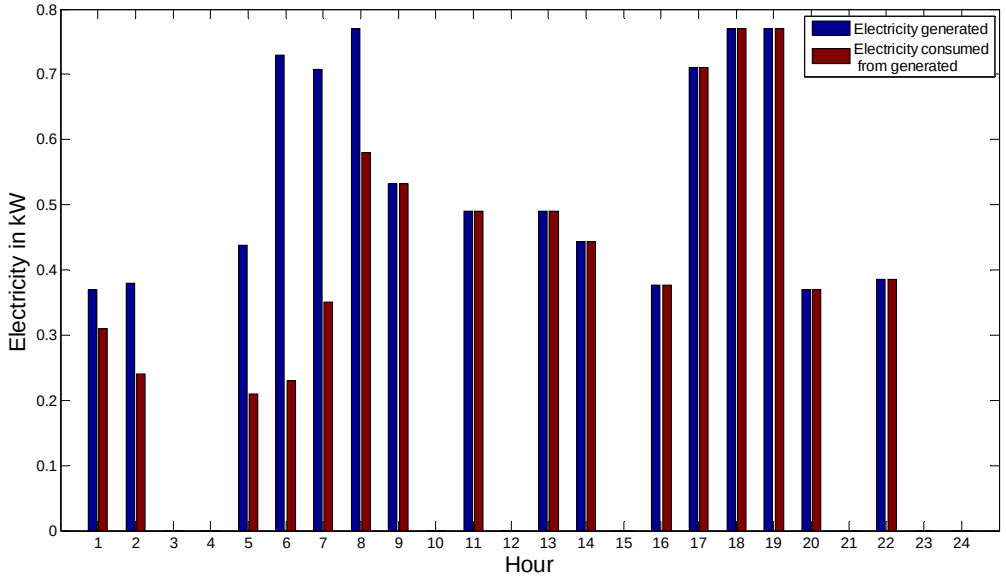

Figure 6.1.7 Generated electricity by micro-CHP and the consumed part of this electricity

Figure 6.1.8 shows that the controller tracks the heating load fluctuations effectively. For example in hour 18, the generated heat by the micro-CHP is 6.16 kWh, and at this hour the stored heat has been increased from 0.66 kWh at hour 17 to 2.02 kWh at hour 18. This means that from 6.16 kWh of generated heat, 1.36 kWh (2.02–0.66=1.36 kWh) has been stored in the storage tank and 4.8 kWh (6.16–1.36=4.8 kWh) is used for heating, which is equal to the heating load at hour 18 (Figure 6.1.4).

Figure 6.1.8 shows that in hour 24 all the stored heat in the hot water tank is consumed and the stored energy amount is zero, which is the condition that was set by the constraint equation $E_h(0) = E_h(24) = 0$.

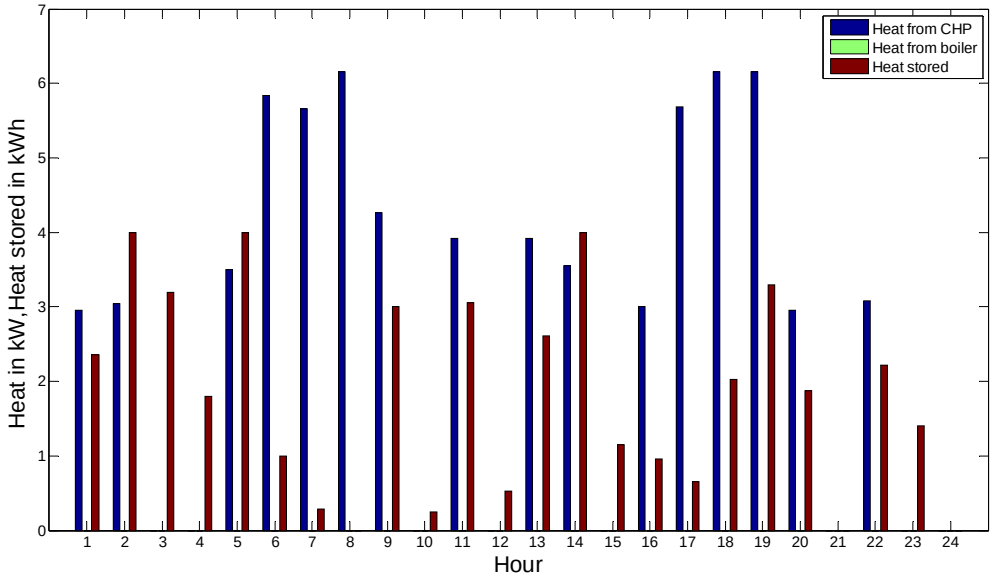

Figure 6.1.8 Heat supplied by the micro-CHP and boiler, and stored heat in the storage tank

The conventional control strategy for micro-CHP systems is heat led control. In this strategy the output of the micro-CHP is controlled by heat demand. If the generated electricity is more than the electrical demand, the extra electricity is exported to the grid, and if the generated electricity is less than the electrical demand, the electrical deficit is imported from the grid. Due to the minimum output limit of the micro-CHP, when the micro-CHP operates at minimum capacity and if there is excess heat, this heat is stored in a storage tank.

The operational cost of the micro-CHP system with the supervisory controller was compared with the operational cost of the micro-CHP system with a heat led control strategy. The results show that the operational cost with the supervisory controller is 3.63 percent less than the operational cost with heat led control strategy.

The CO_2 emission factors of natural gas and electricity are 0.198 and 0.517 kg CO_2 per kWh respectively as shown in Table A.3, Appendix A. The results show that CO_2 emission with the supervisory controller is 1.34 percent less than the CO_2 emission with heat led control strategy.

Solving the optimization problem with different storage tank sizes shows that increasing the tank size has no effect on the total cost. This is because of the feed-in tariff. With the feed-in tariff, the system does not need to store the heat generated by the micro-CHP, and instead of this, the micro-CHP operates whenever there is a need for heating, and exports the extra generated electricity to the grid.

As it is shown in Figure 6.1.8, due to the high capacity of the micro-CHP, the auxiliary boiler is always off. To see the contribution of the auxiliary boiler in the supplying of heating load, the space heating load is increased by 50% (Figure 6.1.9).

In this case the imported and exported electricity are shown in Figure 6.1.10. The generated electricity by the micro-CHP and the consumed part of this electricity are shown in Figure 6.1.11. In Figure 6.1.12 the heat supplied by the micro-CHP and boiler and also the stored heat in the storage tank are shown.

Figures 6.1.10 and 6.1.11 show that, in hours 1 and 2 the micro-CHP supplies the electrical and thermal loads, and the extra heat is stored in the hot water tank. In hour 2, the stored heat in the tank reaches its maximum level, so in the next hour (hour 3) the micro-CHP is turned off. So the electrical load is supplied from the grid and the heating load is supplied from the hot water tank. In hours 4 to 8 and in

hour 17, the heating demand is supplied by the micro-CHP, and the extra generated electricity is exported to the grid.

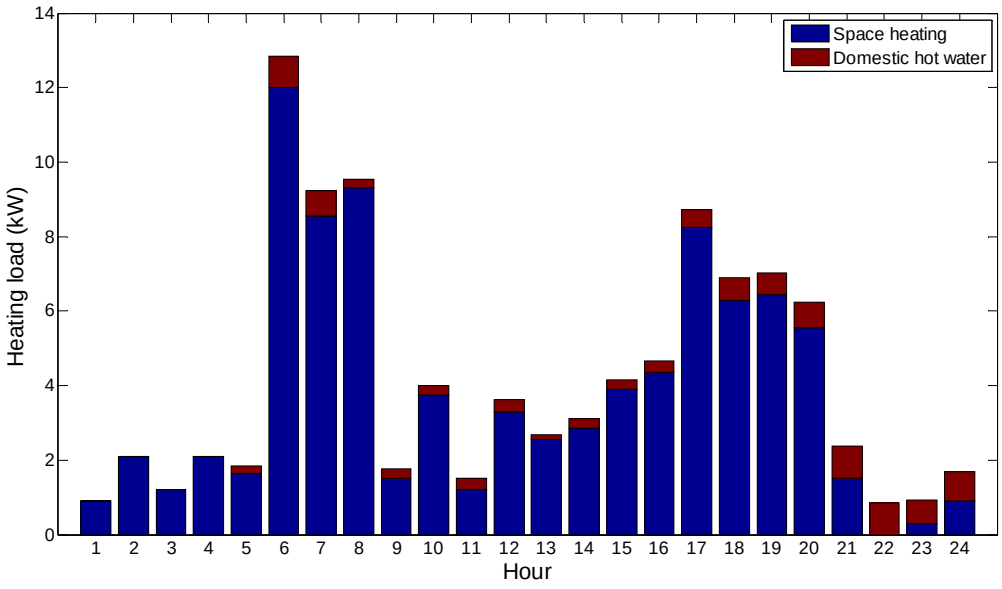

Figure 6.1.9 Space heating load (50% more) and domestic hot water load

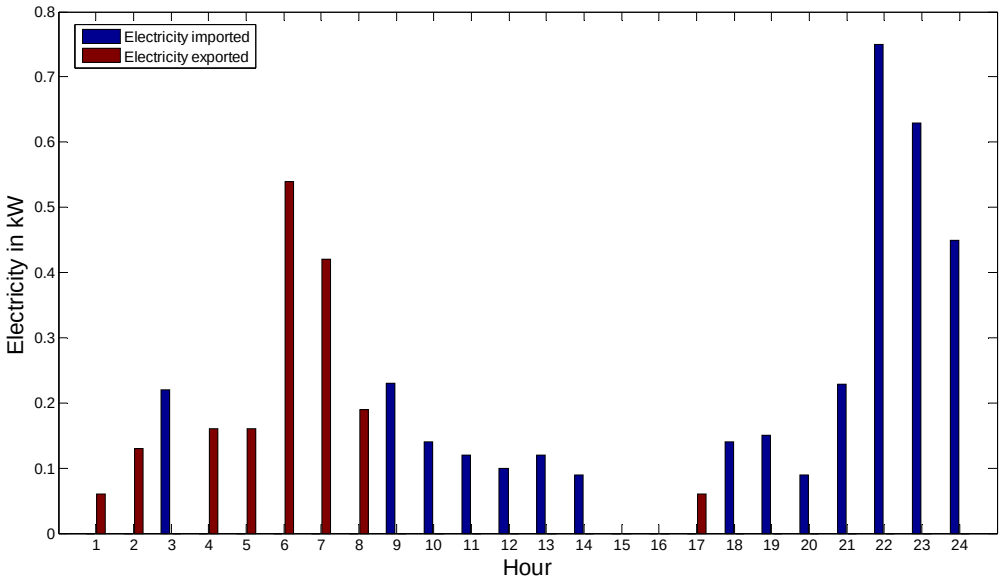

Figure 6.1.10 Imported and exported electricity (case of 50% more heating load)

Figure 6.1.12 shows that in this case, due to the higher heating demand in hours 6,7,8 and 17 and lack of enough stored heat in the hot water tank, the auxiliary

boiler is turned on sequentially, when the output heat from the micro-CHP reaches its maximum limit.

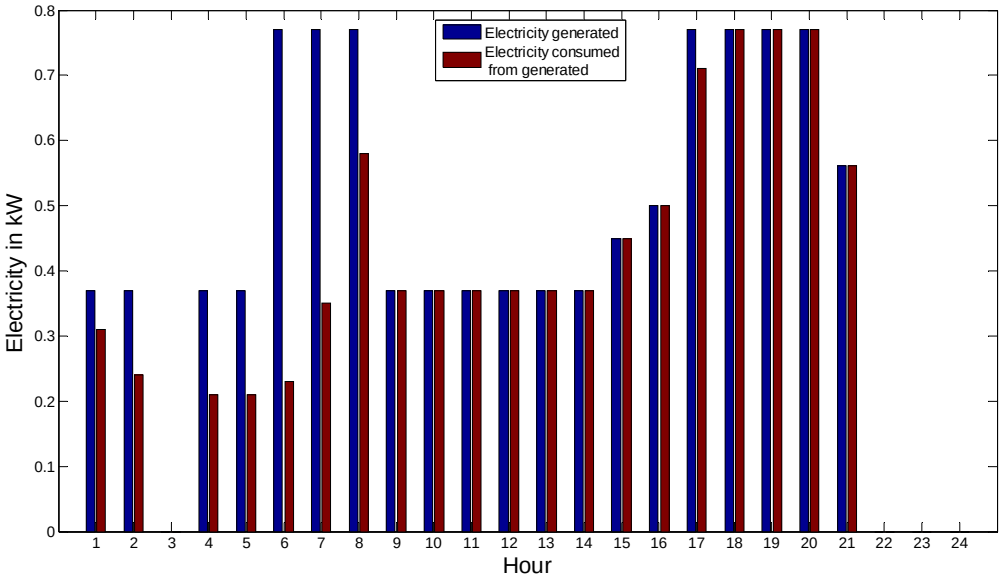

Figure 6.1.11 Generated electricity by micro-CHP and the consumed part of this electricity (case of 50% more heating load)

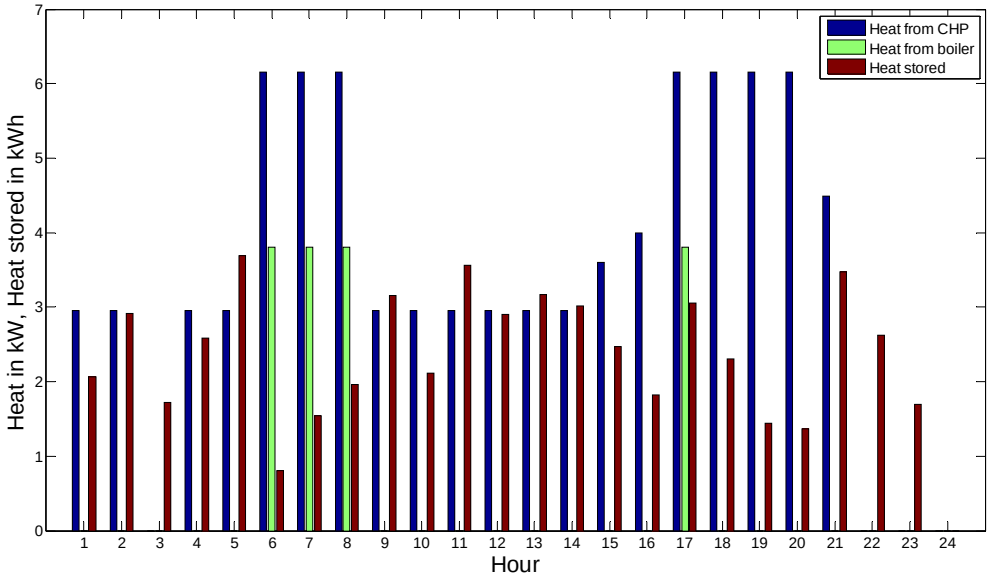

Figure 6.1.12 Heat supplied by micro-CHP and boiler and the stored heat in the storage tank (case of 50% more heating load)

The results of simulations show that in this case, the supervisory optimal controller with respect to the heat led control strategy reduces the operational cost and CO_2 emission by 7.31 percent and 5.19 percent respectively.

6.1.2 Hybrid MPC approach

In this approach, as explained in Section 5.3, the hybrid model of the system is initially derived.

The system has five continuous inputs, $u_r = [P_{hwt}\ P_{ed}\ P_{ex}\ P_{g,chp}\ P_{g,b}\ ]'$, and 4 binary inputs , $u_b = [\delta_1\ \delta_2\ \delta_3\ \delta_4]'$. P_{ed} and P_{ex} are the delivered and exported electrical powers respectively. $P_{g,chp}$, $P_{g,b}$ and P_{hwt} are the input powers to the micro-CHP, the boiler and the storage tank respectively. The binary inputs are defined in Table 6.1.2.

The states of the system are $x_r = [E_{hwt}\ P_{el}\ P_{hl}]'$, and the outputs of the system are $y_r = [E_{hwt}\ P_{el}\ P_{hl}]'$. E_{hwt}, P_{el} and P_{hl} are the stored energy in the tank, the electrical load and the heating load respectively.

The discrete hybrid system is a collection of linear systems:

$$\begin{aligned} x_r(k+1) &= A_{i(k)}x_r(k) + B_{i(k)}u_r(k) \\ y_r(k) &= C_{i(k)}x_r(k) \end{aligned} \qquad (6\text{-}2)$$

The $A_{i(k)}$, $B_{i(k)}$, and $C_{i(k)}$ are as follows:

$$A_{i(k)} = \begin{bmatrix} 1 & 0 & 0 \\ 0 & 0 & 0 \\ 0 & 0 & 0 \end{bmatrix} \quad B_{i(k)} = \begin{bmatrix} 0 & 0 & 0 & 0 & -1 \\ 0 & \delta_1 & -\delta_2 & \delta_3\eta_{ge}^{chp} & 0 \\ 1 & 0 & 0 & \delta_3\eta_{gh}^{chp} & \delta_4\eta_{gh}^{b} \end{bmatrix} \quad C_{i(k)} = \begin{bmatrix} 1 & 0 & 0 \\ 0 & 1 & 0 \\ 0 & 0 & 1 \end{bmatrix}$$

By considering the operational constraints of the system, which were explained in the previous section, the hybrid model of the system is transformed to the MLD

model. For this purpose, HYSDEL (Kvasnica and Herceg, 2009), which is a high-level modelling language for DHA, is used. The MLD matrices have been given in Appendix C. By using the Multi-Parametric Toolbox (Kvasnica, et al., 2004), the hybrid MPC controller is derived.

The controller is simulated for the case of a 50% increased space heating load. In the cost function, input electricity and gas and exported electricity are penalized with prices which are the same as in the previous section. Figure 6.1.13 shows that the controller exactly follows the required electrical (Le) and heating (Lh) outputs from the systems. In this figure, the stored heat in the hot water tank (Eh) also has been shown. The profile of the stored heat in this method is similar to the pervious method (with 50% more space heating load), with a small difference.

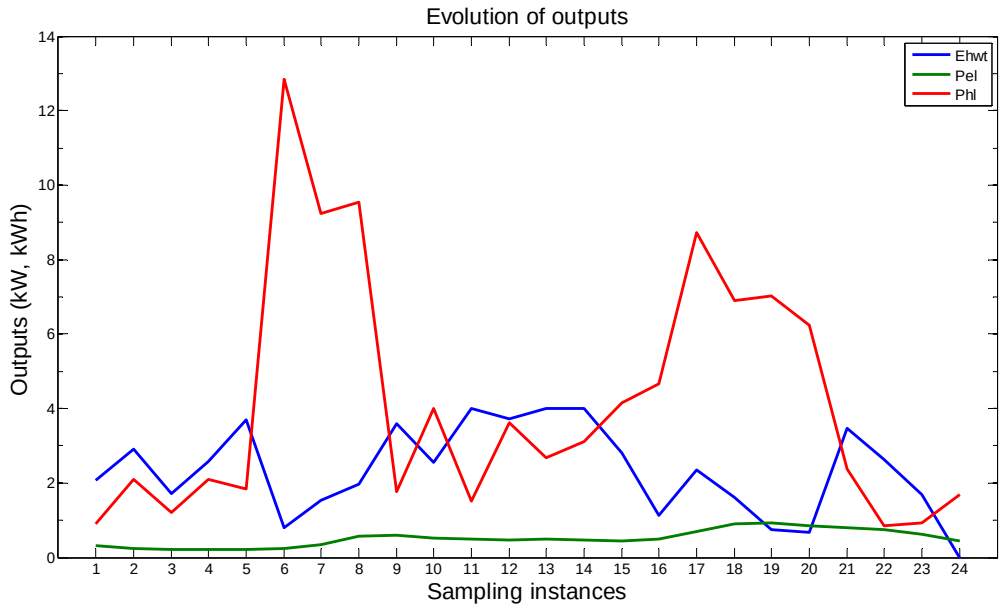

Figure 6.1.13 Stored energy in the tank (E_{hwt}), electrical load (P_{el}) and heating load (P_{hl}) (case of 50% more heating load)

The imported and exported electricity are shown in Figure 6.1.14. The profiles of the imported and exported electricity in this method, are similar to the previous method (with 50% more space heating load), but again there are small differences between the profiles.

The inputs to the micro-CHP ($P_{g,chp}$), the boiler ($P_{g,b}$) and the storage tank (P_{hwt}) are shown in Figure 6.1.15. To obtain the outputs from the micro-CHP and the boiler, the input values should be multiplied by the related efficiencies.

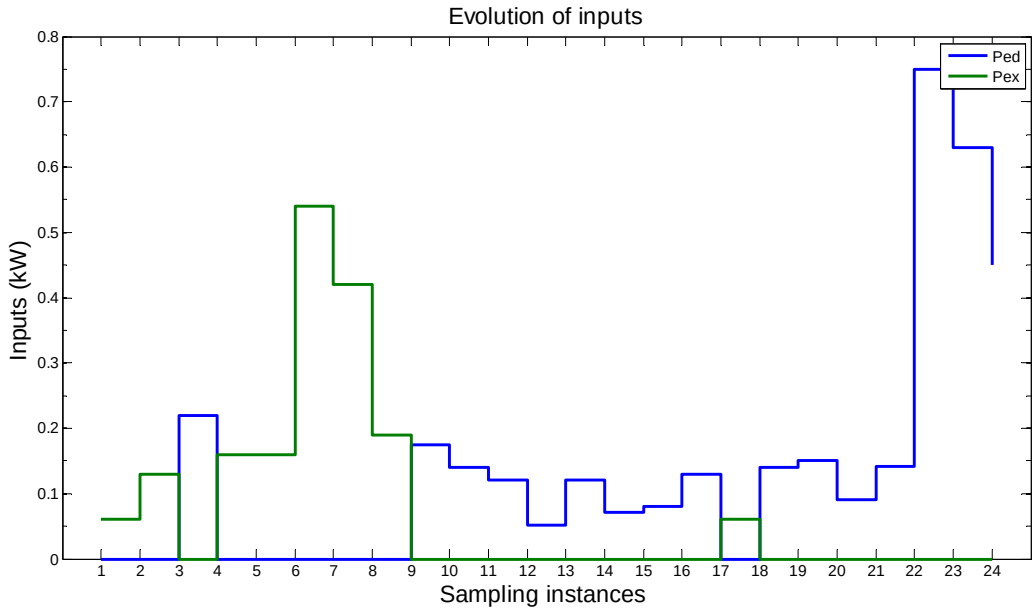

Figure 6.1.14 Delivered (P_{ed}) and exported (P_{ex}) electricity (case of 50% more heating load)

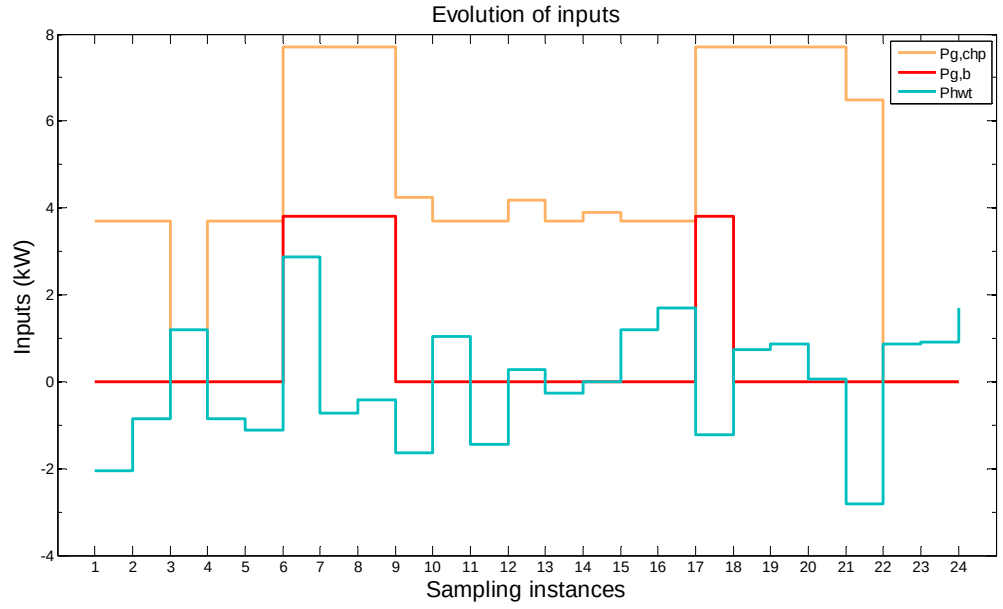

Figure 6.1.15 Inputs to the CHP ($P_{g,chp}$), boiler ($P_{g,b}$) and storage tank (P_{hwt}) (case of 50% more heating load)

Although in this method the optimum values of the inputs are slightly different from the values obtained in the multi-period optimization approach, the optimum cost values are exactly equal in both approaches. This is acceptable, since in linear programming, with a unique objective function value, alternate optimal solutions can exist (Dantzig and Thapa, 2003; Alpay and Shor, 1999).

6.1.3 Explicit hybrid MPC

As described in Section 5.3.3, the explicit controller of the above system is a simple membership test to find the active region with the minimum cost value. Then the inputs sequence is computed by the equation (5-34).

For each time step, there is a distinct explicit controller. For obtaining the explicit controller, the computation time increases by 2^n, where n is the number of binary variables. For this reason, only 2 time steps have been considered in the computation. Figure 6.1.16 shows the controller partition for the control and prediction horizons of 2 time steps. In this figure x_1, x_2 and x_3 are the states of the stored energy in the hot water tank, the electrical load and the heating load respectively.

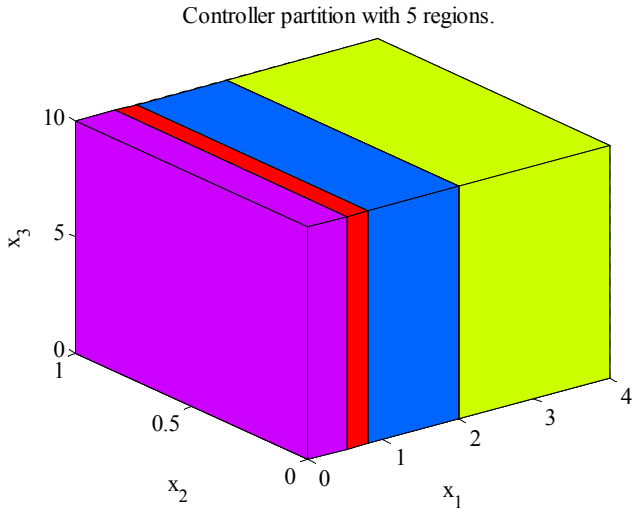

Figure 6.1.16 Explicit controller partition for the control and prediction horizon of 2 time steps

6.2 Application 2

In this application, the electrification of a small farm is considered, located near to London in the UK. The electricity supply system of the farm consists of PV panels, a diesel generator unit and a battery bank.

The electricity supply system of the farm consists of 20 PV panels each of 220 Wp, a diesel generator unit with a nominal capacity of 10 kW and 12 battery packs each of 360 Ah (2.16 kWh) nominal capacity. The tilt angle of the PV panels is 51°.

The hourly electrical load of the farm is shown in Figure 6.2.1. In this figure hourly incident solar radiation on the panels for a sample day in early May is also shown.

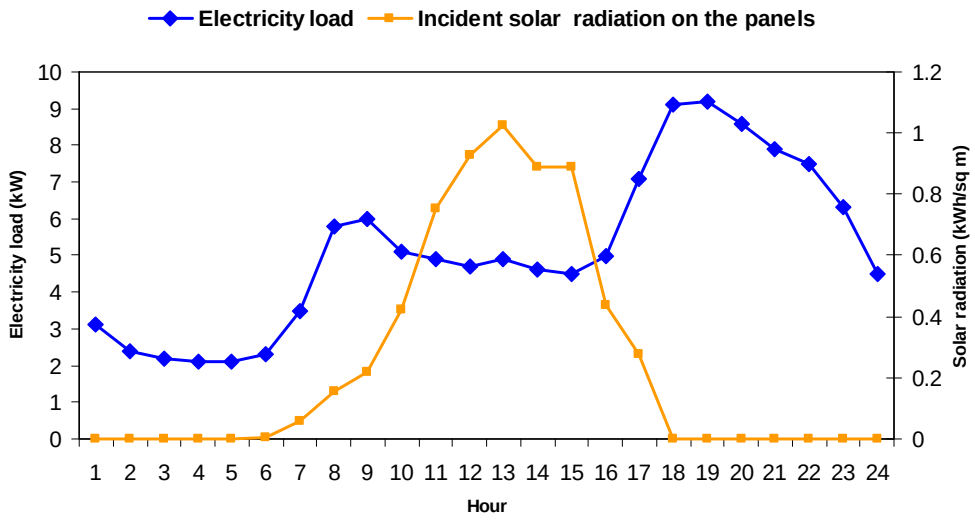

Figure 6.2.1 Electrical load of the farm and incident solar radiation on the panels for a sample day in early May.

The electrical system is shown in Figure 6.2.2. The PV panels are equipped with a Maximum Power Point Tracking (MPPT) unit and a boost converter. The battery has a charge controller and the AC/DC/AC unit converts the AC power to DC

when there is power excess, and when there is a power deficit it converts the DC power of the battery to AC.

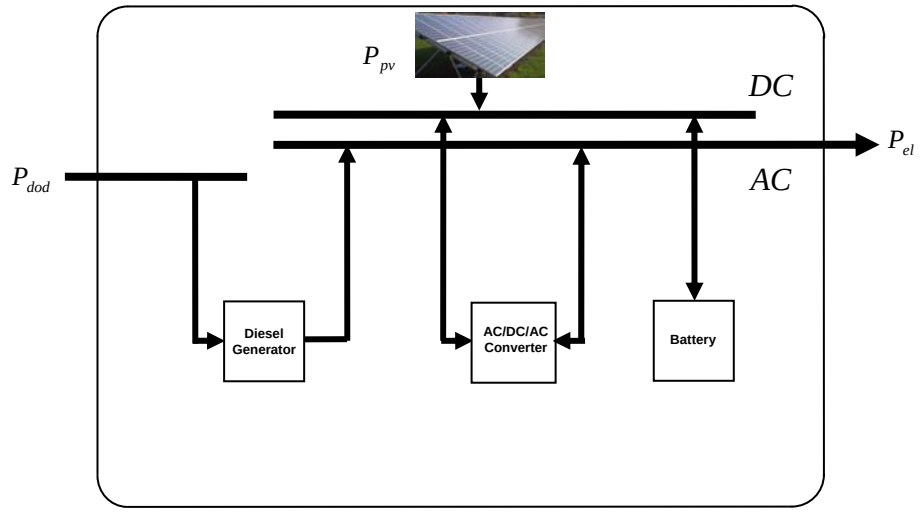

Figure 6.2.2 Diagram of the system in application 2

If the losses of the power electronic devices are neglected the simplified system will be the system as shown in Figure 6.2.3.

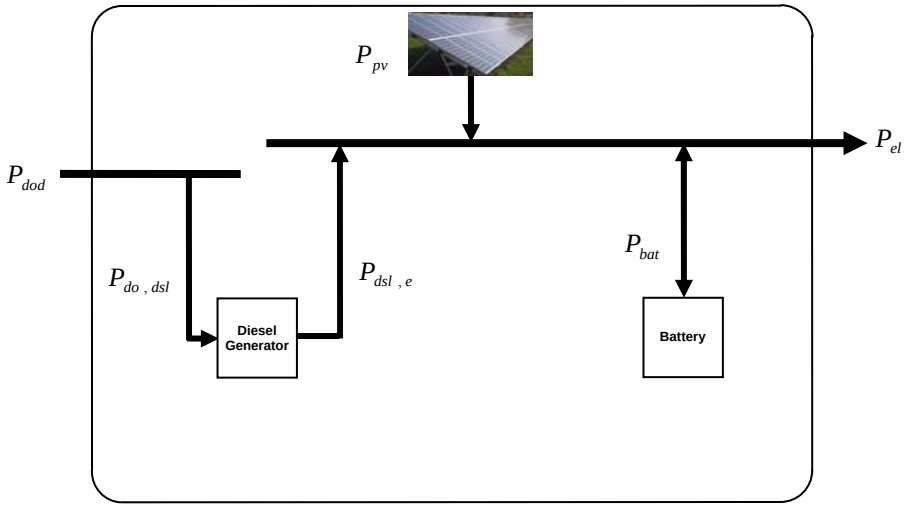

Figure 6.2.3 Simplified diagram of the system in Application 2

The main specifications of the pieces of equipment are shown in Table 6.2.1. The maximum charging and discharging powers of the battery have been selected according to the manufacturer recommendations. The diesel generator nominal power has been selected based on the maximum power demand.

The charging and discharging efficiency is very difficult to measure. In the calculation it is assumed that the charging efficiency is equal to the roundtrip efficiency of the battery (0.85) and the discharging efficiency is equal to 1.

Table 6.2.1 Specifications of the equipment in Application 2

PV panel	
Peak power	220 Wp
Number of panels	40
Diesel generator	
Nominal power	10 kW
Fuel type	Diesel
Battery bank	
Manufacturer-Model	Trojan-L16P
Nominal capacity	360 Ah (2.16 kWh)
Maximum capacity	396 Ah
Maximum charging power	0.65 kW
Maximum discharging power	1.08 kW
Round trip efficiency	0.85
Minimum SOC	0.30
Number of batteries	10

For the modelling of the energy system we consider 3 binary variables: δ_1 for the on/off status of the diesel generator and δ_2 and δ_3 for the charging and discharging states of the battery respectively.

The model of the energy system components in Chapter 4 and the modelling method in Section 5.2.1 are used to obtain the mathematical model of the system.

The energy balance equation (5-12) for the fuel bus is:

$$P_{dod}(t) = P_{do,dsl}(t)$$

The energy balance equation for the electricity bus is:

$$P_{pv}(t)+\delta_1\cdot P_{dsl}(t)+\delta_3\cdot P_{bat,dch}(t)=\delta_2\cdot P_{bat,ch}(t)+P_{el}(t)$$

$$P_{pv}(t)+\delta_1\cdot P_{dsl}(t)=\delta_2\frac{E_{bat}(t)-E_{bat}(t-1)}{\eta_{bch}}+\delta_3\frac{E_{bat}(t)-E_{bat}(t-1)}{1/\eta_{bdc}}+P_{el}(t)$$

The battery cannot charge and discharge at the same time so we have:

$$\delta_2+\delta_3\le 1$$

It is assumed that the initial and final energy stored in the battery bank is equal to 6.48 kWh (SOC = 0.3):

$$E_{bat}(0)=E_{bat}(24)=6.48$$

The other constraints are according to the data given in Table 6.2.1.

The optimization period is 24 hours which is divided into 1 hour time steps. The objective function is the total fuel cost, the battery wear and the diesel generator replacement cost for the 24 hours that should be minimized.

$$J=\sum_{t=1}^{24}\delta_1\cdot(C_{do}F(t)+C_{rep,dsl})+\delta_3\cdot C_{bw}\cdot P_{bat,dch}(t) \qquad (6\text{-}3)$$

Here F is the fuel consumption of the diesel generator which is obtained from equation (4-12). C_{do} is the fuel cost per litre. The diesel engine uses red diesel oil which costs 0.63 £/lit.

$C_{rep,dsl}$ is the diesel generator replacement cost which is :

$$C_{rep,dsl}=\frac{diesel\ \ generator\ \ price}{lifetime}=\frac{3500£}{12000\,hr}=0.29£/hr$$

The depth of discharge and the cycles to failure of the batteries are shown in Table 6.2.2. From this data and using the equation (5-18) for each depth of discharge values, the lifetime of the battery was calculated and is shown in Figure 6.2.4. As can be seen from this figure the lifetime does not so much depend on the depth of discharge, so we can use an average lifetime throughput between the minimum and maximum states of charge which are assumed to be 30% and 100%

respectively (NREL, 2008). The average lifetime throughput is 1182 kWh. Each battery has a price of 510.34 pounds and according to the manufacturer's data the roundtrip efficiency of the battery is 85%. So from the equation (5-17) the wear cost of the battery is equal to 0.468 pounds/kWh.

Table 6.2.2 Cycles to failure vs. depth of discharge (data from NREL, 2008)

Depth of Discharge (%)	Cycles to failure	Depth of Discharge (%)	Cycles to failure
10	4,398	60	884
20	2,322	70	774
30	1,614	80	698
40	1,266	90	633
50	1,036	100	600

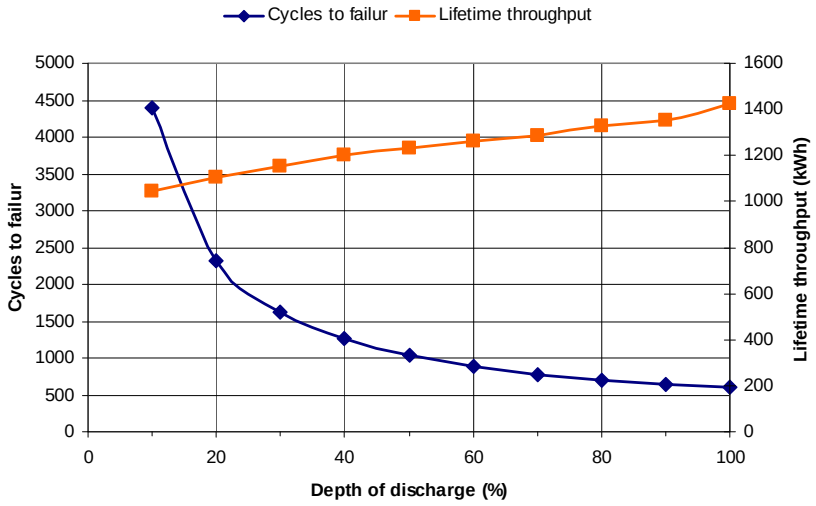

Figure 6.2.4 Battery cycles to failure and lifetime throughput vs. depth of discharge

The results of optimization for the diesel generator output power is shown in Figure 6.2.5. The unit cost of the power generation by the diesel generator is decreased by increasing the output power. So the diesel works at higher outputs and stores the extra power in the batteries. However, for the cost of stored power the wear cost of the batteries should be added when this power is discharged from the batteries. So the controller decides between the extra power generation by the diesel generator and storage of it, or generation of power as much as it is needed.

Figure 6.2.5 shows that the power generation by the diesel generator for less than 3.04 kW is not economical.

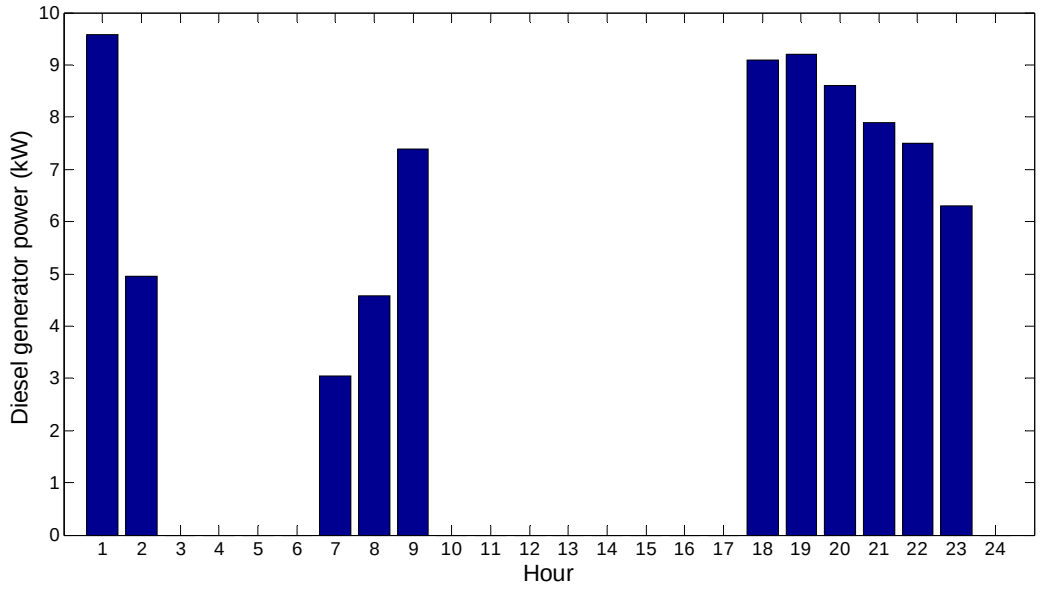

Figure 6.2.5 Diesel generator power output

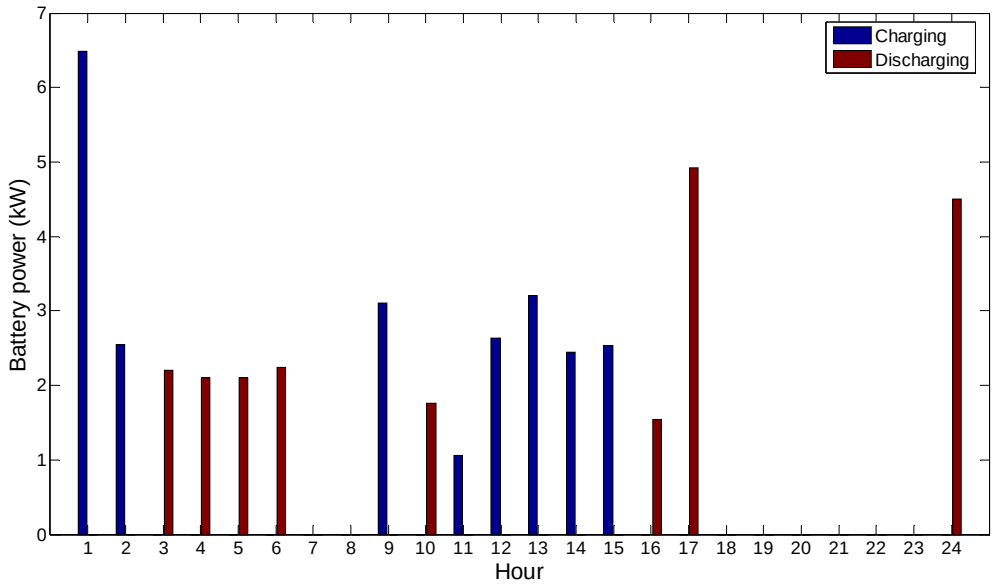

Figure 6.2.6 Battery bank charging and discharging power

Figures 6.2.6 shows the battery bank's charging and discharging power. The charging power comes from the PV panels and the diesel generator. Figure 6.2.7 shows the stored power in the battery bank, which in each hour is equal to the

stored electricity at the previous hour plus the charging power and minus the discharging power at the same hour. The final stored power in the battery is 6.48 kWh which is equal to its initial value.

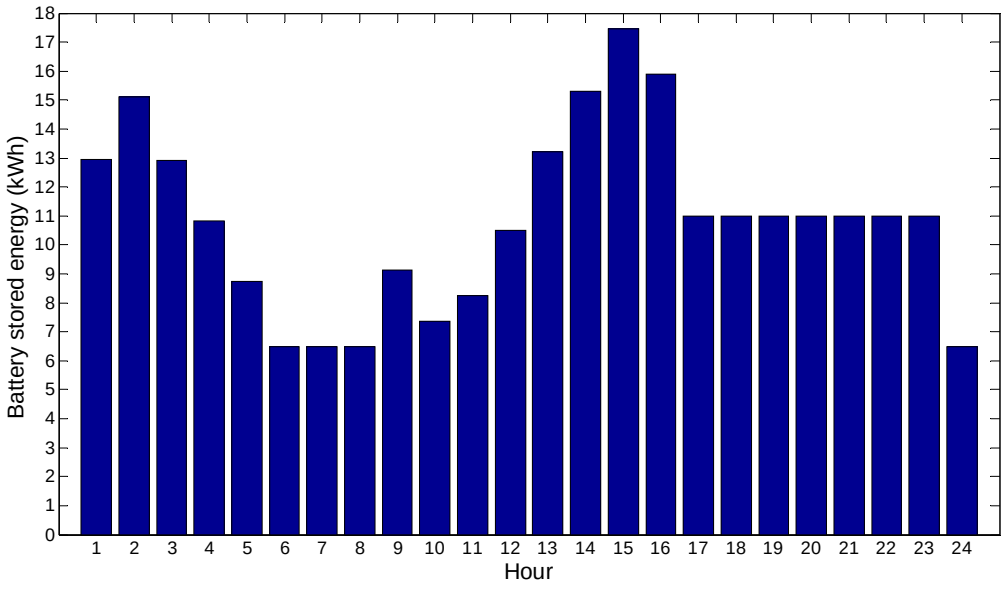

Figure 6.2.7 Battery bank stored power

The simulation results of the supervisory controller are compared with the results of the load following strategy (Barley and Winn, 1996). In the load following strategy, if the batteries cannot meet the electrical load, the diesel generator runs at a rate that produces only enough power to meet the net load. The batteries will be charged whenever the renewable power exceeds the primary load, but they will not be charged by the diesel generator. The results show that the supervisory controller with respect to the load following strategy reduces operational cost by 3.8 percent.

6.3 Application 3

In this application a hybrid power system is used for the electrification of an off grid house. The house is located in London, UK. The electrification of the house is performed by a hybrid power system. The hybrid power system consists of PV

panels, a battery bank, an electrolyzer, a hydrogen storage tank and a fuel cell as shown in Figure 6.3.1.

The solar radiation is converted to electricity by the PV panels. The panels have been equipped with a Maximum Power Point Tracking (MPPT) system and a boost converter. When the power from the PV panels exceeds the load, the extra power is stored in the batteries or is consumed by the electrolyzer to produce hydrogen which is stored in the hydrogen tank. The batteries are equipped with a charge controller that controls the charging/discharging rate and the minimum state of charge (SOC) of the batteries. A buck converter regulates the voltage and current of the electrolyzer. The hydrogen is stored in the hydrogen tank. In this application it is assumed that the pressure of the hydrogen produced by the electrolyzer is high enough so that the hydrogen can easily be stored in the tank and there is no need for a compressor.

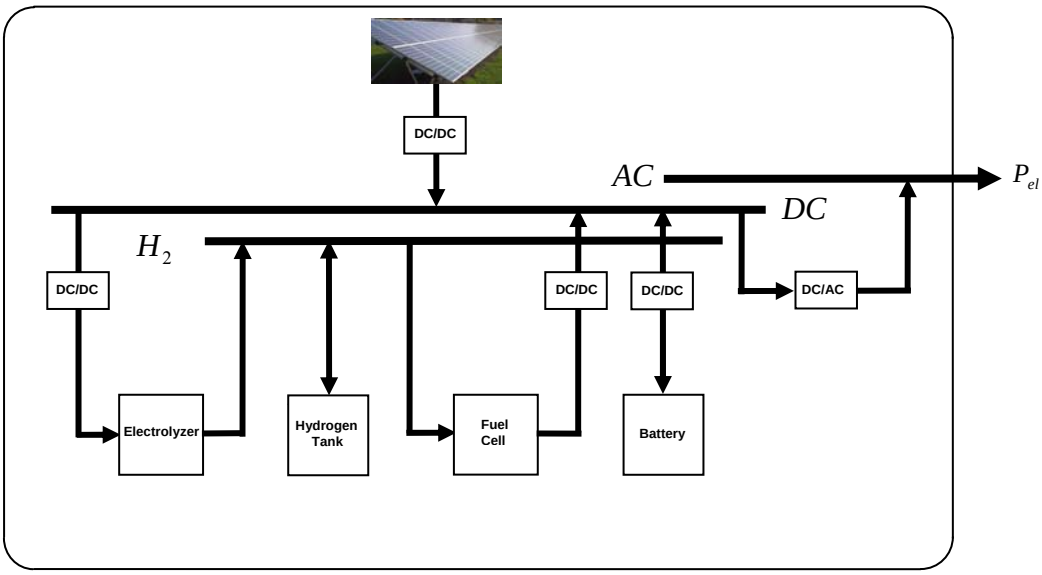

Figure 6.3.1 Diagram of the hybrid power system in Application 3

When the solar radiation is not enough for electricity generation which satisfies the electrical load of the house, the batteries and fuel cell supply the power deficit. For matching the output voltage of the fuel cell with the DC bus a boost converter

has been used. The DC power from the DC bus is converted to AC power by an inverter and supplies the electrical load of the house.

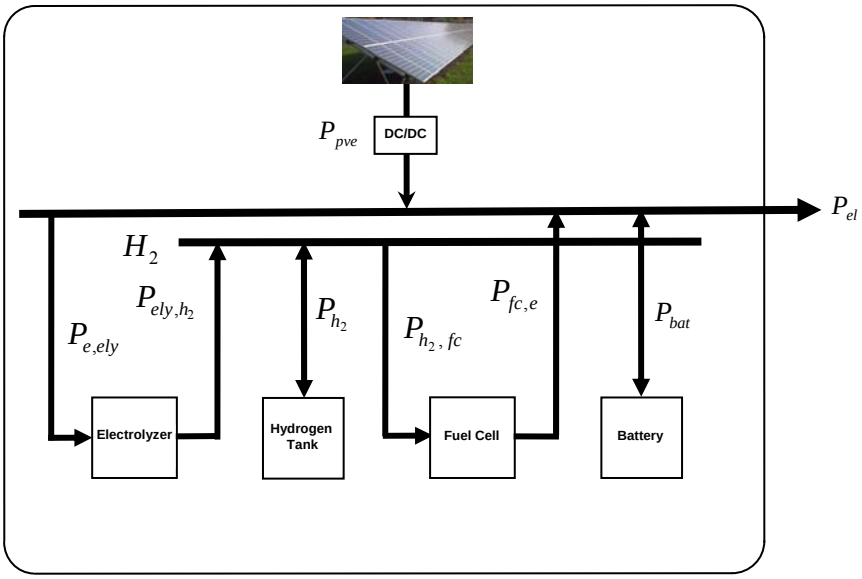

Figure 6.3.2 Simplified diagram of the hybrid power system in Application 3

If the power losses in the power converters, the charge controller and the power inverter are neglected, the diagram of the hybrid power system in Figure 6.3.1 is simplified to the diagram shown in Figure 6.3.2.

The specification of the components is shown in Table 6.3.1. The maximum charging and discharging powers of the battery have been selected according to the manufacturer recommendations. The stored electrical energy in the hydrogen tank has been given based on the higher heating value of the hydrogen. The amount of stored hydrogen can be obtained by dividing it to the heating value of the hydrogen.

The electrical load profile of the house is the same as the electrical load profile in Application 1. Average daily global horizontal radiation values for each month have been used for the calculation of incident solar radiation on the PV panels. Assuming a constant daily load profile, the electricity load profile and the incident solar radiation for three subsequent days in early May are shown in Figure 6.3.3.

Table 6.3.1 Specifications of the equipment in Application 3

PV panel	
Peak power	220 Wp
Number of panels	24
Battery bank	
Manufacturer-Model	Trojan-L16P
Nominal capacity	360 Ah (2.16 kWh)
Maximum capacity	396 Ah (2.38 kWh)
Maximum charging power	0.65 kW
Maximum discharging power	1.08 kW
Round trip efficiency	0.85
Minimum SOC	0.30
Number of batteries	6
Electrolyzer	
Capacity	5.0 kW
Efficiency*	0.8
Fuel cell	
Capacity	1.0 kW
Efficiency*	0.50
Hydrogen tank	
Minimum storage level*	10 kWh
Maximum storage level*	300 kWh

* Based on higher heating value (HHV) of hydrogen (39.4 kWh/kg)

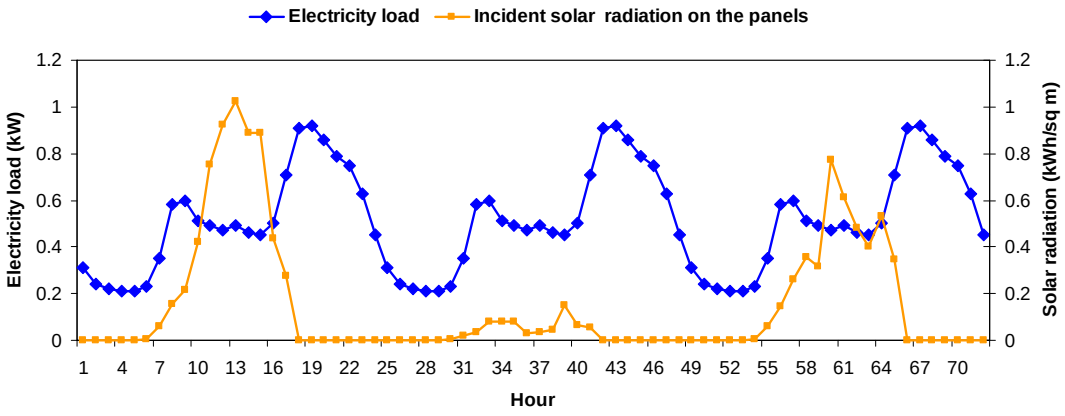

Figure 6.3.3 Electricity load and incident solar radiation on the solar panels

For the modelling of the system, 4 binary variables $\delta_1, \delta_2, \delta_3$ and δ_4 are considered which indicate the charging state of the battery, the discharging state of the battery, the electrolyzer operation and the fuel cell operation respectively.

The model of the energy system components in Chapter 4 and the modelling method in Section 5.2.1 are used to obtain the mathematical model of the system.

The energy balance equation (5-12) for the electricity bus is:

$$P_{pv}(t) = \delta_1 \frac{E_{bat}(t) - E_{bat}(t-1)}{\eta_{bat,ch}} + \delta_2 \frac{E_{bat}(t) - E_{bat}(t-1)}{1/\eta_{bat,dch}} + \delta_3 \frac{E_{h_2}(t) - E_{h_2}(t-1)}{\eta_{ely}} + \delta_4 \frac{E_{h_2}(t) - E_{h_2}(t-1)}{1/\eta_{fc}} + P_{el}(t)$$

The battery cannot charge and discharge at the same time so:

$$\delta_1 + \delta_2 \leq 1$$

In addition the electrolyzer and fuel cell cannot operate simultaneously:

$$\delta_3 + \delta_4 \leq 1$$

The initial stored energy in the battery bank and hydrogen tank are assumed to be equal to 6 kWh and 40 kWh respectively:

$$E_{bat}(0) = 6$$

$$E_{h_2}(0) = 40$$

The other constraints in the optimization are according to the data given in Table 6.3.1.

The optimization period is 3 days which is divided into 72 time steps, each of 1 hour. The objective function is the total energy stored in the battery and the hydrogen tank.

When there is a power surplus the extra power can be stored in the batteries or in the hydrogen tank by the electrolyzer. When there is a power deficit, the remaining power can be supplied by the battery or by converting hydrogen to electricity in the fuel cell. The round trip efficiency of the battery is more than the round trip efficiency of the hydrogen cycle so the extra power should first be stored in the battery, but if the battery is full or the power is more than the maximum charging rate of the battery this power should be stored in the hydrogen tank. The power deficit should be first supplied by the battery, and if the battery is empty or the power deficit is more than the maximum discharging rate of the battery this power should be supplied by the fuel cell.

The results of optimization in Figures 6.3.4 and 6.3.5 show that in the early hours of day 1 the battery starts to discharge and supply the load. At hour 7 of day 1 the sun rises and starts shining on the PV panels. The generated electricity by the PV panels supplies the load and reduces the discharge rate of the battery. At hour 8 and in later hours up to hour 17 the generated power by the PV panels is more than the power consumption, so the extra power is stored in the battery and/or in the hydrogen tank (by electrolyzer). It is seen that in this period the charging power of the battery in hour 13, which has the highest radiation (Figure 6.3.3), is limited by the maximum charging power of the battery bank which is equal to $6 \times 0.65 = 3.9$ kW. At hour 18 when the sun sets, until hour 4 of the next day, the electrical load is supplied by the battery. In hour 5 on day 2 although the stored power in the battery is still more than the minimum SOC value ($6 \times 0.65 \times 0.3 = 1.17$ kWh) and the round trip efficiency of the battery is more than the round trip efficiency of the hydrogen storage, the battery is not discharged below 6.67 kWh. But at the end of day 2 (hours 10, 11 and 12) the battery is discharged to have enough capacity so that it can be charged during day 3. On day 3, where the solar radiation and the load profiles are almost similar to day 1, first the battery is discharged and supplies the load then electricity is generated by the PV panels and the battery and hydrogen tank are charged. At the end of day 3 the battery and the fuel cell supply the load.

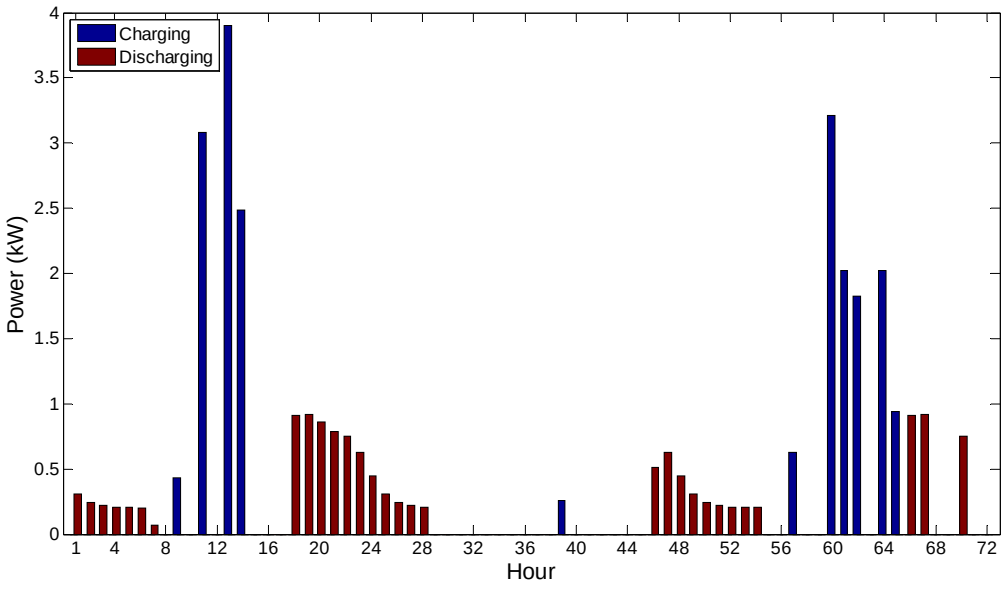

Figure 6.3.4 Charging and discharging power of the batteries

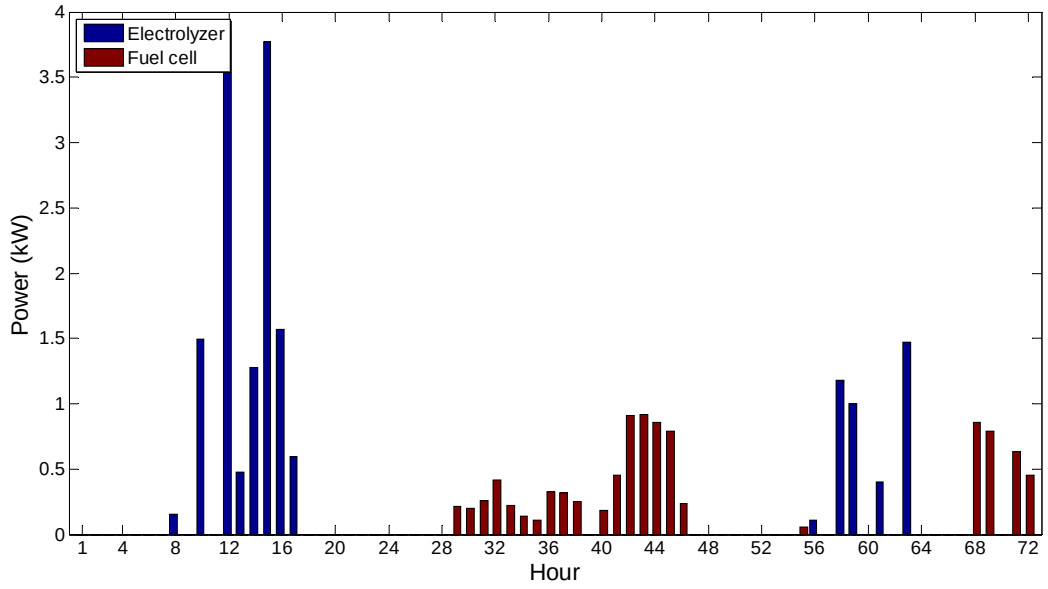

Figure 6.3.5 Input power to the electrolyzer and out put power form the fuel cell

The total stored energy in the battery and hydrogen tank at the beginning of the period is 46 kWh (6 kWh in the battery bank and 40 kWh in the hydrogen tank). Figure 6.3.6 shows that the total stored energy at the end of the period is 45.14 kWh (10.38 kWh in the battery bank and 34.76 kWh in the hydrogen tank). So the

discharged energy from the battery and hydrogen tank during a cloudy day 2, where the PV panel generates less electricity, has almost been compensated by the charged energy on days 1 and 3.

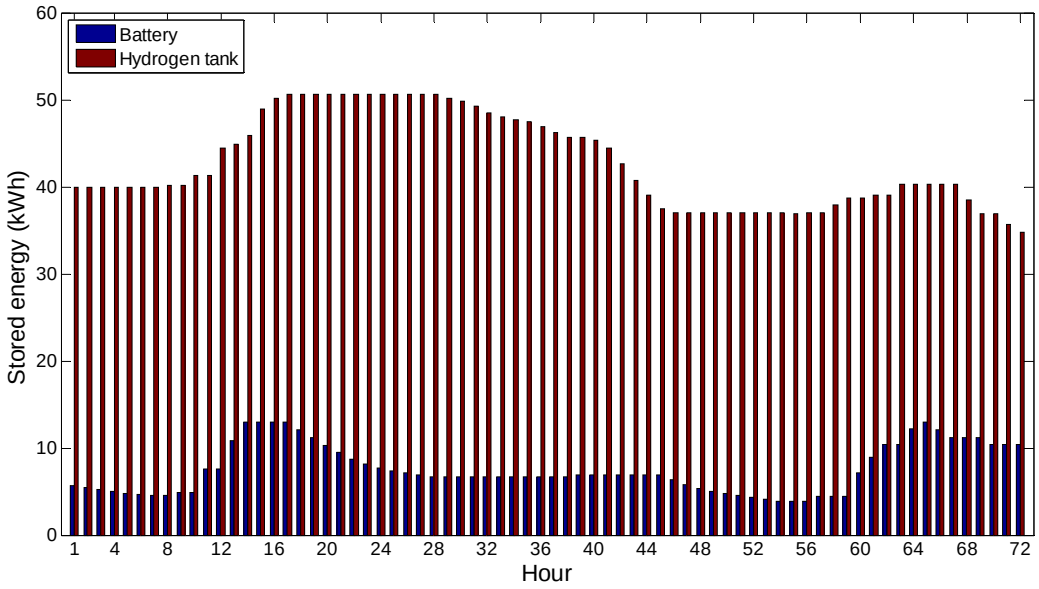

Figure 6.3.6 Stored energy in the batteries and the hydrogen tank

6.4 Conclusions

In this chapter, three applications of the supervisory model predictive controller were studied. These applications have been selected from various applications of the building integrated renewable and low carbon energy systems to show that the designed controller in Chapter 5 is flexible and can be used in different applications. In the first application it was shown that the controller is able to reduce the daily energy cost and CO_2 emission from the heating and electrification of a house in the UK. The second application showed that the controller reduces the diesel generator fuel cost by preventing its operation in low loads and running it in higher loads in order to store the cheaper generated electricity in the batteries. Also the controller compares the battery wear cost and the diesel generator operational cost for reducing the total cost. In the third application, the controller was used in a hybrid power system and it was shown that the controller manages

the power flows between the system components to supply the electrical demand and minimize the losses due to the energy storage in the system.

Chapter 7
Conclusions

In this chapter a summary of the thesis is first given. Then the conclusions which were derived from this research are explained. Next some recommendations are given for the industry. Finally, some related future work are presented.

7.1 Summary

From environmental, economical and energy security points of view, utilization of the renewable and low carbon energy systems in buildings is desirable and inevitable. The integration of different renewable energies gives more reliability for the utilization of them.

A literature review of the various control methods showed that each control method has its advantages and disadvantages. The methods based on multi-period optimization and MPC were recognised as the most appropriate methods for supervisory control and operational management of the integrated renewable and low carbon energy systems, since these methods can consider the predicted values of the available renewable energy and also the building energy demands.

Although the multi-period optimization has been used in some literature, there is not a unified method for the utilization of this technique in the various types of building integrated renewable and low carbon energy systems. The MPC method has been used in chemical process engineering, electrical power networks and building primary and secondary HVAC systems, but it has not been used in the

building integrated renewable and low carbon energy systems. In addition, there are no studies for designing explicit MPCs in this research area.

The multi-period optimization and hybrid MPC methods were used for designing a unified supervisory controller for building integrated renewable and low carbon energy systems. For this purpose, the mathematical models of the energy system were initially obtained, then the related controllers were designed.

In the multi-period optimization method, for each one of the energy carriers an energy bus was considered. Energy converters and energy storage devices are connected to this bus and also energy from grids and renewable energies enter into the bus, and the energy supply of the building and energy exported to the grid exit from the bus. Each one of the energy buses are modelled using the energy conservation law. Then, the optimal inputs of the system are obtained by solving the optimization problem consisting of an objective function, a system model and constraints.

In the hybrid MPC method the model of the system is obtained with the state space equations which are modified to integrate the discrete and the continuous time dynamics of the building energy system (MLD model). Then the optimal inputs of the system are obtained by solving a constraints finite time optimal control problem.

Three applications of the supervisory controller were studied in this research. In the first application it was shown that the controller is able to reduce the daily energy cost and CO_2 emission from the heating and electrification of a house in the UK. The second application showed that the controller reduces the diesel generator fuel cost by preventing its operation in low loads and running it in order to store the cheaper generated electricity in the batteries. In the third application the controller was used in a hybrid power system, and it was shown that the controller manages the power flows between the system components to supply the electrical demand and minimize the losses due to the energy storages in the system.

7.2 Conclusions

The aim of this research was to develop a unified supervisory controller for building integrated renewable and low carbon energy systems. The controller optimised the energy generation and storage in the building in order to reduce the operational cost and CO_2 emissions.

According to the objectives of the research, a mathematical model of the typical energy system components was determined. Then a unified model of the building integrated renewable and low carbon energy system was obtained. This model was used in designing the supervisory controller. The supervisory controller was validated by the simulation of three different applications. In addition, in Application 1 the controller was validated by two methods. The first method was based on multi-period optimization and the second method was based on the hybrid model predictive control. In the second method, the explicit operation of the controller was also considered.

In conclusion, the results of the simulations showed that :

1. The controller is a unified controller and can be tailored to different applications.
2. The controller successfully follows up loads set points.
3. The controller captures inputs and outputs constraints.
4. The controller determines how much energy should be charged or discharged from the energy storage devices.
5. The controller determines the start up and shut down of the non-renewable energy converters and their output capacity when they are in operation.
6. The controller determines the amount of energy which should be imported from the grid or exported to the grid.
7. The controller, with respect to the other non-optimal control strategies, reduces the operational cost and CO_2 emissions.

8. The optimal operational cost of the energy system with the designed controllers based on multi-period optimization and hybrid model predictive control methods are identical.

7.3 Contribution

In Section 2.3, it was highlighted that there was no unified optimal supervisory controller in the existing research for controlling the building integrated renewable and low carbon energy systems. In this research a unified controller was designed based on the linear mathematical model of the system. The linearity of the mathematical model of the system was important, since it resulted in a convex optimization problem which was simple to solve and certain to find a global optima.

The other contribution to knowledge was in using the MLD model and the hybrid model predictive control approach in the design of the supervisory controller. As stated in Section 2.3, using the hybrid model predictive control for the supervisory control of the building integrated renewable and low carbon energy systems has not been reported in the literature. In this approach, high level tools were used in the design of the controller. In addition the supervisory controller was designed in the explicit form.

7.4 Recommendations for industry

Considering the UK government's policies and incentives for utilization of the renewable and low carbon energy technologies in buildings (explained in Section 2.1.9) and also the continuous reduction of the cost of these technologies, there is an increasing market demand for them. Therefore the supervisory controller designed in this research, is attractive to the related industry.

For the implementation of the designed supervisory controller, certain types of hardware and software are needed. The required hardware is a computer with acceptable performance and the required software is numerical computing environment (like MATLAB) with optimization software for MILP.

The commercial optimization software is normally expensive and requires a powerful computer to run it properly. As stated in Section 7.2, in the online operation of the controller, the run time of the optimization program should be less than one time step.

The prediction of the weather data and the building loads that are needed by the controller are performed by dedicated software. In the online operation, these predictions also should be calculated in less than one time step.

Considering the above factors, the following recommendations are given for the implementation of the supervisory controller:

1. In buildings that have a building management system (BMS), the energy converters and energy storage devices (explained in Chapter 4) are connected to the BMS. The Human Machine Interface (HMI) of the BMS normally runs on a powerful workstation(s), which can be used for running the supervisory control program as well. In this case, the control program environment (e.g. MATLAB) can exchange the required data with the energy system components through HMI and a standard communication interface, like Dynamic Data Exchange (DDE).

The predicted weather data can be received via the internet and used for renewable energy and building load predictions. The controller can access the predicted data via a standard method. For instance, MATLAB can communicate with routines written in other programming languages with External Interfaces.

2. In homes and small buildings with no BMS, due to the complexity and/or cost, a computer based controller is not feasible. For these applications two methods are recommended. The first method is using the explicit form of the controller. In this manner there is no need for the optimization. The controller can receive weather

data from a weather station via the internet, and can calculate the available renewable energies. The building loads in each month can be assumed to have a fixed profile for week days, weekends and holidays.

The second method is to use a gateway to connect the energy system components to an Energy Service Provider (ESP). ESP calculates the control inputs and sends them to the energy system via the internet. The ESP predicts the building loads and the available renewable energies, based on the weather prediction data that it receives from the weather stations.

7.5 Future work

The following research objectives are suggested as future work to be investigated:

1. In practical applications the models of the energy converter and the energy storage equipment are non-linear. This non-linearity will be considered in designing a non-linear model predictive controller.

2. Output power from most of the renewable energy technologies, like solar collectors, photovoltaic cells and wind turbines, depends strongly on the weather conditions. Due to the uncertainty of weather forecasting, the prediction of the output power is also uncertain. In addition, the prediction of the energy consumption of a building, which depends on the weather conditions and the occupants' behaviour, is uncertain. These uncertainties will be considered in designing a stochastic model predictive controller.

3. If the supervisory optimal controller minimizes the cost, it may not also optimize the CO_2 emission, and vice versa. A model predictive controller will be designed based on multiple objective functions, which will need to compromise between the minimization of cost and CO_2 emission.

References

ABU-SHARKH, S., ARNOLD, R.J., KOHLER, J., LI, R., MARKVART, T., ROSS, J.N., STEEMERS, K., WILSON, P. and YAO, R., 2006. Can microgrids make a major contribution to UK energy supply? *Renewable and Sustainable Energy Reviews,* **10**(2), pp. 78-127.

AI, B., YANG, H., SHEN, H. and LIAO, X., 2003. Computer-aided design of PV/wind hybrid system. *Renewable Energy,* **28**(10), pp. 1491-1512.

AL-ALAWI, A., M AL-ALAWI, S. and M ISLAM, S., 2007. Predictive control of an integrated PV-diesel water and power supply system using an artificial neural network. *Renewable Energy,* **32**(8), pp. 1426-1439.

ALPAY, M.E. and SHOR, M.H., 1999. Multiple solutions to the l^1-optimal control problem and its dual linear programming problem. *Automatic Control, IEEE Transactions on,* **44**(5; given with a three dimensional constraint region where both problems have multiple solutions), pp. 1089-1093.

ARORA, J., 2011.*Introduction to Optimum Design.* Third edn. Academic Press.

ASHRAE, 2008. *ASHRAE Handbook, HVAC Systems and Equipment.* American Society for Heating, Refrigerating and Air-conditioning Engineers.

BALL, M. and WIETSCHEL, M., 2009. *The hydrogen economy: opportunities and challenges.* Cambridge University Press.

BARLEY, C.D. and WINN, C.B., 1996. Optimal dispatch strategy in remote hybrid power systems. *Solar Energy,* **58**(4-6), pp. 165-179.

BAXI, . Available: http://www.bdrthermeaspecification.co.uk/assets/baxi-ecogen-micro-chp.pdf [July, 2011].

BEAUSLEIL-MORRISON, I., MOTTILLO, M., FERGUSON, A., RIBBERINK, H., YANG, L. and HADDAD, K., 2006. The Simulation of a Renewable-Energy-Powered Hydrogen-Based Residential Electricity System, *Second National IBPSA-USA Conference*, 2nd-4th, August 2006, pp. 67-74.

BELEGUNDU A. D. and CHANDRUPATLA, T.R., 2011. *Optimization Concepts and Applications in Engineering.* Cambridge University Press.

BELFKIRA, R., ZHANG, L. and BARAKAT, G., 2011. Optimal sizing study of hybrid wind/PV/diesel power generation unit. *Solar Energy,* **85**(1), pp. 100-110.

BELLMAN, R., 1957. *Dynamic Programming.* Princeton: Princeton University Press.

BEMPORAD, A. and MORARI, M., 1999. Control of systems integrating logic, dynamics, and constraints. *Automatica,* **35**, pp. 407-427.

BEN SALAH, C., CHAABENE, M. and BEN AMMAR, M., 2008. Multi-criteria fuzzy algorithm for energy management of a domestic photovoltaic panel. *Renewable Energy,* **33**(5), pp. 993-1001.

BEN SALAH, C. and OUALI, M., 2010. Energy management of a hybrid photovoltaic system. *International Journal of Energy Research*, pp. 130-138.

BERNAL-AGUSTÍN, J.L. and DUFO-LÓPEZ, R., 2010. Techno-economical optimization of the production of hydrogen from PV-Wind systems connected to the electrical grid. *Renewable Energy,* **35**(4), pp. 747-758.

BLEVINS, T.L., MCMILLAN, G.K., WOJSZNIS, W.K. and BROWN, M.W., 2005. *Advanced Control Unleashed.* Research Triangle Park, NC: ISA Society.

BOROWY, B.S. and SALAMEH, Z.M., 1996. Methodology for optimally sizing the combination of a battery bank and PV array in a wind/PV hybrid system. *Energy Conversion, IEEE Transactions on,* **11**(2), pp. 367-375.

BOUKETTAYA, G., KRICHEN, L. and OUALI, A., 2007. Fuzzy logic supervisor for power control of an isolated hybrid energy production unit. *International Journal of Electrical and Power Engineering*, pp. 279-285.

BRDYS, M. and TATJEWSKI, P., 2005. *Iterative Algorithms for Multilayer Optimizing Control.* London/Singapore: Imperial College Press/World Scientific.

CAMACHO, E.F. and C. BORDONS, C., 2004. *Model predictive control.* 2 edn. Springer-Verlag.

CARRION, M. and ARROYO, J.M., 2006. A computationally efficient mixed-integer linear formulation for the thermal unit commitment problem. *Power Systems, IEEE Transactions on,* **21**(3), pp. 1371-1378.

CATALÃO, J.P.S., POUSINHO, H.M.I. and MENDES, V.M.F., 2010. Scheduling of head-dependent cascaded hydro systems: Mixed-integer quadratic programming approach. *Energy Conversion and Management,* **51**(3), pp. 524-530.

CCC, 2011-last update, Carbon Budgets. Available: http://www.theccc.org.uk/carbon-budgets [July, 2011].

CHAABENE, M., BEN AMMAR, M. and ELHAJJAJI, A., 2007. Fuzzy Based Energy Management of a Domestic Photovoltaic Panel. *American Journal of Applied Sciences,* **4**(2), pp. 60-65.

CLASTRES, C., HA PHAM, T.T., WURTZ, F. and BACHA, S., 2010. Ancillary services and optimal household energy management with photovoltaic production. *Energy,* **35**(1), pp. 55-64.

COLLAZOS, A., MARÉCHAL, F. and GÄHLER, C., 2009. Predictive optimal management method for the control of polygeneration systems. *Computers and Chemical Engineering*, **33**(10), pp. 1584-1592.

CROWN, 2008b-last update, Energy Act 2008 [Homepage of (UK: The Stationary Office Limited) chapter 32], [Online]. Available: http://www.legislation.gov.uk/ukpga/2008/32/pdfs/ukpga_20080032_en.pdf [July, 2011].

CROWN, 2008a-last update, Climate Change Act 2008 [Homepage of (UK: The Stationary Office Limited) chapter 27], [Online]. Available: http://www.legislation.gov.uk/ukpga/2008/27/pdfs/ukpga_20080027_en.pdf [July, 2011].

DANTZIG, G.B. and THAPA, M.N., 2003. *Linear Programming: Theory and extensions.* Springer.

DCLG, 2010-last update, The housebuilding industry. Available: http://www.communities.gov.uk/documents/housing/pdf/1526670.pdf [July, 2011].

DCLG, 2008-last update, Definition of zero carbon homes and non-domestic buildings . Available: http://www.zerocarbonhub.org/resourcefiles/1101177.pdf [July, 2011].

DCLG, 2006b-last update, Code for Sustainable Homes. Available: http://www.planningportal.gov.uk/uploads/code_for_sust_homes.pdf [July, 2011].

DCLG, 2006a-last update, Building A Greener Future:Towards Zero Carbon Development. Available: http://www.communities.gov.uk/documents/planningandbuilding/pdf/153125.pdf [July, 2011].

DECC, 2011b-last update, Renewable Heat Incentive (RHI) Scheme. Available: http://www.decc.gov.uk/en/content/cms/meeting_energy/Renewable_ener/incentive/incentive.aspx [July, 2011].

DECC, 2011a-last update, Carbon budgets. Available: http://www.decc.gov.uk/en/content/cms/emissions/carbon_budgets/carbon_budgets.aspx [July, 2011].

DECC, 2010c-last update, Feed-in Tariffs Government's Response to the Summer 2009 Consultation. Available: http://www.decc.gov.uk/assets/decc/Consultations/Renewable%20Electricity%20Financial%20Incentives/1_20100204120204_e_@@_FITsconsultationresponseandGovdecisions.pdf [July, 2011].

DECC, 2010b-last update, Fuel poverty monitoring indicators 2010. Available: http://www.decc.gov.uk/assets/decc/Statistics/fuelpoverty/612-fuel-poverty-monitoring-indicators-2010.pdf [July, 2011].

DECC, 2010a-last update, UK energy in brief 2010. Available: http://www.decc.gov.uk/assets/decc/statistics/publications/brief/190-uk-energy-in-brief-2010.pdf [July, 2011].

DECC, 2009c-last update, The Renewable Energy Strategy (RES). Available: http://www.decc.gov.uk/en/content/cms/what_we_do/uk_supply/energy_mix/renewable/res/res.aspx [July, 2011].

DECC, 2009b-last update, The UK Fuel Poverty Strategy. Available: http://www.decc.gov.uk/assets/decc/statistics/fuelpoverty/1_20091021091505_e_@@_ukfuelpovertystrategy7annreport09.pdf [July, 2011].

DECC, 2009a-last update, UK Low Carbon Transition Plan Emissions Projections. Available: http://www.decc.gov.uk/assets/decc/statistics/projections/1_20090812111709_e_@@_lctprojections.pdf [July, 2011].

DECC, 2008-last update, Energy consumption in the United Kingdom. Available: http://www.decc.gov.uk/en/content/cms/statistics/publications/ecuk/ecuk.aspx [July, 2011].

DELL, R.M. and RAND, D.A.J., 2001. Energy storage — a key technology for global energy sustainability. *Journal of Power Sources,* **100**(1-2), pp. 2-17.

DIAF, S., DIAF, D., BELHAMEL, M., HADDADI, M. and LOUCHE, A., 2007. A methodology for optimal sizing of autonomous hybrid PV/wind system. *Energy Policy,* **35**(11), pp. 5708-5718.

DIAF, S., NOTTON, G., BELHAMEL, M., HADDADI, M. and LOUCHE, A., 2008. Design and techno-economical optimization for hybrid PV/wind system under various meteorological conditions. *Applied Energy,* **85**(10), pp. 968-987.

DOHERTY, P.S., AL-HUTHAILI, S., RIFFAT, S.B. and ABODAHAB, N., 2004. Ground source heat pump—description and preliminary results of the Eco House system. *Applied Thermal Engineering,* **24**(17-18), pp. 2627-2641.

DTI AND DEFRA, 2007. *UK Biomass Strategy.* London, Department for Environment, Food and Rural Affairs (DEFRA).

DUFFIE, J.A. and BECKMAN, W.A., 1991. *Solar Engineering of Thermal Processes.* New York: John Wiley & Sons, Inc.

DUFO-LÓPEZ, R., BERNAL-AGUSTÍN, J.L. and CONTRERAS, J., 2007. Optimization of control strategies for stand-alone renewable energy systems with hydrogen storage. *Renewable Energy,* **32**(7), pp. 1102-1126.

ECI, 2005. *40% house.* Research report 31. Environmental Change Institute University of Oxford.

EEA (ENERGY AND ENVIRONMENTAL ANALYSIS, INC.), 2008. *Catalog of CHP technologies: Fuel cells.* Environmental Protection Agency.

EIA, 2010-last update, International Energy Outlook 2010. Available: http://www.eia.gov/oiaf/ieo/pdf/0484%282010%29.pdf [July, 2011].

ENERGY SAVING TRUST, 2005. *Pimilco District Heating Undertaking: a case study of community heating.* Energy Saving Trust.

ENGELL, S., 2007. Feedback control for optimal process operation. *Journal of Process Control,* **17**(3), pp. 203-219.

ENVIRONMENTAL PROTECT UK, 2007-last update, Small scale wind turbines. Available: http://www.environmental-protection.org.uk/assets/library/documents/Small_wind_turbines_scotland_Nov07.pdf [July, 2011].

FAILLE, D., MONDON, C. and AL-NASRAWI, B., 2007. mCHP Optimization by Dynamic Programming and Mixed Integer Linear Programming. *Intelligent Systems Applications to Power Systems, 2007. ISAP 2007. International Conference on*, pp. 1-6.

FAVRE-PERROD, P., 2005. A vision of future energy networks. *Power Engineering Society Inaugural Conference and Exposition in Africa, 2005 IEEE,* , pp. 13-17.

FINDEISEN, W., BAILEY, F.N., BRDY´S, M., MALINOWSKI, K., TATJEWSKI, P. and WO´ZNIAK, A., 1980. *Control and Coordination in Hierarchical Systems.* Chichester/New York, NY/Brisbane/Toronto. J. Wiley&Sons.

FLETCHER, R., 2000. *Practical methods of optimization.* Wiley.

FLOUDAS, C.A. and GROSSMANN, I.E., 1987. Automatic generation of multiperiod heat exchanger network configurations. *Computers & Chemical Engineering,* **11**(2), pp. 123-142.

FLOUDAS, C.A. and GROSSMANN, I.E., 1986. Synthesis of flexible heat exchanger networks for multiperiod operation. *Computers & Chemical Engineering,* **10**(2), pp. 153-168.

FUNG, L.C.C., 2000. Combined fuzzy-logic and genetic algorithm technique for the scheduling of remote area power system. *Power Engineering Society Winter Meeting, 2000. IEEE,* **2**, pp. 1069-1074 vol.2.

GEIDL, M., KOEPPEL, G., FAVRE-PERROD, P., KLOCKL, B., ANDERSSON, G. and FROHLICH, K., 2007b. Energy hubs for the future. *Power and Energy Magazine, IEEE,* **5**(1), pp. 24-30.

GEIDL, M. and ANDERSSON, G., 2007a. Optimal Coupling of Energy Infrastructures. *Power Tech, 2007 IEEE Lausanne*, pp. 1398-1403.

HENZE, G.P., FELSMANN, C. and KNABE, G., 2004a. Evaluation of optimal control for active and passive building thermal storage. *International Journal of Thermal Sciences,* **43**(2), pp. 173-183.

HENZE, G.P., KALZ, D.E., FELSMANN, C. and KNABE, G., 2004b. Impact of Forecasting Accuracy on Predictive Optimal Control of Active and Passive Building Thermal Storage Inventory. *HVAC&R Research,* **10**(2), pp. 153-178.

HENZE, G.P., KRARTI, M. and BRANDEMUEHL, M.J., 2003. Guidelines for improved performance of ice storage systems. *Energy and Buildings,* **35**(2), pp. 111-127.

HENZE, G.P., PFAFFEROTT, J., HERKEL, S. and FELSMANN, C., 2007. Impact of adaptive comfort criteria and heat waves on optimal building thermal mass control. *Energy and Buildings,* **39**(2), pp. 221-235.

HEPHAESTUS BOOKS, 2011. *Hydrogen Infrastructure, including: Tank Car, Hydrogen Highway, Hydrogen Station, Hydrogen Piping, Hynor, California Hydrogen Highway*, Hephaestus Books.

HILLIER, F. and LIEBERMAN, G., 2005. *Introduction to Operations Research.* Eighth edn.

HMGS, 2011-last update, Hydrogen generation. Available: http://www.hydrogen-yorkshire.co.uk/documents/Hydrogen_Generation_HMGS_fact_sheet.pdf [July, 2011].

HOUWING, M., NEGENBORN, R.R. and DE SCHUTTER, B., 2008. Economic advantages of applying model predictive control to distributed energy resources: The case of micro-CHP systems. *Control and Automation, 2008 16th Mediterranean Conference on*, pp. 1550-1555.

HUANG, G., WANG, S. and XU, X., 2009. A robust model predictive control strategy for improving the control performance of air-conditioning systems. *Energy Conversion and Management,* **50**(10), pp. 2650-2658.

ICAX, 2011-last update, Renewable Heat Incentive. Available: http://www.icax.co.uk/Renewable_Heat_Incentive.html [July, 2011].

IHM, P., KRARTI, M. and HENZE, G.P., 2004. Development of a thermal energy storage model for EnergyPlus. *Energy and Buildings,* **36**(8), pp. 807-814.

ILINCA, A., MCCARTHY, E., CHAUMEL, J. and RÉTIVEAU, J., 2003. Wind potential assessment of Quebec Province. *Renewable Energy,* **28**(12), pp. 1881-1897.

IYER, R.R. and GROSSMANN, I.E., 1998. Synthesis and operational planning of utility systems for multiperiod operation. *Computers & Chemical Engineering,* **22**(7–8), pp. 979-993.

JAIN, L.C. and MARTIN M., N., 1999. *Fusion of neural networks, fuzzy sets, and genetic algorithms: industrial applications.* CRC press.

JEONG, K., LEE, W. and KIM, C., 2005. Energy management strategies of a fuel cell/battery hybrid system using fuzzy logics. *Journal of Power Sources,* **145**(2), pp. 319-326.

JIFANG, L., TIANHAO, T. and JINGANG, H., 2010. A neural network control strategy for Multi-energy common dc bus hybrid power supply. *Power Electronics Electrical Drives Automation and Motion (SPEEDAM), 2010 International Symposium on*, pp. 1827-1831.

JOHNSON, G.L., 1985. *Wind Energy Systems.* Englewood Cliffs, NJ: Prentice-Hall Inc.

JONES, D.R., PERTTUNEN, C.D. and STUCKMAN, B.E., 1993. *Lipschitzian optimization without the Lipschitz constant.* Springer Netherlands.

KAVVADIAS, K.C. and MAROULIS, Z.B., 2010. Multi-objective optimization of a trigeneration plant. *Energy Policy,* **38**(2), pp. 945-954.

KOLHE, M., AGBOSSOU, K., HAMELIN, J. and BOSE, T.K., 2003. Analytical model for predicting the performance of photovoltaic array coupled with a wind turbine in a stand-alone renewable energy system based on hydrogen. *Renewable Energy,* **28**(5), pp. 727-742.

KOLOKOTSA, D., POULIEZOS, A., STAVRAKAKIS, G. and LAZOS, C., 2009. Predictive control techniques for energy and indoor environmental quality management in buildings. *Building and Environment,* **44**(9), pp. 1850-1863.

KORPAS, M. and HOLEN, A.T., 2006. Operation planning of hydrogen storage connected to wind power operating in a power market. *Energy Conversion, IEEE Transactions on,* **21**(3), pp. 742-749.

KOUTROULIS, E., KOLOKOTSA, D., POTIRAKIS, A. and KALAITZAKIS, K., 2006. Methodology for optimal sizing of stand-alone photovoltaic/wind-generator systems using genetic algorithms. *Solar Energy,* **80**(9), pp. 1072-1088.

KREITH, F. and GOSWAMI, D.Y., 2007. *Handbook of energy efficiency and renewable energy.* CRC press.

KVASNICA, M. and HERCEG, M., 2009. *HYSDEL 3.0.*

KVASNICA, M., GRIEDER, P. and BAOTI´C., M., 2004. *M. Kvasnica, P. Grieder, and M. Baoti´c. Multi-Parametric Toolbox (MPT), Available from* http://control.ee.ethz.ch/˜mpt/. .

LAUTIER, P., PREVOST, M., ETHIER, P., MARTEL, P. and LAVOIE, L., 2007. Off-Grid Diesel Power Plant Efficiency Optimization and Integration of Renewable Energy Sources. *Electrical Power Conference, 2007. EPC 2007. IEEE Canada*, pp. 274-279.

ŁAWRYŃCZUK, M., 2011. Online set-point optimisation cooperating with predictive control of a yeast fermentation process: A neural network approach. *Engineering Applications of Artificial Intelligence,* **24**(6), pp. 968-982.

LE XIE and ILIC, M.D., 2009. Model predictive economic/environmental dispatch of power systems with intermittent resources. *Power & Energy Society General Meeting, 2009. PES '09. IEEE*, pp. 1-6.

LEVENBERG, K., 1944. A Method for the Solution of Certain Non-linear Problems in Least Squares. *Quarterly of Applied Mathematics,* **2**(2), pp. 164-168.

LITTLE, M., THOMSON, M. and INFIELD, D., 2007. Electrical integration of renewable energy into stand-alone power supplies incorporating hydrogen storage. *International Journal of Hydrogen Energy,* **32**(10-11), pp. 1582-1588.

LIU, S. and HENZE, G.P., 2006. Experimental analysis of simulated reinforcement learning control for active and passive building thermal storage inventory: Part 2: Results and analysis. *Energy and Buildings,* **38**(2), pp. 148-161.

LOGENTHIRAN, T. and SRINIVASAN, D., 2009. Short term generation scheduling of a Microgrid. *TENCON 2009 - 2009 IEEE Region 10 Conference*, pp. 1-6.

LU, L., YANG, H. and BURNETT, J., 2002. Investigation on wind power potential on Hong Kong islands—an analysis of wind power and wind turbine characteristics. *Renewable Energy,* **27**(1), pp. 1-12.

MA, Y., BORRELLI, F., HENCEY, B., COFFEY, B., BENGEA, S. and HAVES, P., 2011. Model Predictive Control for the Operation of Building Cooling Systems. *Control Systems Technology, IEEE Transactions on,* **PP**(99), pp. 1-8.

MACIEJ, Ł., 2011. Online set-point optimisation cooperating with predictive control of a yeast fermentation process: A neural network approach. *Engineering Applications of Artificial Intelligence,* **24**(6), pp. 968-982.

MACIEJOWSKI, J.M., 2002. *Predictive control with constraints.* London, U.K. Prentice-Hall Inc.

MACKAY, D.J.C., 2008-last update, Sustainable energy–without the hot air [Homepage of UIT Cambridge], [Online]. Available: www.withouthotair.com [July, 2011].

MANWELL, J.F. and MCGOWAN, J.G., 1993. Lead acid battery storage model for hybrid energy systems. *Solar Energy,* **50**(5), pp. 399-405.

MARECHAL, F. and KALITVENTZEFF, B., 2003. Targeting the integration of multi-period utility systems for site scale process integration. *Applied Thermal Engineering,* **23**(14), pp. 1763-1784.

MARLIN, T.E., 1995. *Process Control.* New York, NY: McGraw-Hill.

MARQUARDT, D.W., 1963. An Algorithm for the Least-Squares Estimation of Nonlinear Parameters. *SIAM Journal of Applied Mathematics,* **11**(2), pp. 431-441.

NATIONAL GRID, 2011-last update. Available: http://www.nationalgrid.com/uk/LandandDevelopment/DDC/GasElectricNW/ [July, 2011].

NELSON, D.B., NEHRIR, M.H. and WANG, C., 2006. Unit sizing and cost analysis of stand-alone hybrid wind/PV/fuel cell power generation systems. *Renewable Energy,* **31**(10), pp. 1641-1656.

NEMHAUSER, G. and WOLSEY, L., 1999. *Integer and Combinatorial Optimization.* John Wiley & Sons.

NREL, 2008. *HOMER (The Hybrid Optimization Model for Electric Renewables).* National Renewable Energy Laboratory, Available from: http://www.homerenergy.com/.

OECD/IEA, 2004. *Coming from the cold. Improving district heating policy in transition economies.* Paris: OECD/IEA.

OHSAWA, Y., EMURA, S. and ARAI, K., 1993. Optimal operation of photovoltaic/diesel power generation system by neural network. *Neural Networks to Power Systems, 1993. ANNPS '93., Proceedings of the Second International Forum on Applications of*, pp. 99-103.

OVE ARUP, 2008. *Ashford Sustainable Energy Feasibility Study.*

QIN, S.J. and BADGWELL, T.A., 2003. A survey of industrial model predictive control technology. *Control Engineering Practice,* **11**(7), pp. 733-764.

REN21, 2010-last update, Renewables 2010, global status report. Available: http://www.ren21.net/Portals/97/documents/GSR/REN21_GSR_2010_full_revised%20Sept2010.pdf [July, 2011].

RENEWABLE ENERGY TARIFF, 2011-last update, Feed-in Tariff. Available: http://www.renewableenergytariff.co.uk/Tariffs/FiT/FiT.html [July, 2011].

SAHINIDIS, N.V. and GROSSMANN, I.E., 1991. Reformulation of multiperiod MILP models for planning and scheduling of chemical processes. *Computers & Chemical Engineering,* **15**(4), pp. 255-272.

SAP 2009, *The Government's Standard Assessment Procedure for Energy Rating of Dwellings, rev October 2010, DECC for BRE (2011).*

SARKER, R.A. and NEWTON, C.S., 2008. *Optimization modelling: a practical approach.* CRC Press.

SCRI, 2010-last update, A Review of the UK Domestic Energy System. Available: http://live.scri.salford.ac.uk/wp-content/uploads/2010/12/SCRIenergyReport.pdf [July, 2011].

SEBORG, D.E., EDGAR, T.F. and MELLICHAMP, D.A., 2004. *Process Dynamics and Control.* 2 edn. New Jersey: John Wiley & Sons.

SENJYU, T., HAYASHI, D., YONA, A., URASAKI, N. and FUNABASHI, T., 2007. Optimal configuration of power generating systems in isolated island with renewable energy. *Renewable Energy,* **32**(11), pp. 1917-1933.

SHEARER, D. and ANDERSON, B., 2005. *Low and Zero Carbon Technologies in the Scottish Building Standards .* Scottish Enterprise Technology Park, East Kilbride, Glasgow, G75 0RZ: BRE.

ŠIROKÝ, J., OLDEWURTEL, F., CIGLER, J. and PRÍVARA, S., 2011. Experimental analysis of model predictive control for an energy efficient building heating system. *Applied Energy,* **88**(9), pp. 3079-3087.

SKARSTEIN, O. and UHLEN, K., 1989. Design considerations with respect to long-term diesel saving in wind/diesel plants. *Wind Engineering,* **13**(2), pp. 72-87.

SONTAG, E., 1981. Nonlinear regulation: The piecewise linear approach. *Automatic Control, IEEE Transactions on,* **26**(2), pp. 346-358.

SONTAG, R. and LANGE, A., 2003. Cost effectiveness of decentralized energy supply systems taking solar and wind utilization plants into account. *Renewable Energy,* **28**(12), pp. 1865-1880.

SWEENEY, D.J., ANDERSON, D.R., WILLIAMS, T.A., CAMM, J.D. and MARTIN, R.K., 2009. *Quantitative methods for business.* Cengage Learning.

TAO LI and SHAHIDEHPOUR, M., 2005. Price-based unit commitment: a case of Lagrangian relaxation versus mixed integer programming. *Power Systems, IEEE Transactions on,* **20**(4), pp. 2015-2025.

TATJEWSKI, P., 2008. Advanced control and on-line process optimization in multilayer structures. *Annual Reviews in Control,* **32**(1), pp. 71-85.

TATJEWSKI, P., 2007. *Advanced Control of Industrial Processes.* London, Springer.

TATJEWSKI, P., ŁAWRYN´ CZUK, M. and MARUSAK, P., 2009. Integrated predictive optimiser and constraint supervisor for processes with basic feedback control algorithm. *In: Proceedings of the European Control Conference,ECC2009, Budapest, Hungary*, pp. 3359-3364.

TATJEWSKI, P., 2010. Supervisory predictive control and on-line set-point optimization. *International Journal of Applied Mathematics and Computer Science,* **20**(3), pp. 483-495.

TORRISI, F.D. and BEMPORAD, A., 2004. HYSDEL-a tool for generating computational hybrid models for analysis and synthesis problems. *Control Systems Technology, IEEE Transactions on,* **12**(2), pp. 235-249.

TRNSYS (A TRANSIENT SYSTEMS SIMULATION PROGRAM), Available from: http://sel.me.wisc.edu/trnsys/.

TVRZSKÁ DE GOUVEA, M. and ODLOAK, D., 1998. One-layer real time optimization of LPG production in the FCC unit: procedure, advantages and disadvantages. *Computers & Chemical Engineering,* **22, Supplement 1**(0), pp. S191-S198.

ULLEBERG, Ø., 2004. The importance of control strategies in PV–hydrogen systems. *Solar Energy,* **76**(1-3), pp. 323-329.

VANDERBEI, R.J., 2008. *Linear programming: foundations and extensions.* Springer.

VARVAREZOS, D.K., BIEGLER, L.T. and GROSSMANN, I.E., 1995. Modeling uncertainty and analyzing bottleneck characteristics in multiperiod design optimization. *Computers & Chemical Engineering,* **19**(5), pp. 497-511.

VENAYAGAMOORTHY, G.K. and WELCH, R.L., 2010. Energy dispatch controllers for a photovoltaic system. *Engineering Applications of Artificial Intelligence,* **23**(2), pp. 249-261.

WELCH, R. and VENAYAGAMOORTHY, G.K., 2007. A Fuzzy-PSO Based Controller for a Grid Independent Photovoltaic System. *Swarm Intelligence Symposium, 2007. SIS 2007. IEEE*, pp. 227-233.

WINSTON, W.L. and GOLDBERG, J.B., 2004. *Operation research:applications and algorithms.* Fourth edn. Thomson Brooks/Cole.

XIA, X. and ELAIW, A.M., 2010. Optimal dynamic economic dispatch of generation: A review. *Electric Power Systems Research,* **80**(8), pp. 975-986.

XIAOHUA XIA, JIANGFENG ZHANG and ELAIW, A., 2009. A Model Predictive Control approach to dynamic economic dispatch problem. *PowerTech, 2009 IEEE Bucharest*, pp. 1-7.

YANG, H.X., LU, L. and BURNETT, J., 2003. Weather data and probability analysis of hybrid photovoltaic–wind power generation systems in Hong Kong. *Renewable Energy,* **28**(11), pp. 1813-1824.

YANG, H., LU, L. and ZHOU, W., 2007. A novel optimization sizing model for hybrid solar-wind power generation system. *Solar Energy,* **81**(1), pp. 76-84.

YANG, H., WEI, Z. and CHENGZHI, L., 2009. Optimal design and techno-economic analysis of a hybrid solar–wind power generation system. *Applied Energy,* **86**(2), pp. 163-169.

YUAN, S. and PEREZ, R., 2006. Multiple-zone ventilation and temperature control of a single-duct VAV system using model predictive strategy. *Energy and Buildings,* **38**(10), pp. 1248-1261.

YUDONG MA, ANDERSON, G. and BORRELLI, F., 2011. A distributed predictive control approach to building temperature regulation. *American Control Conference (ACC), 2011*, pp. 2089-2094.

YUDONG MA, BORRELLI, F., HENCEY, B., PACKARD, A. and BORTOFF, S., 2009. Model Predictive Control of thermal energy storage in building cooling systems. *Decision and Control, 2009 held jointly with the 2009 28th Chinese Control Conference. CDC/CCC 2009. Proceedings of the 48th IEEE Conference on*, pp. 392-397.

ZADEH, L.A., 1973. The concept of a linguistic variable and its application to approximate reasoning. *Memorandum ERL-M 411, Berkeley, October 1973*, pp. 43-80.

ZADEH, L.A., 1965. Fuzzy sets. *Information and Control,* **8**, pp. 335-353.

ZANIN, A.C., DE GOUVÊA, M.T. and ODLOAK, D., 2000. Industrial implementation of a real-time optimization strategy for maximizing production of LPG in a FCC unit. *Computers & Chemical Engineering,* **24**(2–7), pp. 525-531.

ZANIN, A.C., TVRZSKÁ DE GOUVÊA, M. and ODLOAK, D., 2002. Integrating real-time optimization into the model predictive controller of the FCC system. *Control Engineering Practice,* **10**(8), pp. 819-831.

ZERVAS, P.L., SARIMVEIS, H., PALYVOS, J.A. and MARKATOS, N.C.G., 2008. Model-based optimal control of a hybrid power generation system consisting of photovoltaic arrays and fuel cells. *Journal of Power Sources,* **181**(2), pp. 327-338.

ZHANG, B.J. and HUA, B., 2007. Effective MILP model for oil refinery-wide production planning and better energy utilization. *Journal of Cleaner Production,* **15**(5), pp. 439-448.

ZHANG, J.D. and RONG, G., 2008. An MILP model for multi-period optimization of fuel gas system scheduling in refinery and its marginal value analysis. *Chemical Engineering Research and Design,* **86**(2), pp. 141-151.

Appendix A

In this Appendix, Table A.1 shows feed-in tariff levels for the installation of microgeneration technologies. Table A.2 shows the renewable heat tariff levels and Table A.3 shows various fuel prices, emission factors and primary energy factors in the UK.

Table A. 1 Feed-in tariff levels for technologies installed between 1st April 2010 to 31st March 2013 (DECC, 2010c)

Technology	Scale	Tariff level for new installations in period (p/kWh) [NB tariffs will be inflated annually]			Tariff lifetime (years)
		Year 1: 1/4/10 – 31/3/11	Year 2: 1/4/11 – 31/3/12	Year 3: 1/4/12 – 31/3/13	
Anaerobic digestion	≤500kW	11.5	11.5	11.5	20
Anaerobic digestion	>500kW	9.0	9.0	9.0	20
Hydro	≤15 kW	19.9	19.9	19.9	20
Hydro	>15-100 kW	17.8	17.8	17.8	20
Hydro	>100 kW-2 MW	11.0	11.0	11.0	20
Hydro	>2 MW – 5 MW	4.5	4.5	4.5	20
MicroCHP pilot*	≤2 kW*	10*	10*	10*	10
PV	≤4 kW (new build)	36.1	36.1	33.0	25
PV	≤4 kW (retrofit)	41.3	41.3	37.8	25
PV	>4-10 kW	36.1	36.1	33.0	25
PV	>10-100 kW	31.4	31.4	28.7	25
PV	>100kW-5MW	29.3	29.3	26.8	25
PV	Stand alone system	29.3	29.3	26.8	25
Wind	≤1.5kW	34.5	34.5	32.6	20
Wind	>1.5-15kW	26.7	26.7	25.5	20
Wind	>15-100kW	24.1	24.1	23.0	20
Wind	>100-500kW	18.8	18.8	18.8	20
Wind	>500kW-1.5MW	9.4	9.4	9.4	20
Wind	>1.5MW-5MW	4.5	4.5	4.5	20
Existing microgenerators transferred from the RO		9.0	9.0	9.0	to 2027

* Note the microCHP pilot will support up to 30,000 installations with a review to start when the 12,000th installation has occurred

Table A. 2 Renewable heat tariff levels (ICAX, 2011)

RHI	Scale	RHI tariffs pence/kWh	Tariff lifetime in years
Solid biomass	45 kW	9.0	15
Bioliquids	45 kW	6.5	15
Biogas on-site	45 kW	5.5	10
Ground source heat pumps	45 kW	7.0	23
Air source heat pumps	45 kW	7.5	18
Solar thermal	20 kW	18.0	20
Solid biomass	45-500 kW	6.5	15
Biogas on-site	45-200 kW	5.5	10
Ground source heat pumps	45-350 kW	**5.5**	**20**
Air source heat pumps	45-350 kW	2.0	20
Solar thermal	20-100 kW	**17.0**	**20**
Solid biomass	500 kW	1.6-2.5	15
Ground source heat pumps	350 kW	1.5	20
Biomethane injection	All scales	4.0	15

Table A. 3 Fuel prices, additional standing charges, emission factors and primary energy factors (SAP 2009)

Fuel	Additional standing charge, £[a]	Unit price p/kWh	Emissions kg CO_2 per kWh	Primary energy factor	Fuel code
Gas:					
mains gas	106	3.10	0.198	1.02	1
LNG	106	3.10	0.198	1.02	8
bulk LPG	70	5.73	0.245	1.06	2
bottled LPG		8.34	0.245	1.06	3
LPG subject to Special Condition 18 [b]	106	3.10	0.245	1.06	9
Oil:					
heating oil		4.06	0.274	1.06	4
biodiesel from any biomass source [c]		5.7	0.047	1.30	71
biodiesel from used cooking oil only [d]		5.7	0.004	1.08	72
rapeseed oil		5.7	0.009	1.12	73
appliances able to use mineral oil or liquid biofuel B30K [e]		4.06	0.274	1.06	74
		4.6	0.193	1.06	75
bioethanol from any biomass source		42.0	0.064	1.34	76
Solid fuel: [f]					
house coal		2.97	0.301	1.02	11
anthracite		2.86	0.318	1.02	15
manufactured smokeless fuel		3.73	0.347	1.08	12
wood logs		3.42	0.008	1.05	20
wood pellets (in bags for secondary heating)		5.45	0.028	1.20	22
wood pellets (bulk supply for main heating)		4.93	0.028	1.20	23
wood chips		2.49	0.009	1.07	21
dual fuel appliance (mineral and wood)		3.21	0.206	1.04	10
Electricity:					
standard tariff		11.46	0.517	2.92	30
7-hour tariff (high rate) [g]		12.82	0.517	2.92	32
7-hour tariff (low rate) [g]	27	4.78	0.517	2.92	31
10-hour tariff (high rate) [g]		11.83	0.517	2.92	34
10-hour tariff (low rate) [g]	18	6.17	0.517	2.92	33
24-hour heating tariff	57	5.64	0.517	2.92	35
electricity sold to grid		11.46 [h]			36
electricity displaced from grid			0.529 [h]	2.92 [h]	37
electricity, unspecified tariff [i]					39
Community heating schemes: [j]	106 [k]				
heat from boilers – mains gas		3.78	0.198	1.02	51
heat from boilers – LPG		3.78	0.245	1.06	52
heat from boilers – oil		3.78	0.297 [l]	1.06	53
heat from boilers – B30D [e]		3.78	0.199	1.06	55
heat from boilers – coal		3.78	0.350 [m]	1.02	54
heat from electric heat pump		3.78	0.517	2.92	41
heat from boilers – waste combustion		3.78	0.040	1.28	42
heat from boilers – biomass		3.78	0.013 [n]	1.07	43
heat from boilers – biogas (landfill or sewage gas)		3.78	0.018	1.10	44
waste heat from power station		2.65	0.058 [o]	1.20	45
geothermal heat source		2.65	0.036	1.16	46
heat from CHP		2.65	as above[p]	as above[p]	48
electricity generated by CHP			0.529 [h]	2.92 [h]	49
electricity for pumping in distribution network			0.517	2.92	50

Energy Cost Deflator [q] = 0.47

Notes to Table 12:

(a) The standing charge given for electricity is extra amount for the off-peak tariffs, over and above the amount for the standard domestic tariff, as it is assumed that the dwelling has a supply of electricity for reasons other than space and water heating. The standing charge for off-peak electricity is added to space and water heating costs where either main heating or hot water uses off-peak electricity. The standing charge for gas is added to space and water heating costs where gas is used for space heating (main or secondary) or for water heating.

(b) www.ofgem.gov.uk/networks/gasdistr/otherwork/Documents1/7940-Independentnetworksopenletter.pdf

(c) For appliances that specifically use biodiesel (FAME) and fuel verified as wholly derived from biomass sources

(d) For appliances that specifically use biodiesel (FAME) and fuel verified as wholly derived from used cooking oil

(e) For appliances that specifically use a blend of 30% biodiesel from cooking oil and 70% kerosene (B30K) or 70% fuel oil (B30D)

(f) The specific fuel should be assumed for those appliances that can only burn the particular fuel (including Exempted Appliances within Smoke Control Areas).
Where a main heating appliance is classed as dual fuel (i.e mineral and wood), the data for dual fuel should be used, except where the dwelling is in a Smoke Control Area, when the data for solid mineral fuel should be used.
Wood should be specified as fuel for a main heating system only if there is adequate provision (at least 1.5 m³) for storage of the fuel.
Outside Smoke Control Areas an open fire should be considered as dual fuel, and a closed room heater without boiler if capable of burning wood as burning wood logs.

(g) With certain appliances using an off-peak tariff, some of the consumption is at the low rate and some at the high rate. The high-rate fractions to be used are given in Table 12a, the remainder being provided at the low rate.

(h) Deducted from costs, emissions or primary energy

(i) This code is used to define the fuel for any electric system. Other codes for electricity are to provide cost data, depending on the applicable electricity tariff.

(j) Cost is per unit of heat supplied, emission and primary factors are per unit of fuel used

(k) Include half this value if the community scheme is for DHW only

(l) Based on the mix of petroleum products used to generated heat in the UK (predominantly gas oil).

(m) Value for non-domestic coal

(n) Based on the mix of biomass sources used to generate heat in the UK.

(o) Takes account of the reduction in electricity generation that occurs where heat is produced at a high enough temperature to provide community heating.

(p) Use factor for community heat from boilers according to fuel used.

(q) An energy cost deflator term is applied before the rating is calculated. It will vary with the weighted average price of heating fuels in future so that the SAP rating is not affected by the general rate of fuel price inflation. However, individual SAP ratings are affected by relative changes in the price of particular heating fuels.

Appendix B

B.1 Chiller

A chiller is a machine that removes heat from a liquid via a vapor-compression or absorption refrigeration cycle. Most often water is chilled, but this water may also contain ~20% glycol and corrosion inhibitors; other fluids such as thin oils can be chilled as well (ASHRAE, 2008).

There are basically two types of chillers: compression and absorption. Compression chillers, including reciprocating compression, scroll compression, screw-driven compression, and centrifugal compression, are all mechanical machines that can be powered by electric motors, steam, or gas turbines (ASHRAE, 2008). They produce their cooling effect via the reverse-Rankine cycle, also known as vapor-compression. The heat of the cooling process is absorbed in the evaporator and rejected from the condenser.

The absorption chiller's thermodynamic cycle is driven by a heat source; this heat is usually delivered to the chiller via steam, hot water, or combustion. Compared to electrically powered chillers, they have very low electrical power requirements - very rarely above 15 kW in combined consumption for both the solution pump and the refrigerant pump. However, their heat input requirements are large, and their COPs are often 0.5 (single-effect) to 1.0 (double-effect) (ASHRAE, 2008). For the same cooling capacity, they require much larger cooling towers than vapor-compression chillers. However, absorption chillers, from an energy-efficiency point of view, excel where cheap, high grade heat or waste heat is readily available like heat rejection from heat engines or thermal power plants. In extremely sunny climates, solar energy has been used to operate absorption chillers.

The condenser of the chillers can be air-cooled or water-cooled. Water-cooled condensers are cooled by cooling towers and have better heat rejection performance. This is due to heat transfer at or near the air's wet-bulb temperature

rather than the higher dry-bulb temperature of the air. To increase the effectiveness of the air cooled condenser, a spray of water is used to wet down the condenser. This condenser is called an evaporative condenser.

For the vapour compression chillers, the coefficient of performance (COP) is defined as the ratio of the cooling capacity of the chiller to the electric energy input to the chiller (ASHRAE, 2008):

$$COP_{cooling} = \frac{cooling\ capacity}{input\ electric\ power} \qquad (1)$$

So the cooling power of the chiller can be determined from:

$$P_{cchi}(t) = COP_{cooling} P_{ech} \qquad (2)$$

Similarly the coefficient of performance and the cooling power for absorption chillers can be determined from the following equations respectively:

$$COP_{cooling} = \frac{cooling\ capacity}{input\ heat\ power} \qquad (3)$$

$$P_{cchi}(t) = COP_{cooling} P_{hch} \qquad (4)$$

The results of the mechanistic chiller model indicate that the chiller COP is primarily a function of only two variables, the load and the temperature difference between the leaving condenser and the chilled water flows. In this research we will consider an average constant COP that includes the total power consumption by the chiller, the cooling tower and the related pumps in the cooling system.

B.2 Heat Pump

A heat pump is a piece of equipment that moves heat from a low temperature location (the source) to a higher temperature location (the sink or heat sink), by using work or high temperature heat.

The source of the heat for a heat pump can be outside air or underground heat. The sink is normally the hot water of the heating system in the building.

Heat pumps can be thought of as a refrigeration machine, which is operating in reverse. So the above formulation for the chiller's power consumption can be used for heat pumps as well. The coefficient of performance for a vapour compression heat pump is defined as the ratio of the heating capacity of the heat pump to the electric power input (ASHRAE, 2008):

$$COP_{heating} = \frac{heating\ capacity}{electric\ power\ input} \qquad (5)$$

So the output heat from the heat pump can be determined by:

$$P_{hhp}(t) = COP_{heating} P_{ehp} \qquad (6)$$

In the case of the absorption heat pump $COP_{heating}$ and output heat power of the heat pump can be determined from the following equations:

$$COP_{heating} = \frac{heating\ capacity}{heating\ power\ input} \qquad (7)$$

$$P_{h_{out}hp}(t) = COP_{heating} P_{h_{in}hp} \qquad (8)$$

The results of the mechanistic heat pump model indicate that heating COP is a function of heating load and the temperature difference between the evaporator and condenser temperatures. In this research we will consider an average constant COP for heat pumps which includes all the electricity consumption by pumps, fans, etc.

B.3 Wind Turbine

A wind turbine is a rotating machine that converts the kinetic energy of wind into mechanical energy. If the mechanical energy is then converted to electricity, the

machine is called a Wind Generator, Wind Turbine, Wind Power Unit or Wind Energy Converter.

In building applications, small scale wind turbines have become more widely available over the past few years (Environmental Protect UK, 2007). These turbines vary in size according to how much electricity they generate, ranging from 100 watts to 6 kilowatts. The average house would need a system of 1-6 kilowatts depending on the location and size of the property, whilst a public building such as a community hall would require around 5-6 kilowatts. There are two types of small scale wind turbines available: mast mounted and roof mounted. Although mast mounted systems are generally more cost effective, they may not be appropriate for many properties. However, smaller roof mounted systems are capable of generating a reasonable proportion of the energy requirements given the right conditions. Most small wind turbines generate direct current electricity (DC) and require an inverter to convert it to alternating current electricity (AC).

For the estimation of wind turbine power, several models exist in the literature, such as the linear model (Yang, 2003; Yang, 2007), the model based on Weibull parameters (Lu, et al., 2002; Borowy and Salameh, 1996), the quadratic model (Diaf, et al., 2008) and the cubic model (Diaf, et al., 2007).

If we have the wind turbine characteristic curve that shows the relation between wind speed and power output, then we can use a linear interpolation to find the power output in the desired wind speed (Koutroulis, et al., 2006):

$$P_{wt} = (v - v_1)(\frac{P_2 - P_1}{v_2 - v_1}) + P_1 \qquad (9)$$

Here v is the wind speed (m/s) at turbine height and (P_1, v_1) , (P_2, v_2) are the wind turbine power and the wind speed pairs stored in the lookup table, such that $v_1 < v < v_2$.

If we have only the rated power of the wind turbine (P_{wtr}), the cut-in speed (v_{cin}) and the cut-out speed (v_{cout}) then we can use the following quadratic model to calculate the power generated by the wind turbine in the desired wind speed:

$$P_{wt} = \begin{cases} P_{wtr} \dfrac{v^2 - v_{cin}^2}{v_r^2 - v_{cin}^2} & v_{cin} < v < v_r \\ P_{wtr} & v_r \le v < v_{cout} \\ 0 & v \le v_{cin} \text{ and } v \ge v_{cout} \end{cases} \quad (10)$$

Wind speed should be adjusted for the wind turbine hub level. The adjusted wind speed is derived by the vertical profile of the wind speed which is determined from the power law:

$$v = v_{ref}\left(\frac{H}{H_{ref}}\right)^{\alpha} \quad (11)$$

Here v is the wind speed (m/s) measured at the hub height H (m); v_{ref} is the wind speed (m/s) measured at the reference height H_{ref} (m) and a is the wind speed power law coefficient, ranging from 1/7 to 1/4 (Ilinca, et al., 2003; Johnson, 1985).

B.4 Solar Collector

Solar collectors receive the sun's radiation, transform it into heat and then transfer that heat to water, solar fluid, or air. The solar thermal energy can be used in solar water heating systems, solar pool heaters, and solar space-heating systems. Solar collectors can be flat-plate collectors or evacuated-tube collectors. Here we derive a mathematical model for the flat plate collector.

Flat plate solar collector efficiency η is defined as the ratio of useful heat collection Q_u to the radiation that is incident on the surface of collector AI_T (Duffie and Beckmann, 1991):

$$\eta = \frac{Q_u}{AI_T} \quad (12)$$

Here I_T is global radiation incident on the solar collector (tilted surface) and A is the total collector array aperture or gross area.

In practice thermal efficiency of solar collector can be determined from a quadratic efficiency model originating from theoretical equations developed by Duffie and Beckmann (1991):

$$\eta = a_0 - a_1 \frac{(\Delta T)}{I_T} - a_2 \frac{(\Delta T)^2}{I_T} \qquad (13)$$

Here ΔT is the temperature difference between the inlet temperature of the fluid to the collector T_i and the ambient (air) temperature T_a. The thermal efficiency is defined by 3 parameters: a_0, a_1 and a_2. These 3 parameters are available for collectors tested according to American ASHRAE Standard 93-77, as well as for collectors tested according to the European Standards on solar collectors DIN EN 12975. Many examples of collector parameters can be found on the manufacturers' websites on the internet.

Collector test reports sometimes provide the efficiency curve using a different temperature difference (TRNSYS):

$$\Delta T = \begin{cases} \Delta T_i = T_i - T_a \\ \Delta T_{av} = T_{av} - T_a \\ \Delta T_o = T_o - T_a \end{cases} \qquad (14)$$

Here T_i is the inlet temperature of the fluid to the collector, T_a is the ambient (air) temperature, T_{av} is the average collector fluid temperature and T_o is the outlet temperature of the fluid from the collector. The first formulation is usually preferred in the US, while the second one is used in most European documents. Equation (13) can use any of those definitions of the temperature difference and the user can specify the a_0, a_1 and a_2 coefficients using any of the definitions. If the coefficients are given in terms of the average or the outlet temperature, correction factors are applied.

The total collector array may consist of collectors connected in series and in parallel. The thermal performance of the total collector array is determined by the number of modules in series and the characteristics of each module.

B.5 Cool storage

The cooling energy demand of buildings is normally supplied by the chilled water that is prepared by compression or absorption chillers. Compression chillers consume electrical energy which is cheap at night-time. This cheap electricity can be used to produce cooling energy which can be stored and used in the following day-time.

The cooling energy can be stored as cold water or ice. Cold water storage needs a large storage tank but the stored cold water can be directly connected to the building chilled water system. Ice storage needs a smaller storage tank but requires a complex control system.

Ihm, et al. (2004) have developed a model for ice storage system. In a steady state a simplified energy balance for cool storage can be written as:

$$E_c(t+\Delta t) = E_c(t) + eP_c(t)\Delta t \qquad (15)$$

Here E_c is the stored cool, P_c is the cooling power charged or discharged from the cooling tank and e is the efficiency of the system:

$$e = \begin{cases} COP_{ch} & P_c > 0 \\ 1 & P_c < 0 \end{cases} \qquad (16)$$

Appendix C

The MLD matrices of the hybrid model predictive control approach used in the application 1 (Section 6.1.2) are given below:

$$A = \begin{bmatrix} 1 & 0 & 0 \\ 0 & 0 & 0 \\ 0 & 0 & 0 \end{bmatrix} \qquad B_1 = \begin{bmatrix} 0 & 0 & 0 & 0 & -1 & 0 & 0 & 0 & 0 \\ 0 & 0 & 0 & 0 & 0 & 0 & 0 & 0 & 0 \\ 0 & 0 & 0 & 0 & 1 & 0 & 0 & 0 & 0 \end{bmatrix} \qquad B_2 = \begin{bmatrix} 0 \\ 0 \\ 0 \end{bmatrix}$$

$$B_3 = \begin{bmatrix} 0 & 0 & 0 & 0 \\ 1 & -1 & 0.1 & 0 \\ 0 & 0 & 0.8 & 1 \end{bmatrix} \qquad C = \begin{bmatrix} 1 & 0 & 0 \\ 0 & 0 & 0 \\ 0 & 0 & 0 \end{bmatrix}$$

$$D_1 = \begin{bmatrix} 0 & 0 & 0 & 0 & -1 & 0 & 0 & 0 & 0 \\ 0 & 0 & 0 & 0 & 0 & 0 & 0 & 0 & 0 \\ 0 & 0 & 0 & 0 & 1 & 0 & 0 & 0 & 0 \end{bmatrix} \qquad D_2 = \begin{bmatrix} 0 \\ 0 \\ 0 \end{bmatrix}$$

$$D_3 = \begin{bmatrix} 0 & 0 & 0 & 0 \\ 1 & -1 & 0.1 & 0 \\ 0 & 0 & 0.8 & 1 \end{bmatrix}$$

$$E_1 = \begin{bmatrix} 0 & 0 & -1 & 0 & 0 & 0 & 0 & 0 & 0 \\ 0 & 0 & 1 & 0 & 0 & 0 & 0 & 0 & 0 \\ -1 & 0 & 0 & 0 & 0 & -3 & 0 & 0 & 0 \\ 1 & 0 & 0 & 0 & 0 & 0 & 0 & 0 & 0 \\ 0 & 0 & 0 & 0 & 0 & 0 & 0 & 0 & 0 \\ 0 & 0 & 0 & 0 & 0 & 3 & 0 & 0 & 0 \\ 0 & -1 & 0 & 0 & 0 & 0 & -3 & 0 & 0 \\ 0 & 1 & 0 & 0 & 0 & 0 & 0 & 0 & 0 \\ 0 & 0 & 0 & 0 & 0 & 0 & 0 & 0 & 0 \\ 0 & 0 & 0 & 0 & 0 & 0 & 3 & 0 & 0 \\ 0 & 0 & -1 & 0 & 0 & 0 & 0 & -7.7 & 0 \\ 0 & 0 & 1 & 0 & 0 & 0 & 0 & 3.7 & 0 \\ 0 & 0 & 0 & 0 & 0 & 0 & 0 & -3.7 & 0 \\ 0 & 0 & 0 & 0 & 0 & 0 & 0 & 7.7 & 0 \\ 0 & 0 & 0 & -1 & 0 & 0 & 0 & 0 & -18 \\ 0 & 0 & 0 & 1 & 0 & 0 & 0 & 0 & 3.8 \\ 0 & 0 & 0 & 0 & 0 & 0 & 0 & 0 & -3.8 \\ 0 & 0 & 0 & 0 & 0 & 0 & 0 & 0 & 18 \\ 0 & 0 & 0 & 0 & 0 & -1 & -1 & 0 & 0 \\ 0 & 0 & 0 & 0 & 0 & 0 & 0 & 1 & -1 \\ 0 & 0 & 0 & 0 & 0 & 0 & 0 & 0 & -1 \end{bmatrix} \qquad E_2 = \begin{bmatrix} 0 \\ 4 \\ 0 \\ 0 \\ 0 \\ 0 \\ 0 \\ 0 \\ 0 \\ 0 \\ 0 \\ 0 \\ 0 \\ 0 \\ 0 \\ 0 \\ 0 \\ 0 \\ 0 \\ 0 \\ 0 \end{bmatrix}$$

$$E_3 = \begin{bmatrix} 0 & 0 & 0 & 0 \\ 0 & 0 & 0 & 0 \\ -1 & 0 & 0 & 0 \\ 1 & 0 & 0 & 0 \\ -1 & 0 & 0 & 0 \\ 1 & 0 & 0 & 0 \\ 0 & -1 & 0 & 0 \\ 0 & 1 & 0 & 0 \\ 0 & -1 & 0 & 0 \\ 0 & 1 & 0 & 0 \\ 0 & 0 & -1 & 0 \\ 0 & 0 & 1 & 0 \\ 0 & 0 & -1 & 0 \\ 0 & 0 & 1 & 0 \\ 0 & 0 & 0 & -1 \\ 0 & 0 & 0 & 1 \\ 0 & 0 & 0 & -1 \\ 0 & 0 & 0 & 1 \\ 0 & 0 & 0 & 0 \\ 0 & 0 & 0 & 0 \\ 0 & 0 & 0 & 0 \end{bmatrix} \quad E_4 = \begin{bmatrix} 0 & 0 & 0 \\ 0 & 0 & 0 \end{bmatrix} \quad E_5 = \begin{bmatrix} 7.7 \\ -3.7 \\ 3 \\ 0 \\ 0 \\ 0 \\ 3 \\ 0 \\ 0 \\ 0 \\ 7.7 \\ -3.7 \\ 0 \\ 0 \\ 18 \\ -3.8 \\ 0 \\ 0 \\ 1 \\ 0 \\ 0 \end{bmatrix}$$